2013-05-08

The Relationship Between Carbonate Chemistry and Calcification on the Florida Reef Tract, and in the Symbiotic Reef Coral, Acropora cervicornis

Nancy Muehllehner
University of Miami, nancymuehllehner@gmail.com

UNIVERSITY OF MIAMI

THE RELATIONSHIP BETWEEN CARBONATE CHEMISTRY AND CALCIFICATION ON THE FLORIDA REEF TRACT, AND IN THE SYMBIOTIC REEF CORAL, *ACROPORA CERVICORNIS*

By

Nancy Muehllehner

A DISSERTATION

Submitted to the Faculty
of the University of Miami
in partial fulfillment of the requirements for
the degree of Doctor of Philosophy

Coral Gables, Florida

May 2013

UNIVERSITY OF MIAMI

A dissertation submitted in partial fulfillment of
the requirements for the degree of
Doctor of Philosophy

THE RELATIONSHIP BETWEEN CARBONATE CHEMISTRY AND CALCIFICATION ON THE FLORIDA REEF TRACT, AND IN THE SYMBIOTIC REEF CORAL, *ACROPORA CERVICORNIS*

Nancy Muehllehner

Approved:

_____ Chris Langdon, Ph.D. Professor of Marine Biology and Fisheries	_____ M. Brian Blake, Ph.D. Dean of the Graduate School
_____ Andrew C. Baker, Ph.D. Associate Professor of Marine Biology and Fisheries	_____ Martin Grosell, Ph.D. Professor of Marine Biology and Fisheries
_____ Diego Lirman, Ph.D. Associate Professor of Marine Biology and Fisheries	_____ Joan Kleypas, Ph.D. Scientist III National Center for Atmospheric Research Boulder, Colorado

MUEHLLEHNER, NANCY (Ph.D., Marine Biology and Fisheries)
The Relationship between Carbonate Chemistry and Calcification on the Florida Reef Tract, and in the Symbiotic Reef Coral, *Acropora cervicornis* (May 2013)

Abstract of a dissertation at the University of Miami.

Dissertation supervised by Professor Chris Langdon.
No. of pages in text. (164)

Increasing atmospheric carbon dioxide (pCO_2) dissolves in the ocean, decreasing the calcium carbonate saturation state ($\Omega_{aragonite}$) and creating conditions unfavorable for calcification (G) in reef-building corals. Understanding the effects of ocean acidification on coral reefs requires a robust description of the relationship between Ω and calcification (Ω-G) at both the reef scale and at the organismal scale. To evaluate the Ω-G relationship on the reef, we conducted repeat surveys across 200 km of the Florida Reef Tract over a 2 year period. Results showed that net community calcification switches from positive in the summer to negative in the winter, indicating net dissolution and revealing that the reef tract is currently straddling the tipping point between reef growth and loss. To evaluate the Ω-G relationship at the organismal scale, we grew *Acropora cervicornis* under six CO_2 levels, 2-3 times more than typically achieved in laboratory settings. The associated Ω stretched from current levels to highly undersaturated seawater, creating a robust test of linearity of the Ω-G relationship. Our results show that the Ω-G relationship is linear and maintained even in highly undersaturated seawater. The effect of pCO_2 on calcification was also strongly mediated by heterotrophy, which significantly alleviated the effect of ocean

acidification at all pCO_2 levels. The obligate symbiont, *Symbiodinium microadriacticum*, also showed a significant response to increasing pCO_2 and declined in density in both corals in the laboratory (*A. cervicornis*), and in corals at natural CO_2 vents in the South Pacific (*Acropora millepora* and *Pocillopora damicornis*). This dissertation demonstrates that while heterotrophy can offset a significant portion of the negative effects of ocean acidification, coral calcification still declines in direct proportion to reductions in Ω. At the community level, evidence is presented that calcification on the Florida Reef Tract exists near the threshold for net carbonate accretion. Thus, while corals can utilize heterotrophic sources of nutrients to alleviate the effects of ocean acidification, it is unlikely to translate into net reef growth in the natural environment, where net annual dissolution is already occurring.

This thesis is dedicated to my husband, Scott Alexander Smith.

For being the one person who always believed I could do everything I said I could.

To my parents:

I am grateful for setting an example of strong work ethics balanced with perspective.

To my children:

I am grateful for making my life enjoyable,

and reminding me how much I have left to learn.

ACKNOWLEDGEMENTS

My committee:

Dr. Chris Langdon, Dr. Diego Lirman., Dr. Andrew Baker, Dr. Martin Grosell and Dr. Joan Kleypas

Laboratory and field support:

Katharina Fabricius, Sven Uthicke, Craig Humphrey, Ross Cunning, Remy Okazaki, Rebecca Albright, Jay Fisch, Carolina Mor, Alyson Venti, Erica Towle, Paul Jones, Rachel Pausch, Marc Fruitema

Scott Alexander Smith, for never-ending sacrifice and blanket approval for my desire to achieve my ambitions,

Rachel Pausch, for being the most talented and dedicated partner, and making the science fun.

Remy Okazaki, for being a great role model and a willing participant for intellectual debate.

Sean Bignami, for being an active partner in the RSMAS community with me, and a good friend.

Gary Hitchcock, for laboratory support and technical advice.

Chris Kelbe, for laboratory support and guidance.

Larry Brand, for laboratory support and guidance.

Tom Capo, for smiling, helping out and hatchery support.

Su Sponaugle, Sharon Smith, Lynne Fieber and Margie Oleksiak for recurring support and being sources of inspiration.

Funding sources:
This project was in part funded by National Science Foundation grant 0825578 to Chris Langdon and David Kadko. Additional support was provided by a University of Miami Maytag Fellowship, the Marine Science Graduate Student Organization (MSGSO) Student Travel Fund, and a Marine Technology and Science (MTS) grant.

TABLE OF CONTENTS

List of Figures

List of Tables

Chapter 1: Introduction
Corals, Coral Reefs and Ocean Acidification

1.1 Reefs in Decline

Tropical coral reefs are among the most biologically diverse and monetarily valuable ecosystems on the planet (Moberg and Folke 1999, Hoegh-Guldberg et al., 2007). However, due to anthropogenic and natural sources of degradation, coral reefs are also some of the most threatened ecosystems (Hoegh-Guldberg 2005).

The process of calcification by reef-building corals creates much of the three dimensional complexity of the reef structure (Smith and Buddemeier, 1992). Reefs are unique in that this creation of the 3-dimensional structure is done primarily by one taxonomic group, and thus provides a community that would not otherwise occur nor persist over time (Bruno and Bertness 2001). Tropical stony corals have therefore been coined "autogenic ecosystem engineers" (Jones *et al*., 1997) as the biogenic habitat they construct provides shelter for multiple species in the community (Reaka-Kudla 1996). The structural complexity produced by coral skeletons has been found to be a direct predictor of fish abundances and diversity (Hixon and Beets, 1993, Holbrook *et al*., 2002, Nanami and Nishihira, 2004) as well as providing critical refuge for a multitude of invertebrates (Idjadi and Edmunds, 2007).

However, the calcium carbonate produced by corals and other organisms is also continually degraded by biological and physical erosion. Biological erosion occurs through the actions of multiple organisms, such as parrotfish, echinoids, boring sponges, polychaete worms and endolithic algae (Hughes *et al*., 2007, Andersson and Gledhill 2012). Microbial remineralization of organic matter can act indirectly by driving pore

water pH to ranges of 7.0-7.4 (Walter and Burton 1990) which is corrosive to calcium carbonate. These biological processes can be further modulated by physical erosion, through tidal flushing and wave energy, to create substantial rates of reef erosion (Hoegh-Guldberg 2005). Thus, both live coral cover and rapid calcification are required to maintain net limestone accretion across the reef (Kleypas *et al*., 2001).

Coral reefs have declined substantially across the globe. Levels of live coral cover have been reduced by ~30% world-wide due to changing conditions surrounding corals, such as increasing coastal sediment, nutrient run-off, disease, and over-harvesting (Wilkinson *et al*., 2000; Bruno and Selig, 2007). The remaining reefs typically exhibit reduced hard coral abundance and diversity (Fabricius *et al*., 2005). While degradation of coral reefs has effectively decimated about one fifth of the worlds reefs (Wilkinson, 2008), Caribbean reefs have experienced multiple stressors that have left them particularly degraded (Gardner *et al*., 2003). Gardener at al., (2003) estimate that there has been an 80% reduction in relative coral cover over the last thirty years in the Caribbean and current coral cover estimates in Florida range from only 2% to 12% (5% Burman *et al*., 2012; 3-12% Palandro *et al*., 2008; 2-7% Soto *et al*., 2011). In addition there is evidence for the Caribbean that ~10% coral cover is the limit for positive carbonate production on reefs therefore reefs with less than 10% coral cover would be at risk for erosion rates being higher than rates of reef growth (Perry *et al*., 2013).

1.2 Ocean Acidification and Carbonate Chemistry

A near-future challenge for coral reefs is the increasing levels of carbon dioxide in the atmosphere and its effect on the chemistry of our ocean. Atmospheric carbon dioxide conditions (pCO_2) have increased from 280 μatm in preindustrial times to over 380 μatm currently. By the end of this century, pCO_2 levels are predicted to more than double relative to preindustrial levels due to human activity (Solomon *et al*., 2007). Approximately one quarter of the pCO_2 produced by human activity is being absorbed in the ocean (Sabine *et al*., 2004) producing carbonic acid that rapidly disassociates causing a reduction in seawater pH (Caldeira and Wickett, 2005), coining the term "Ocean Acidification" (OA). While seawater is naturally buffered against changes in pH, the buffering occurs at the expense of carbonate ions; the decrease of which lowers the carbonate mineral saturation state (i.e. aragonite, calcite). The aragonite saturation state (Ω_{arag}) is defined as:

$$\Omega_{arag} = \frac{[Ca^{2+}] \cdot [CO_3^{2-}]}{K'_{arag}}$$

where K'_{arag} is the apparent solubility product of the mineral and varies slightly with temperature and pressure. Values of $\Omega_{arag} > 1$ indicate supersaturation whereas $\Omega_{arag} < 1$ is undersaturated. Throughout the remainder of this dissertation, saturation state (Ω) refers the saturation state of aragonite (Ω_{arag}) as it is the principal form of calcium carbonate in reef-building corals. Current surface waters in the ocean average 4.02 ± 0.2 (SD) with respect to Ω (Kleypas *et al*., 1999) with considerable variation by latitude

(Caldeira and Wickett, 2005) and in coastal reef regions (Ω 2.84-4.24; Shamberger *et al*., 2011, Gattuso *et al*., 1996).

1.3 CO_2 Predictions and Connections between Carbonate Chemistry and Reef Growth

Atmospheric carbon dioxide (pCO_2) concentrations have risen at a rate that is at least 10, and possibly 100 times, faster than at any other time in the past 420,000 years (Falkowski *et al*., 2000). Estimates of future pCO_2 levels suggest increases from 380 μatm currently, to over 900 μatm by the end of this century (Figure 1.1; Caldeira and Wickett, 2005). The Fourth Assessment Report (AR4) released by the Intergovernmental Panel on Climate Change (IPCC) provides six models (A1FI, A1T, A1B, A2, B2, B1) formulated using the Special Report Emissions Scenarios (SRES). Models differ by their use of different drivers, population projections and economic/technological developments (i.e. alternative sources of energy). For instance the A1 projections include very economic rapid growth and a global population that peaks mid-century and then declines. Scenario A1B is a middle of the road scenario and includes the balanced usage of fossil and non-fossil fuel energy sources, and predicts pCO_2 of ~700 μatm by the end of the century. Model A2, which contains the delayed development of renewable energy and global population growth and economic trends that are similar to current trajectories represent some of the higher pCO_2 estimates and result in almost 1000 μatm by the end of 2100 (Figure 1.1). In any scenario, the rapidly increasing pCO_2 levels are considered inevitable, and are already being detected (Wei *et al*., 2009)

Using a mean pH concentration in the ocean of 8.1 in 2000, increased pCO_2 translates into a decline in pH by almost 0.3 units in scenario A2 or 0.2 units in scenario B2 (Figure 1.3; Caldeira and Wickett, 2005). The corresponding reduction in carbonate ion concentration is ~60% per 0.2 pH units in oceanic waters, and is one of the best correlatives to reduced calcification rates of tropical scleractinian corals (Langdon *et al*., 2000, Schneider and Erez 2006, Marubini *et al*., 2003, Hoegh-Guldberg 2005). Coral reefs are currently not found in regions where the annual average $\Omega < 3.3$, although this may in part be due to lower temperatures and less light penetration which are strongly correlated with Ω (Kleypas *et al*., 1999b). Models of future Ω indicate that coastal waters in some reef regions may become marginal for coral calcification as soon as 2040 (Kleypas *et al*., 2006). By 2100, mean average Ω is predicted to be under 3 under all major scenarios (B1, A1b, B2, A2; Figure 1.3), indicating that reefs may rapidly decline in the acidifying ocean.

Concerns have been raised that ocean acidification could cause reefs to transition from net carbonate production to net erosion (Hoegh-Guldberg, 2005; Andersson *et al*., 2009; Silverman *et al*., 2009). Models of future carbonate production hinge on the experimentally derived relationship between aragonite saturation state and calcification (Ω-G). Based on physical chemistry, inorganic calcification ceases in undersaturated water ($\Omega<1$) and calcium carbonate production may decrease by as much as 40% by the year 2100 (Andersson *et al*., 2003, 2005; Buddemeier *et al*., 2004) and 85-100% by the year 2300 (Andersson *et al*, 2005, 2007). As the net accumulation of carbonate on the reef declines, dissolution could exceed the production of carbonate, creating drastic

consequences for their function as coastal ecosystems (Hoegh-Guldberg, 2005; Andersson *et al*., 2009; Silverman *et al*., 2009).

1.4 Ocean Acidification Effects on Scleractinian Corals

The number of studies devoted to the potential impacts of OA on corals have risen over the past several years. Growing experimental evidence suggests that numerous biological and pysiological process will be impacted; reproduction (Holcomb *et al*, 2011), early life hisotry stages (Albright *et al*., 2011, Nakamura *et al*., 2011) and bioerosion rates (Tribollet *et al*., 2009). In addition, the obligate coral symbiont, *Symbiodinium microadriacticum*, has been found to respond to increasing ocean acidification (Anthony *et al*., 2008), with declines in symbiont density and changes in gene expression, photosynthesis and respiration (Kaniewska *et al*., 2012).

Reductions in coral calcification rates due to decreased Ω occur independently of coral morphology, and across genera, (e.g., *Stylophora, Acropora, Porites, Galaxea, Turbinaria* and *Pavona*), suggesting that the effects of reduced Ω will have reef-wide impacts. Signs of acclimation to lowered Ω have not been detected in short-term experiments (i.e., days) (Marubini and Atkinson 1999) or long-term experiments (i.e., years; see Langdon *et al*., 2000).

The rate of $CaCO_3$ precipitation in corals is typically directly proportional to Ω (Marubini *et al*., 2001; Langdon *et al*., 2000; Chan and Connolly, 2012). A direct relationship has been demonstrated between Ω and calcification rate across a reef in both long-term (i.e., years), large-scale experiments (Langdon *et al*., 2000), as well as in smaller, short-term (i.e., weeks) experimental studies (Marubini and Atkinson, 1999,

LeClercq *et al*., 2000, Marubini *et al*., 2003, Langdon and Atkinson, 2005). However recent experimental work using pCO_2 levels associated WITH undersaturation ($\Omega<1$) shows evidence of a chemical tipping point where calcification rate will decline more rapidly (Ries *et al*., 2010). Nonlinear relationships between Ω and calcification rate have been found in tropical coral larvae (Cohen *et al*., 2009; de Putron *et al*., 2011) and temperate corals (Ries *et al*., 2010), however such studies have been few and it is unknown if other coral species or life history stages will exhibit similar relationships in undersaturated waters.

Coral calcification is complex, in part because it can be energetically enhanced by both heterotrophy and autotrophy (Odum and Odum, 1955; Muscatine and Porter, 1977). Autotrophy by photosynthetic dinoflagellates from the genus *Symbiodinium* augments the carbon supply to the host, providing 70% or more of the daily carbon requirements (Muscatine, 1981). Corals also obtain carbon through heterotrophic feeding from a variety of sources such as zooplankton (Palardy *et al*., 2005), suspended particulate matter (Anthony, 1999), dissolved organic matter (Trench, 1974), and bacteria and pico- and nanoplankton (Bak *et al*., 1998;, Houlbréque *et al*., 2004b). The role of the micro-diet is now known to play an important role in heterotrophic feeding, and can amount to 84-94% of the total carbon and 52-85% of the total nitrogen ingested by coral (Houlbréque *et al*., 2004b). In addition, feeding has been shown to play a strong role in determining the total energy budget even in high light when photosynthetic rates are high, suggesting that the two processes (heterotrophy and autotrophy) mutually enhance each other (Hoogenboom *et al*., 2010),

Reductions in calcification rate due to ocean acidification are variable, with studies ranging from 15-54% declines (Kleypas *et al*., 2006). Some of this variability is likely due to differences between feeding regimes within experiments, as food provision that is not sufficient is suspected to alter physiological responses in hosts and symbionts (Hoogenboom *et al*., 2010). Early ocean acidification studies occurred without consideration of symbiont dynamics and heterotrophic feeding, and it is still unknown to what degree these factors can modify the calcification declines due to increasing pCO_2 (Pandolfi *et al*., 2011). Thus, there remains much to be done to understand the declines in calcification we expect to see in our acidfying ocean.

1.5 Carbonate Chemistry Analysis and Manipulation

The following chapters present the findings of an ecosystem scale survey and experiments conducted in an outdoor seawater facility. Chapter 2 investigates the seasonal changes in seawater chemistry and benthic coastal metabolism and calcification. Chapter 3 utilizes a six level OA design to test the effects on the calcification rates of *Acropora cervicornis*. Chapter 4 investigates the effect of OA on the symbiotic dinoflagellate, *Symbiodinium microadriacticum,* in two Pacific species, *Acropora millepora* and *Pocillopora damicornis*, and one Atlantic species, *Acropora cervicornis*.

1.5.1 Carbonate Chemistry Analysis

For all surveys and experiments detailed in the following chapters, seawater carbonate chemistry was analyzed by the use of discrete water samples. Water samples

from experimental surveys were analyzed for total alkalinity (TA) and pH. TA was determined in duplicate using 40 ml aliquots in an automated, open-cell Gran titration (Dickson *et al*, SOP3b). pH is reported and determined on the total scale with an Orion Ross combination pH electrode calibrated daily at 25°C against seawater TRIS buffer (Dickson *et al*., 2007, SOP6). Water samples from ecosystem surveys were analyzed for TA, pH and dissolved inorganic carbon (DIC). A subset of surveys also had continuous shipboard pCO_2 monitoring systems. DIC was analyzed. Accuracy of TA and DIC measures was checked against certified seawater reference standards. (A. Dickson, Scripps Institute of Oceanography). All other carbonate system parameters were calculated using the program CO2SYS (E. Lewis, Brookhaven National Laboratory), with the dissociation constants for carbonate determined by Mehrbach *et al* (1973), as refit by Dickson & Miller (1987) and dissociation constant for boric acid determined by Dickson (Dickson, 1990).

1.5.2 Experimental Carbon Dioxide System

For coral growth experiments in this study, an outdoor seawater facility at the University of Miami's Experimental Hatchery (UMEH) was utilized. The facility contains twelve 60 L fiberglass aquaria, hereafter referred to as tanks. Tanks are arranged in rows of 3 in 2 meter long sections. Each tank is positioned on top of a 200 l sump tank. Tanks were exposed to natural outdoor lighting with UV filtration. Seawater from Bear Cut, Virginia Key, FL was pumped through a sand filter and 10 μm filter into a holding tank. Fresh seawater was continuously fed into sump tanks with a total turnover in the sump and coral tank of approximately once per day. The CO_2 level

of the sump tank is achieved by controlling the mixing air and pure CO_2 through mass flow controllers (Sierra Instruments) and pumping gas mixtures using Venturi injectors. Circulation to the above coral tank and in the sump tank was attained issuing 500 GPH pumps. Coral tanks have a refreshment rate of once per every 10-15 minutes with the sump tank below. Temperature was controlled by chilled water (26°C) that flowed through plastic tubing coiled in the sump tank and heating elements. Temperature controllers (OMEGA CN7500) regulated temperatures to ± 0.1°C. All tanks were monitored using a HOBO U30 data logger (Onset Computer, MA, USA) recorded temperatures for each tank every 5 minutes along with light through a centrally-located PAR sensor for light logging which provides alarms for temperature outside of the desired range. Sump tanks were darkened to prevent algal growth and coral tanks were cleaned weekly and the water discarded to prevent organic matter from building up in the sump tank. Sump tanks were cleaned before experimentation. Schematic and photographs of the system are presented in Figure 1.3.

1.5.3 Monitoring of Carbonate Chemistry Experiments

During tank experiments the carbonate chemistry was monitored randomly and continuously in any 2 of the 12 tanks and with discrete water samples in all tanks 2-3 times weekly. Real-time monitoring was conducted with a carbon dioxide equilibrator. This system uses a continuous flow of seawater that is pumped into a closed equilibrator chamber through a spiral cone spray nozzle. The fine spray that is produced by the spiral nozzle enhances the rate of gas exchange between the water and overlaying air. The overlying air is continuously pumped into a Li-Cor model (6251) infrared CO_2 analyzer to measure CO_2 concentration in the sample gases. The samples flow through

the sample cell where the CO_2 concentration is determined by infrared absorption. Calibration is done using reference gases of pure nitrogen and pure gases of known CO_2 concentrations that span the range of expected environmental CO_2 levels. Continual airflow was maintained by a small pump that drives air through a closed system. Leaks in the closed system can be identified by the movement of air through a manometer, a small water filled tube that indicates pressure differences within the equilibration chamber. Samples were dried by an inline desiccant-filled chamber and the data were continually streamed online. The continuous monitoring system was moved from tank to tank as needed. Discrete water samples were collected in 250ml polyethylene terephthalate (PET) bottles that were rinsed with sample water prior to filling with samples. Samples were taken carefully to avoid bubbles and were capped with little to no headspace. Samples were preserved using mercuric chloride (HgCl) to cease all biological activity.

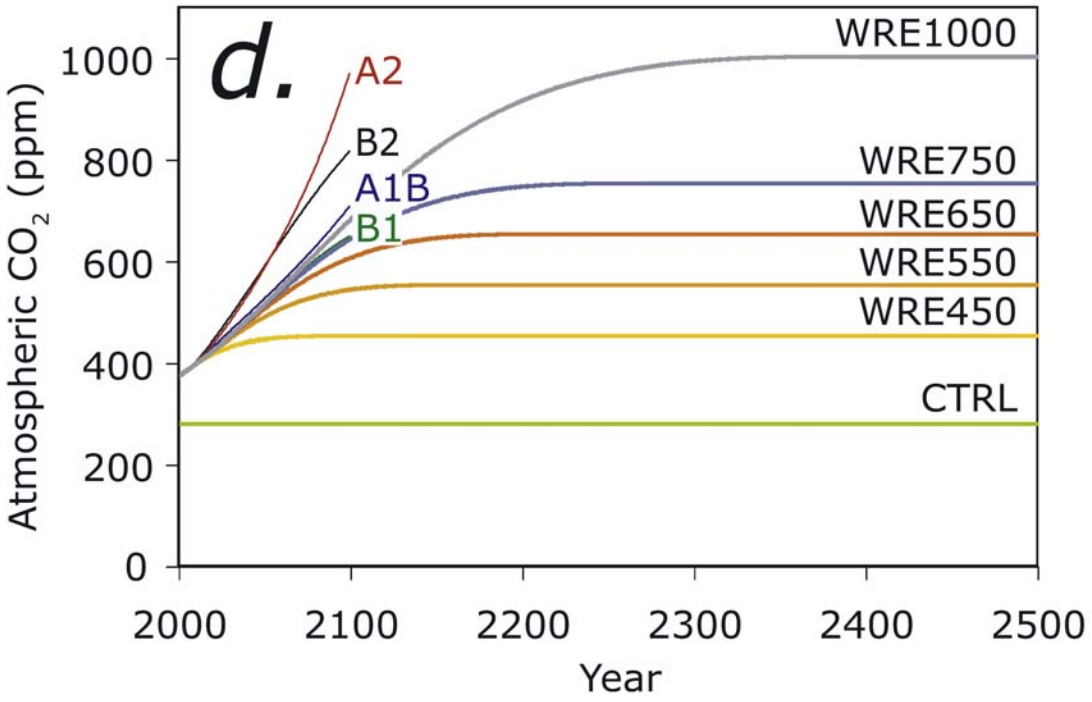

Figure 1.1. Atmospheric CO_2 contents predicted from emissions scenarios releasing 1250 to 20,000 Tg C (4580-73,3000 Pg CO_2) after year 2000 specified in the Special Report on Emissions Scenarios (SREA) A1, A2, B1, B2 pathways and specified in Caldeira and Wicket's (2005) ocean model for CO_2 stabilization scenarios. (Caldeira and Wicket 2005)

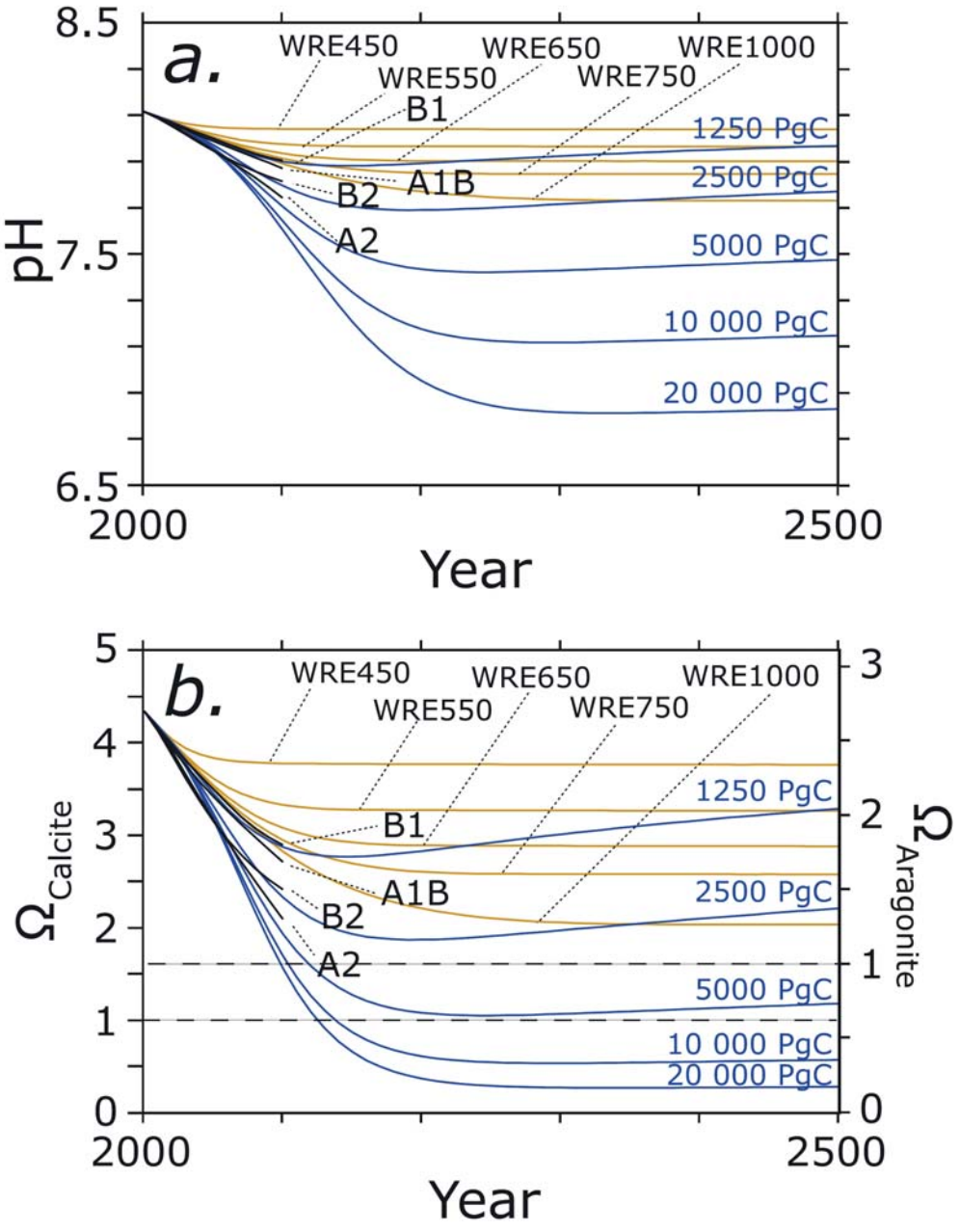

Figure 1.2. (a) Surface ocean pH and (b) saturation states of calcite ($\Omega_{calcite}$) and aragonite ($\Omega_{aragonite}$) starting from horizontal mean observed concentrations (Key *et al*., 2004). Dashed lines show calcite and aragonite saturation. (Caldeira and Wickett, 2005).

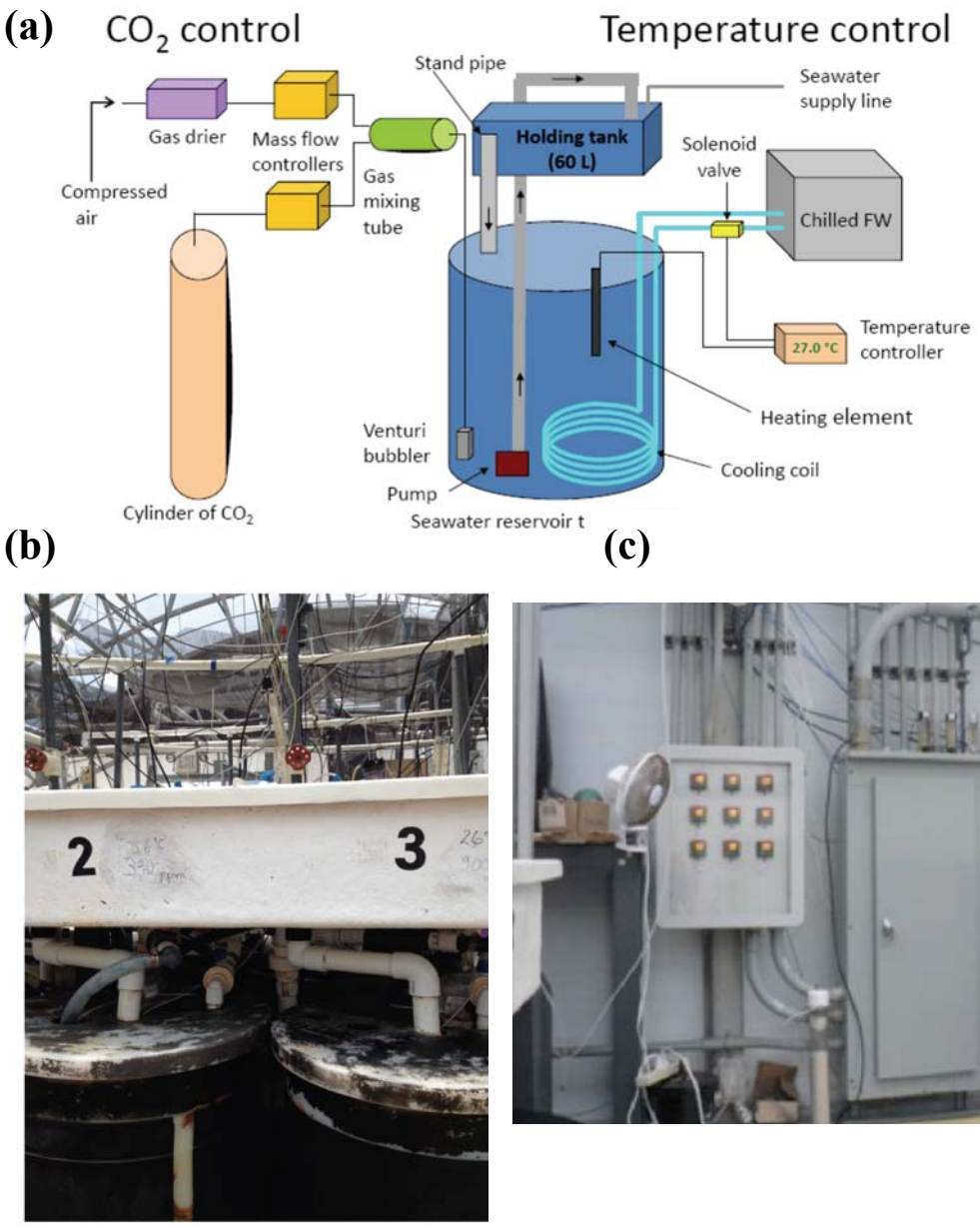

Figure 1.3. Schematic diagram (courtesy of R. Okazaki, C. Langdon and A. Baker) (a) and photographs (b,c) of CO_2 experimental system at the University of Miami Experimental Hatchery (UMEH) for culturing corals under controlled temperature and natural light. Elevated pCO_2 is achieved by mixing pure CO_2 with ambient air, then passing the gas through a Venturi injector into the 200 L sump tank. Water temperature is regulated with a sensor than turns on heating or countercurrent cooling as needed. Seawater from the sump tank circulates to the top holding tank and gravity feeds back into the sump

Chapter 2: Seasonal Dissolution and Biological Feedbacks on Carbonate Chemistry of the Florida Reef Tract

2.1 Summary

In order for a coral reef to maintain its structure in the face of natural erosive processes over time, there must be a positive balance of calcification over dissolution. Ocean acidification threatens this balance by making seawater less conducive to calcification and more conducive to dissolution. This study represents the first broad scale measure of the rates of calcification and dissolution on the Florida Reef Tract. It uses a method that provides average rates over a long temporal scale (>5 days) and calcification rates on a spatial scale of several kilometers. Seven transects in the upper, middle and low keys were surveyed seven times over two years. These repeat surveys reveal that in winter the Florida Reef Tract exhibits widespread dissolution (-19 ± 12 mmol m^{-2} d^{-1}). Average calcification on an annual basis reveals the carbonate balance for the reef tract is just slightly negative (-1 ± 8.2 mmol m^{-2} d^{-1}). While saturation states in this region (3.63) are similar to most reefs, we observe dissolution during winter months during relatively mild seasonal swings in Ω (Δ 0.46). Dissolution may be reflecting the influence of high seagrass cover and organic matter decomposition. Oxygen transport by seagrass rhizomes and the carbon dioxide produced by organic matter decomposition can both contribute to undersaturated pore water within the reef structure leading to dissolution. As ocean acidification further decreases the Ω of ocean

water entering the reef system, calcification on the reef is expected to decline along with concomitant increases in dissolution.

2.2 Background

The rapid rise in atmospheric pCO_2 is driving greater CO_2 absorption by the oceans, changing its carbonate chemistry, particularly within the surface layers (Sabine *et al*., 2004). Carbonate saturation states (Ω) and ion concentrations [CO^{2-}_3] are declining throughout our oceans in a process coined "ocean acidification" due to declines in pH. The changes in carbonate chemistry affect skeletal growth rates in corals as they build their calcium carbonate skeletons, with multiple lab and mesocosm experiments showing coral calcification declines as Ω declines (Pandolfi *et al*., 2011). Recent in situ CO_2 enrichment experiments have found that net calcification within the reef environment also declines when pCO_2 is experimentally increased (Kline *et al*., 2012). Based on these ocean acidification experiments, coral reefs globally are generally predicted to experience a significant decrease in calcification rate by the middle of the 21st century (Kleypas *et al*., 1999; Chan and Connelly 2012).

The benthic community on a coral reef can strongly modify the carbonate chemistry of the overlaying water as the community metabolism (photosynthesis/respiration and calcification/dissolution) affects the flux of carbon (e.g. Kinsey 1985). Studies of benthic community composition show that reefs with a higher proportion of photosynthesizing organisms to calcifying organisms can result in a partially compensation of the affects of ocean acidification, but the effect is dependent on the benthic community structure (Kleypas *et al*., 2011). For instance, Kleypas *et al*.,

(2011) found that modest increases in calcification (5.8%) on the reef flat could occur by a phase shift to a macroalgae dominated upstream community, which alters the carbonate chemistry of the waters subsequently flowing over the reef. Seagrasses beds, which are predicted to increase in productivity under ocean acidification (Koch *et al*., 2012), have also been identified as altering the local carbonate chemistry and possibly creating refugia for coral reefs in an acidifying ocean (Manzello *et al*., 2012). However limited field data, particularly on the feedbacks between carbonate chemistry, benthic production and reef calcification, currently constrain our ability to understand the current and future community metabolism on coral reefs. (Silverman *et al*., 2007b; Bates *et al*., 2010; Shamberger *et al*., 2011; Silverman *et al*., 2012).

Coral calcification on reefs creates a habitat of great topographical complexity that it is continuously being built and degraded. As corals build their skeletons, processes such as bioerosion, breakage and grazing, simultaneously breakdown the accreted skeleton and reef structure. Net reef growth therefore, represents the growth that is in excess of destructive processes as breakdown, export and dissolution act upon the existing carbonate structure (Glynn 1997). Loss of the reef substrate can be measured as net carbonate dissolution in reef waters, though only when the rates of dissolution are larger than those of calcification. Field measurements of net carbonate dissolution are rare and when net dissolution does occur, it is observed almost exclusively at night (e.g. Barnes and Devereux, 1984; Yates and Halley, 2006; Silverman *et al* 2007a, b; Shamberger *et al*., 2011). Currently on most reefs, the high rates of calcification during the day and lower calcification rates at night far outweigh the daily dissolution. However as ocean acidification lowers the Ω of surface ocean

water, it is predicted to reduce calcification rates, thus shifting the calcium carbonate budget on the reef closer to net dissolution (Silverman *et al*., 2009).

Understanding when a reef system crosses the threshold from one of net calcification to net dissolution is important because it provides an estimated tipping point for when oceanic conditions become unfavorable for reef growth. It is complicated, however, by the fact that reefs vary by an order of magnitude in their calcification rates (Shamberger *et al*., 2011). The rate of calcium carbonate production per unit area varies between reefs primarily due to differences in coral cover, species composition, temperature, salinity and light. Reefs that exist in colder high latitudes like Bermuda have been classified at higher risk for net dissolution than warmer lower latitude reefs because the waters have a lower Revelle factor and thus a greater capacity for CO_2 absorbance (Bates *et al*., 2010, 2011). In Bermuda, predictions of seasonal swings that may result in zero net calcification in winter have been predicted to occur in the next 10 years at a Ω of ~2.65. For reefs that have not been carefully surveyed, predicting where the calcification threshold occurs is complicated by the range of processes that affect dissolution rates. Spatially, dissolution of the reef occurs both in the framework and in the reef sediments (Andersson *et al*., 2007). Rates of dissolution vary widely as they are modulated by factors like tidal flushing, porosity and metabolic dissolution due to organic matter remineralization (Andersson and Gledhill., 2012). Furthermore, dissolution rates are enhanced by bioerosion by grazing fish, sea cucumbers and echinoderms or borers such as sponges, crustaceans, endolithic algae and marine worms (See Glynn 1997, Wisshak and Tapanila, 2008, Andersson and Gledhill 2012 for a full review). Current modeling efforts are not sufficiently

constrained to take all of these widely varying factors into account, and thus may be lacking in their ability to identify high risk systems. However recent modeling efforts to predict the shift from reef-building to reef dissolution have tried to account for differences in coral cover and temperature (Silverman *et al*., 2009: Anthony *et al*., 2011). Their results show that dissolution may occur much earlier than expected; e.g., at a pCO_2 of only 560 μatm (Silverman *et al*., 2009). In summary, reef calcification rates vary greatly due to combined biological and physical differences, which suggest that the timing of the calcification to dissolution threshold is likely to vary across reef systems.

While there is a growing body of studies on benthic calcification and metabolism, many are confined to small spatial scales and/or relatively short time scales. These studies excel at elucidating patterns, such as the relationship of community calcification to light and temperature, but challenges arise when trying to integrate hourly rates into 24-hour rates or extrapolating to weekly or annual scale. Nighttime rates of calcification can be 10 fold less than those in the daytime and may/may not exhibit dissolution that varies widely over space and time (Yates and Halley, 2006). Extrapolating across seasons or across regions should be done with caution due to factors known to strongly affect calcification and dissolution like differing hydrodynamic regimes (Falter *et al*., 2012) or shifts in the biological communities (Kleypas *et al*., 2011). Few ecosystem scale surveys have been undertaken due to the large time and monetary expense incurred. Those that have occurred in places such as in Bermuda (Bates *et al*., 2010), Puerto Rico (Gray *et al*., 2012) or Hawaii (Shamberger *et al*., 2012) have provided seasonal changes in

carbonate chemistry. Other than a few smaller scale estimates of community in the Northern Florida Reef Tract (e.g., Brock *et al*. 2006), no reef tract scale measurements of NEC have been completed for the Florida Reef Tract.

This study uses carbon chemistry changes over the Florida Reef Tract to provide spatially and temporally integrated rates of net community production/respiration and net community calcification/dissolution. By surveying across the 200 km of the reef, we can assess how biological processes of the reef community drives changes in both TA and DIC both spatially and temporally in the shelf waters of the Florida Reef Tract. The resulting broad picture of carbonate chemistry dynamics across the reef allows us to report the current status of this reef ecosystem and predict the future effects of ocean acidification in this region. Here we present evidence of a tropical coral reef where net dissolution is already occurring regularly on a seasonal scale, which suggests that the system may be operating very close to its carbonate balance. The data presented here are only from a 2-year time period but substantiates that accurately predicting the effects of ocean acidification requires first and foremost, an understanding of regional coastal dynamics and second, an understanding of the biological and physical processes that drive the carbonate chemistry in these systems.

2.3 Methods

2.3.1 Site Description

This study was conducted from May of 2009 to December of 2010 along ~200 km of the Florida Reef Tract (FRT) from north of Biscayne National Park to the Looe

Key National Marine Sanctuary (Figure 2.1). This system supports a diverse and productive community with extensive seagrass beds and patch reefs lying adjacent to the string of keys facing the Atlantic Ocean. The inshore region (< 2 km from shore) includes bands of seagrass habitat interrupted by channels. Channels occur between the keys, connecting the reef to Florida Bay, and a single channel (Hawk Channel) runs parallel to the keys in a north south direction. Water flow to and from Florida Bay and the Atlantic varies with wind and season, and has been found to intrude 1-2 km towards the Atlantic as it moves into Hawk Channel (Smith, 2002). The midshelf region (1-6 offshore) includes patch reefs, seagrass beds and hard bottom (Burman *et al*., 2012). The narrow outer shelf (~8 km offshore) is defined by the reef crest, which sits at a depth range of 2 to 20m. The average depth for the inshore stations in this study was 5.2 ± 1.6 m while offshore stations were 19.1 ± 13.9 m. Waters moving onto the reef originate from the Florida Current, which flows northward in the Atlantic Ocean. These waters are the beginning of the Gulf Stream and represent the source of seawater that moves inshore (Lee and Williams, 1999), with reported current speeds of around 2-10 cm s^{-1} at the reef crest (Sponaugle *et al*., 2005; Porter and Porter, 2002). Mid to inner-shelf currents are primarily toward the west in the Lower Keys due to prevailing westward winds, and shift toward the north in the Upper Keys due to northwestward winds (Lee and Williams, 1999; Lee *et al*., 2002).

Recent mapping surveys have shown that seagrass beds cover up to 55% of the 3,141 km^2 Florida Keys area (Lidz *et al*., 2007) and macroalgae covers up to 56% of some reef areas in summer months (Lirman and Biber, 2000). Calcifying organisms in the community include crustose coralline algae, calcifying macroalgae, foraminifera and

corals (Burman *et al*., 2012; Koch *et al*., 2012). Areal coverage of reef building corals in patch reefs, inshore and offshore reefs (excluding hardbottom areas) is estimated to be only 2% and 7% (Soto *et al*., 2011). Well known reefs such as Carysfort Reef in the Upper Keys and Looe Key Reef in the Lower Keys have coral cover up to12% (Palandro *et al*., 2008).

2.3.2 Sampling and Chemical Analysis

Water samples were collected along seven transects that extended perpendicular from shore. Each transect was composed of 3-5 stations with the innermost station 2-3 km off shore and the outermost station 8.3km offshore (Figure 2.1) Carbonate chemistry collected on the reef was classified by the collection location and averaged to describe the trends over the reef. Water classified as oceanic was collected 19.1 km from shore in the Gulf Stream. Two offshore stations in the Fiesta Key and Looe Reef transects that were 13-14 km from shore where also classified as having oceanic water, when the properties of samples collected matched those of the Gulf Stream waters.

Discrete water samples were collected from approximately 2 m depth in 250 ml polyethylene terephthalate (PET) bottles from either the flow through system or the CTD along with temperature and salinity aboard the *R/V F. G. Walton Smith* Oceanographic Vessel. Samples were poisoned with 150 µl mercuric chloride to halt biological perturbation. The carbonate chemistry of the samples was determined based on total alkalinity (TA), pH, and total dissolved inorganic carbon (DIC) analyses performed in the Langdon lab at the Rosenstiel School of Marine and Atmospheric Sciences. TA was determined in duplicate or triplicate (30-40 ml per analysis) by

potentiometric titration with HCl using an automated open-cell temperature controlled Gran titration. Certified Reference Materials were used for calibration and were within ± 2.4 μmol kg^{-1} of certified TA values reported by A. G. Dickson (http//www.dickson.ucsd.edu, Dickson *et al*., 2003). pH was determined on the total scale using an Orion Ross combination pH electrode calibrated at 25°C using a seawater TRIS buffer (Dickson *et al*., 2007, SOP6). DIC was analyzed by coulometry (Dickson *et al*., 2007, SOP6) coupled to a Single Operator Multi-parameter Metabolic Analyzer (SOMMA) and using an Apollo SciTech DIC analyzer (AS-C3, Apollotech, USA). Precision of the SOMMA-Coulometer system was 0.2% while the Apollo SciTech averages a precision of ~0.5%. In addition, an underway pCO_2 analyzer system was used shipboard with a seawater equilibrator through NOAA's Ships of Opportunity (SOOP) program. The resulting pCO_2 data provided another carbon system parameter to calculate and verify the accuracy of the TA, DIC and/or pH measurements. DIC, TA, pH, pCO_2 (when available), temperature and salinity were used to calculate Ω, HCO_3^-, CO_3^{2-} and CO_2 using CO2SYS (Pierrot *et al*., 2006) with dissociation constants for boric acid and K1 and K2 from Mehrbach *et al*., (1973) refit by Dickson and Millero (1987), KSO_4 from Dickson 1990 and pH on the total scale. Air-sea CO_2 fluxes were not measured and there was no correction for gas exchange occurring between offshore or inshore stations. Values reported here represent the average of both the direct and indirect methods of obtaining the carbonate chemistry of the system. By measuring multiple parameters of the system and comparing the results to calculated values, we were able to achieve better quality control and higher confidence in our results.

2.3.3 Calculation of Production and Calcification Rates

Net ecosystem calcification (NEC) was calculated by the change in alkalinity between oceanic and coastal stations using the alkalinity anomaly technique (Smith & Key 1975). The formation of 1 mol of $CaCO_3$ decreases seawater TA by 2 mol and DIC by 1 mol. Thus the change in TA and DIC in water moving over the benthos serves as a measure of the integrated processes of calcification and dissolution. Inshore is defined as stations that were less than 1.6 km from land while offshore stations were greater than 3.0 km from land. The average depth of inshore stations used for primary production and calcification calculations was 5.2± 1.6 m while offshore stations had an average depth of 19.1 ± 13.9 m. The average distance from shore of samples that were categorized as oceanic was 12.7 km. These samples were from both the Gulf Stream and from stations having virtually the same temperature and TA as Gulf Stream waters. Assuming a well-mixed water column over the benthos, net ecosystem calcification (NEC) in units of mmol $CaCO_3$ m^{-2} d^{-1} was calculated by:

Equation 1:
$$NEC = \frac{(-\frac{1}{2}\,\Delta nTA * \rho * h)}{\tau}$$

where, ΔnTA is the difference in salinity normalized total alkalinity between the oceanic stations minus the reef station, ρ is seawater density, h is water depth, and τ is the water residence time.

Similarly, net community production (NCP) in units of mmol C m^{-2} d^{-1} was calculated through its effect on dissolved inorganic carbon minus the effect of calcification on dissolved inorganic carbon and accounting for the depth (h), density (ρ) and residence time (τ).

Equation 2: $$NCP = \frac{-(\Delta nDIC - \frac{1}{2}\Delta nTA)\rho * h}{\tau}$$

We use the oceanic stations as reference, rather than the outermost reef points along each transect, to ensure that the difference in calculated TA or DIC reflects the full NCP and NEC that has occurred during the transit of water across the reef tract. The height or depth of the seawater used is the average for each station over all cruises to reduce the effect of any slight fluctuations in bottom morphology. Density was calculated using standard equations based on temperature, salinity and pressure. For each calculation of NCP or NEC, the residence time of the waters at that station is used for the NCP/NEC rate for that station. The values of τ at each station were provided by a David Kadko (University of Miami), using a novel Be-7 technique (described below).

2.3.4 Residence time

Residence time was measured on 5 of the 7 cruises for a total 33 times on 15 different stations across the reef tract during 2009 and 2010 (Table 2.5). Inshore stations were measured a total of 15 times and offshore stations were measured a total of 14 times over the two years. The method used to estimate reef water residence times is

based on the difference in ^{7}Be activities between off shore and reef waters. ^{7}Be is a naturally occurring, cosmogenic radionuclide whose decay (t½ = 53.3 days) provides a timescale suitable for reef environments with residence times ranging from a day to several weeks. ^{7}Be enters the ocean via precipitation and is subsequently homogenized within the surface mixed layer (Kadko and Olson, 1996). Of relevance to the present application, the open ocean inventory of ^{7}Be is diluted throughout the mixed layer, while the same inventory over the reef is concentrated on the shallow reef platform. This results in higher ^{7}Be activities over the reef as compared to the offshore water. The persistence of this contrast in ^{7}Be activity between the open-ocean and reef platform can be used to estimate the residence time of water over the reef. For example, a high flushing rate, or short residence time, would tend to diminish this contrast in ^{7}Be activity whereas a long residence time would result in a higher contrast between the ocean and the reef. The ^{7}Be method has been vetted during use in Bermuda and found to be comparable to the salinity method of calculating residence time (Venti *et al*., 2012). This method is appropriate for determining rates occurring over timescales of days to months, thus providing a suitable tracer for a model estimating residence times in dynamic reef environments (Moran *et al*., 2003).

With no river or ground water input, there are two sources of ^{7}Be to the reef: (1) rainwater input, and (2) flushing with offshore water, and three loss terms: (1) radioactive decay, (2) flushing to offshore water, and (3) particle removal. The resolve the net flushing rate, we measured or estimated the other inputs and outputs. Atmospheric flux of ^{7}Be was estimated from rainwater samples collected from Virginia Key, Florida. Radioactive decay is a known rate. Estimating the particle removal

required a second tracer, thorium-234 (^{234}Th), to resolve the model for estimating residence time (See Venti *et al*., 2012). ^{234}Th is a short lived (t½ = 24.1 days) particle reactive radionuclide. Disequilibria between ^{234}Th and its parent ^{238}U have often been used as a tracer of particle dynamics in marine environments (e.g. Muir *et al*., 2005).

To determine ^{7}Be seawater at the sample sites, 200 l of surface water were filtered through iron impregnated acrylic fibers (Lee *et al*., 1991). Samples were analyzed for ^{7}Be using a low background germanium gamma detector by integration of its peak at 478KeV. Atomic absorption analysis of stable Be in the precipitate determined the overall chemical yield (Kadko, 2000). Particulate matter was filtered from approximately 200 l of reef water using GF/F under vacuum and analyzed for both ^{7}Be and ^{234}Th. ^{234}Th was analyzed on particle samples, as well as 10 l seawater samples to account for the scavenging of ^{7}Be by particles in the water column.

2.4. Results

Cruises occurring in October (n=2) and December (n=2) showed similar carbonate chemistry and community metabolism trends, thus they are grouped together for discussion as "winter". The three cruises in April, May and August have also been grouped together and are discussed as "summer" data. Any departures from the trend by transect or within season are discussed in the results section below.

2.4.1 Total Alkalinity and Dissolved Inorganic Carbon

In the summer, salinity normalized total alkalinity (nTA) decreased by an average of 70 ± 47 μmol kg^{-1} (standard deviation) as water flowed inshore and benthic

calcification occurred (Figure 2.2). The average decrease in salinity normalized dissolved inorganic carbon (nDIC) during summer months was 106 ± 64 μmol kg^{-1} (standard deviation) due to photosynthetic drawdown of pCO_2. The combined effect of photosynthesis-respiration and calcification-dissolution on the seawater chemistry over all summer months is summarized in Figure 2.2 with examples of trendlines that would occur solely from the processes of photosynthesis (slope = 0.0) or calcification (slope = 2.0) in isolation of one another.

Across all sites, the slope of the summer community metabolism line in Figure 2.2 is 0.56, excluding 2 extreme outliers for the following reasons. On 1 of the 7 cruises, two southern stations (one at Bahia Honda and the other at Looe Key) display extremely low nDIC values of 1743 & 1788 μmol kg^{-1} which were also associated with hyper saline conditions (37.2 and 37.7). We suspect these inshore stations were impacted by water emerging from between the Keys, which underwent an extended period of evaporation, however residence times were not collected during this cruise and the source of this water is not known.. This hypothesis is supported by the normal salinities (36.2 and 36.0) of the two nearest stations closer to the ocean, which are indistinguishable from the average cruise salinity of 35.9 ± 0.2. These neighboring stations also have normal nDIC values in the 1920 to 2050 range. Thus, the slope of 0.56 without the outliers more accurately portrays the trend on the reef tract of all 7 transects and 7 cruises.

In winter, the inshore nTA increased relative to offshore water by an average of 19 ± 57 μmol kg^{-1}. This indicates net dissolution of calcium carbonate and a high degree of spatial variability (Figure 2.2). In addition, winter inshore nDIC increased

inshore relative to offshore water by an average of 53 ± 63 μmol kg^{-1}, which indicates net respiration. Oceanic waters, i.e., Gulf Stream water and stations that were far enough from shore (>10 km) and over deeper portions of the shelf (>80 m) that their water chemistry did not differ from oceanic water samples, also exhibit slight seasonal oscillations. Average nTA and nDIC in oceanic waters in summer were 2304 ± 10 μmol kg^{-1} and 1995 ± 20 μmol kg^{-1} while winter values were slightly lower at 2287 ± 22 μmol kg^{-1} and 1970 ± 19 μmol kg^{-1} (average ± standard deviation).

2.4.2 Aragonite Saturation State

The calcium carbonate saturation state is defined as:

Equation 3: $$\Omega = [Ca^{2+}][CO_3^{2-}] / K_{sp}$$

where K_{sp} is the solubility product constant specific to the $CaCO_3$ mineral phase, such as calcite or aragonite. Because $CaCO_3$ production on the Florida Reef Tract is dominated by aragonite producers, we present our analyses relative to the aragonite saturation state (Ω).

Ω shows seasonal and spatial patterns. There is a clear trend in the onshore to offshore Ω values that reverses by season (Table 2.1), but there is no consistent north to south trends. Seasonally, the winter had a low average Ω of 3.41 ± 0.04 (± standard deviation) while the summer had a higher average Ω of 3.87 ± 0.12. In winter, inshore stations (<1.6 km) had an average Ω of 3.38 ± 0.21 while offshore stations (>3.1 km from shore) had higher Ω (3.71 ± 0.09). In summer, this trend is generally reversed as

can be seen in the maps in Figure 2.4. The summer inshore to offshore trend shows higher inshore Ω in 2 of 3 cruises (See Table 2.1). In August of 2009, the average inshore Ω is lower than offshore water; however this may be influenced by a few unusually low saturation states in the southernmost stations (See Figure 2.4, WS0914 August 2009). Because the August 2009 cruise only included sampling in the lower half the reef, these values further bias the seasonal average values. The high spatial variability of Ω across the Florida Keys is visible in the maps in Figure 2.4, and demonstrates the necessity for repeated measures over time to detect seasonal trends over broad spatial scales.

Another factor impacting the summer average Ω was a probable oceanic eddy that occurred offshore in May of 2010, visible in Figure 2.4, Cruise WS1007. Evidence of an eddy was detected in offshore waters by the crew of the *R.S. Walton Smith* oceanographic vessel during our cruise (Personal communication). During this cruise, high Ω states occurred across the reef tract. The eddy may have influenced the flow of water on the reef, as the highest saturation states at Pennecamp were also associated with higher than normal residence times of 7 and 9 days compared to the reef average of 5.7 days. Longer residence times could contribute to the high Ω observed by increasing the period over which the benthos can influence the carbonate chemistry of the overlying seawater..

The Ω of oceanic waters entering the reef varies naturally over time, particularly with season. While the year-to-year variation in average oceanic Ω is only 0.10 (2010, n=3, Ω= 3.75; 2009, n=4, Ω=3.65), average oceanic Ω is higher by 0.26 in winter (3.78 ± 0.06, average ± standard deviation) and lower in summer (3.52 ± 0.19). Comparable

Ω ranges of oceanic water in Caribbean region (0.35) have been reported by Gledhill *et al*. (2008).

Over the Florida Reef Tract, Ω varied considerably between seasons. Table 2.2 shows the summer and winter trend by transect, and includes only stations where the residence time was measured for the calculation of calcification and production rates. On a transect by transect basis, average Ω in summer versus winter varied as much as 0.8 Ω Ω with the largest differences occurring in the upper and middle Florida Keys near Fowey Rocks, Pennecamp Park and Fiesta Key. Looe Key is an exception, with an average Ω of 3.41 in both summer and winter.

2.4.3 Residence Time

Residence times varied from a minimum of 2 days at station at Fiesta Key to a maximum of 10 to 11 days at Pennecamp Park and Marathon Key respectively (Table 2.5). Over the 2009-2010 period, however, the average residence times for each transect were remarkably uniform, from 4.4 to 6.8 days with standard deviations of 1 to 2.8 days between transects (Table 2.2). Residence times of inshore stations (1.6 km from shore) averaged 5.9 ± 2.5 days (N=15, average ± standard deviation) and were similar to those of offshore stations (5.4 ± 2.5, N=14, > 3 km from shore). Residence time on the Florida Reef Tract (averaged first by transect) was 5.7 ± 0.4 days (standard error).

2.4.4 Ecosystem Metabolism: Net Community Production and Net Ecosystem Calcification

Net community production (NCP) and net ecosystem calcification (NEC) were calculated only for cruises where residence time was measured (Table 2.2). Average production and calcification were first averaged by station, then by transect and lastly by season to avoid errors associated with unequal sampling across the stations..

Net community production (NCP) was positive in summer and negative in winter, averaging 44 ± 8 mmol m^{-2} d^{-1} and -48 ± 21 mmol m^{-2} d^{-1} respectively (average ± standard error). The magnitude of the standard error in winter is largely due to spatial differences in NCP across the Florida Reef Tract (Figure 2.5) rather than differences between years. In both 2009 and 2010 all transects experienced net community production in summer and net community respiration in winter. The processes of yearly net production and respiration were not always spatially coupled. For example, while the highest average net community production was observed at Long Key (78 mmol m^{-2} d^{-1}), the highest average respiration occurred at Fowey Rocks (-151 ± 3 mmol m^{-2} d^{-1}). The factors driving the differences between production and respiration per transect per year are unknown but likely influenced by differences in hydrodynamics, residence time and benthic community composition.

Net ecosystem calcification (NEC) on the reef mirrored the seasonal pattern seen in net community production (Figure 2.7). NEC was positive (calcification) across the entirety of the Florida Reef Tract in summer, averaging 16 ± 5 mmol m^{-2} d^{-1} (± standard error), and was negative (dissolution) in winter (-19 ± 12 mmol m^{-2} d^{-1}) (Table 2.2). Dissolution rates varied almost 10-fold with the highest dissolution rates in the north at

Fowey Rocks (-78 mmol m^{-2} d^{-1}). Calcification did occur in winter but it was temporally and spatially limited. Dissolution in the southernmost tip of the Looe Key, was observed only once, in October of 2010 (-2 mmol m^{-2} d^{-1}), and average winter NEC for this transect was 8 ± 10 mmol m^{-2} d^{-1} (Table 2.3). At Looe Key, the average summer NEC was not strongly different than that in the winter. This average included an unusually high NEC measured once in the winter (17 mmol m^{-2} d^{-1}), which may reflect either increased calcification and/or reduced dissolution. We detected no unusual temperature or weather patterns during this measurement, thus the positive NEC in winter at Looe Key is likely attributable to some other factor, such as hydrodynamics that cause lower than normal pore water dissolution. .

This study did not document a strong influence of Florida Bay waters on NCP in the Florida Reef Tract. The temperature, salinity, and production in Florida Bay are distinct from those in the Florida Reef Tract (Fourqurean *et al*., 2002), and waters from the Bay rarely interact with those of he Florida Reef Tract. . The bay is hypersaline in summer so that water intrusions onto the Reef Tract are distinguishable based on anomalous salinity readings (Porter *et al*., 1999). The magnitude and recurrence of such events tend to be sporadic in nature (Porter *et al*., 1999). We detected intrusions only twice in the 181 observations of this study, and these were omitted from analyses where appropriate (Results section 3.1). If the intrusion of water from Florida Bay waters were contributing to the net dissolution measured, we would expect that over time, higher dissolution would occur near "Channel 5" between the keys. Instead we observe even higher dissolution at Pennecamp Park (-16 mmol m^{-2} d^{-1}) where the reef and Florida Bay

are separated by the ~30km long Key Largo, generally considered a barrier between the bay and reef waters (Lidz and Hallock, 2000).

2.5. Discussion

Understanding coastal seawater carbon dynamics on coral reefs is required to both understand the role biological processes play in determining the carbonate chemistry of coastal waters and to predict the enhancement and decline of these processes under ocean acidification. As ocean acidification continues to reduce the aragonite saturation state (Ω) of oceanic waters flowing onto the reef, it could result in both reduced calcification and greater dissolution on a yearly basis. Our study illustrates that net dissolution within the reef is already occurring seasonally at Ω levels that are over saturated (3.63), increasing the risk that ocean acidification will result in the loss of net reef accretion. We observe a strong correlation between community production and calcification, where higher production is associated with higher calcification and net respiration is associated with net dissolution. It is unknown how the processes of community production might change under ocean acidification, and the subsequent effect on carbonate chemistry of coastal waters and rates of community calcification. This study presents important baseline data for the current oscillations in coastal carbonate chemistry and aids in our understanding of how ocean acidification may further impact the Florida Reef Tract.

2.5.1 Seasonality of Carbonate Chemistry

The strong summer-winter changes in total alkalinity (TA) and dissolved inorganic carbon (DIC) on the Florida Reef Tract primarily reflect changes in the underlying biological processes on the reef. As oceanic water flows over the reef, its carbonate chemistry is altered by the metabolism of the benthic community. The drawdown in nTA and nDIC during summer (Figure 2.2a) illustrate that net calcification and net photosynthesis, respectively, are active. Conversely, the increase in nTA and nDIC in the winter (Figure 2.2b) indicate that the Florida Reef Tract is undergoing both net dissolution and net respiration (Figure 2.2b).

While the processes of photosynthesis-respiration and calcification-dissolution are the primary drivers of the changes in seawater chemistry, the degree of TA and DIC drawdowns also reflects the local hydrography in this region. Oceanic water enters the reef system and generally flows inshore but also moves back and forth across the reef due to the semidiurnal tides. Since the average residence time on the reef is ~ 6 days, this means that our measured changes in TA and DIC are integrated over multiple tidal cycles that retain water over the wide reef tract before moving into Hawk channel and out of the reef system. Thus, the relatively large TA (70 ± 47 μmol kg^{-1} average ± standard deviation) and DIC drawdowns (106 ± 64 μmol kg^{-1}) that occur in summer reflect the long residence times of water on the reef tract.

In winter, DIC on the reef is frequently higher than the incoming oceanic water, indicating net respiration on the reef tract. Net respiration is likely a result of lower wintertime photosynthetic rates due to a lower light and temperature regimes, as well as wintertime declines in the benthic community biomass. Lower percent cover of

photosynthesizing organisms such as macroalgae (Lirman and Biber, 2000) and seagrasses (Fourqurean *et al*., 2001; Collado *et al* 2005) are well documented in winter months and would amplify the effects of reduced light and temperature on community photosynthesis rates.

Similarly in winter, most transects show an increase in TA relative to ocean water, indicating net calcium carbonate dissolution. Dissolution is likely occurring throughout the year, yet only emerges as a net signal in the winter when rates of calcification have declined substantially due to lower light and temperature. Total alkalinity drawdowns on other reefs such as those by the Pacific island of Palau (Watanabe *et al* 2006; Kawahata *et al*., 1997) and at the Majuro atoll (Kawahata *et al*., 1997) have exhibited TA-DIC diagrams with slopes on or near the modeled calcification trendline in Figure 2.9a. This is reflective of the stronger nTA drawdowns in these regions due to higher percent coral cover and a net photosynthesis to respiration ratio of 1.0. Comparatively, the Florida Reef Tract, excluding hard bottom areas averages ~7% scleractinian coral cover (Soto *et al*., 2011). Thus the drawdown in nTA in our plots representing net calcification is likely due to a combination of calcareous algae and coral calcification. The calcifying genera *Halimeda* alone comprises ~40% of the algal community in Biscayne National Park in the northern region of this study (Lirman and Biber, 2000). Further evidence of the wide distribution of calcareous algae species can be see in sediment analyses stretching across the 200 km long reef tract (Lidz and Hallock, 2000).

2.5.2 Ω Seasonality

The net affect of the drawdown in nTA and nDIC in summer and the increase in nTA and nDIC in winter lies along a slope of 0.53 and 0.56 in Figure 2.2a and 2.2b respectively. The figures include Ω isopleths, which show what the Ω would be at any given combination of nTA and nDIC at the seasonal average temperature and salinity. Where the slope of the nTA:nDIC relationship ("community metabolism") exceeds the slope of the Ω isopleths (slope 0.9) indicates that biologically produced/consumed carbon dioxide plays a role in changing the Ω in these waters. In summer, the slope of the community metabolism line exceeds the slope of the isopleths and represents an elevation in Ω (average Ω = 3.87 ± 0.12 (± standard error)). In winter, the community metabolism slope is less than the slope of the Ω isopleths, and represents a depression in Ω (average Ω = 3.41 ± 0.04 (± standard error). These winter-summer trends illustrate a positive biological feedback where higher production causes a DIC drawdown that elevates Ω and thus promotes higher calcification. The biological feedback on carbonate chemistry observed here is not unusual, and has been demonstrated for several coastal environments over diurnal and seasonal timescales (Suzuki *et al*., 1995; Semesi *et al*., 2009; Bates *et al*., 2010).

While Figure 2.2 shows the biological influence on coastal Ω, other factors such as temperature, salinity and pressure also contribute to fluctuations in Ω. In the definition of Ω (equation 1) K_{sp} is the temperature, pressure and salinity dependent solubility product constant. While pressure doesn't vary in the surface waters measured, the temperature and salinity fluctuate on broad spatial and temporal scales (Andersson and Gledhill, 2012). Based on CO2SYS calculations and using the maximum winter-to-

summer change in average temperature across transects of 2.8°C (25.3 to 28.1°C), temperature accounts for a shift in Ω of 0.05. Average salinity across transects ranged from 35.2 to 36.7, which could shift Ω by 0.04 units. The temperature and salinity changes thus account for only 10-20% of the observed seasonal oscillation of 0.46 Ω.

Our work demonstrates the additional challenges of predicting the impacts of ocean acidification in coastal regions. Predictions of Ω on reefs are typically made using SSA declines predicted for the open ocean, such as the 40% decline in Ω from3.85 to 2.28 when global atmospheric pCO_2 increases to 840 μatm (Feely *et al*., 2009). By comparison, Ω measured on the Florida Reef Tract ranged from < 3 (e.g. 2.63, 2.93) and to just over 4 (e.g. 4.13, 4.61) driven mostly by the benthic metabolism and long residence time of water on the reef tract. The Ω of water passing from the ocean and over the Florida Reef Tract decreased by an average of 0.18, but in winter, the average Ω decreases is as much as 0.41 as oceanic water moves over the reef. This reduction is accompanied by increased seawater pCO_2 to ~470 μatm in winter, which is substantially higher than that of the air (~390 μatm). Due to the long diffusion time of carbon dioxide in and out of seawater, carbon dioxide created by benthic processes can play a significant role on the local carbonate chemistry. Future predictions of reefs under ocean acidification necessitate accounting for the existing seasonal Ω patterns. These finding suggests the coastal environment currently represents an large and generally unaccounted for contribution to predictions of future Ω and pCO_2 levels on reefs.

2.5.3 Net Community Production (NCP)

Productivity on any given reef is determined by the proportion of bare substrate to the biomass of benthic photosynthesis per unit water passing over it. The flux of carbon in and out of the benthic community can have a dominating effect on the coastal carbonate chemistry (Unsworth *et al*., 2012). On the Florida Reef Tract, summer net community productivity (NCP) rates averaged 44 ± 8 mmol m^{-2} d^{-1} and peaked as high as 78 mmol m^{-2} d^{-1} at Long Key (Table 2.2). In winter, the Florida Reef Tract experienced net respiration, averaging -48 ± 21 mmol m^{-2} d^{-1} This low value was influenced by a particularly high respiration rate at Fowey Rocks (-151 mmol m^{-2} d^{-1}), but even upon its removal, the pattern of strong net respiration in winter remained (-27 ± 4 mmol m^{-2} d^{-1}). The NCP rates we observed are influenced by the large expanses of relatively shallow (average inshore depth of 5.2 ± 1.6 m) regions composed of sandy areas interspersed with benthic photosynthesizing organisms. Macroalgae and seagrass beds cover ~56% of the 3141 km^2 of reef tract (Lidz *et al*., 2007; Lirman and Biber, 2000). This benthic community seems to be driving the strong seasonal trends in NCP on the Florida Reef Tract, with respiration being the dominant force in the winter and high amounts of benthic photosynthesis being evident in the summer (Figure 2.5). Our results show the Florida Reef Tract to be slightly net heterotrophic, similar to what other smaller scale studies in this area have concluded (Brock *et al*., 2006).

Modeled estimates of NCP exist for the northern region of Florida off of Biscayne Bay and coincide with the Fowey Rocks and Pennecamp Park transects (Figure 2.1). These estimates utilized combined benthic incubation chambers, biotope mapping and remote sensing (Brock *et al*., 2006). Comparatively, these modeled

estimates found excess NCP rates of -47 mmol m^{-2} d^{-1} (Brock *et al*., 2006) in this region, exhibiting net heterotrophy.

2.5.4 Net Ecosystem Calcification (NEC)

The Florida Reef Tract experienced net calcification in the summer (16 ± 5 mmol m^{-2} d^{-1}) but this was balanced by slightly higher net dissolution in the winter (-19 ± 12 mmol m^{-2} d^{-1}). Integrated over the year, NEC was -1 ± 8.2 mmol m^{-2} d^{-1}. In winter, the northern reef tract experienced high dissolution rates (-78 to -12 mmol m^{-2} d^{-1}), and the southern tract experienced intermittent net calcification and dissolution (8 to -19 mmol m^{-2} d^{-1}; Table 2.2). Aside from Bahia Honda, which showed intermittent calcification and dissolution during different surveys, $CaCO_3$ dissolution in winter on the Florida Reef Tract was widespread and recurring. The highest dissolution at Fowey Rocks (-78 mmol m^{-2} d^{-1}; n=1) was matched by equally high respiration in winter (-151 mmol m^{-2} d^{-1}; n=3), indicating that wintertime decomposition of seagrass beds in Biscayne Bay may be a particularly strong source of organic matter decomposition (Moses *et al*., 2009). Net dissolution in this region has also been observed using submersible mesocosms (Yates and Halley, 2003) and modeled using Landsat imagery of the benthic community (Brock *et al*., 2006; Moses *et al*., 2009). To examine the impact of the strong dissolution at Fowey Rocks on the average for the entire reef tract, we can exclude the northernmost region (transect 1, Figure 2.1) from our averages, yet we still observe net dissolution for the Florida Reef Tract in winter (-7 ± 4 mmol m^{-2} d^{-1}). Excluding the high dissolution at Fowey Rocks, does change the annual NEC from negative (-1 ± 8.2 mmol m^{-2} d^{-1}) to positive (5 ± 4.8 mmol m^{-2} d^{-1}) but the both values

still suggest that the reef tract as a whole currently exists close to its tipping point between gain and loss of carbonate substrate.

Reports of dissolution on coral reefs are relatively rare and generally restricted to nighttime when calcification rates are very low (Andersson and Gledhill, 2012). Dissolution in reef structures and sediments tends to occur where isolated water pockets accumulate CO_2 or experience other chemical changes that substantially lower Ω_a; e.g., microbial decomposition of organic matter in the substrate (Tribble, 1993) and the action of bioeroding organisms in the reef framework (Tribollet and Golubic, 2011). The contribution of each process is difficult to isolate, however the role of bioeroder dissolution is believed to typically be higher than dissolution in the sediment (Andersson and Gledhill 2012). In the Florida Reef Tract, bioerosion occurs due to the actions of echinoderms, euendoliths (Tribollet *et al*., 2009), red algae (Walter and Burton, 1990), mollusks (Lidz and Hallock, 2000) and a high density of encrusting and excavating sponges, the latter of which occur in up to 23% of all corals (Chiappone *et al*., 2007). However there is also ample evidence of carbonate dissolution in the sediment. Carbonate dissolution is known to play a paleontological role in the Florida Reef Tract region (Stanely, 1966; Lidz and Hallock, 2000; Walter and Burton, 1990) and can also be amplified due to the biological community such as encrusting sponges and seagrass beds (Burdige *et al*., 2010).

The decomposition of organic matter and the subsequent drop in pH likely contributes to much of the dissolution observed in the sediment on the Florida Reef Tract (Stabenau *et al*., 2004). Oxidation of organic matter in reef sediments often causes anoxia in porewater and the production of carbonic acid, thereby lowering the pH to

ranges of 7.0-7.4 (Walter and Burton, 1990) and facilitating the dissolution of calcium carbonate (Sansone *et al*., 1990; Tribble *et al*., 1990). This process occurs relatively close to the overlying water and anoxic porewaters have been measured as shallow as a few centimeters from the interface (Entsch *et al*., 1983). On the Florida Reef Tract, organic matter builds up in winter following the die-off of annual seagrasses (*Halophila decipiens*) or the leaf-shedding of perennial seagrasses like *Thalassia testudium* (Zieman *et al*., 1999; Thayer *et al*., 1982). The standing stock of seagrasses has been estimated as ~ 15% less in winter (Zieman *et al*., 1999) and the extensive coverage of seagrass beds on the reef tract provides a ready supply of decomposing organic detritus (Thayer *et al*., 1982). In the summer, seagrasses also contribute to sediment dissolution in the summer by enhancing microbial respiration (Walter and Burton, 1990; Burdige and Zimmerman, 2002; Yates and Halley, 2006; Burdige *et al*., 2010), and photosynthetically produced O_2 released from seagrass roots and rhizomes produces higher rates of aerobic respiration, a process studied extensively in the nearby Bahamas Bank (Burdige *et al*., 2010). These below ground dynamics reduce the Ω in sediment banks, with Ω in the Bahamas bank dropping to 1 at depths as little as 4cm (Burdige *et al*., 2010). Thus, in addition to bioerosion processes, metabolic dissolution rates on the Florida Reef Tract are likely to be higher due to both the remineralization of organic matter and the propensity of seagrass enhanced sediment dissolution.

While the occurrence of net dissolution or calcification is independent of residence time, residence time does affect the magnitude of dissolution/calcification measured in the overlying water.. While the average residence time over the entire reef tract was 5.7 days, we observed residence times from 2 to 11 days. Thus detailed

comparisons of NEC over space and time may be influenced by differences in residence time and contribute to the spatial variability in calcification or dissolution.

Our calcification rates are similar to modeled estimates for the Caribbean region, adding to the evidence that the dissolution we measured over 2 years could be continuous and widespread (Perry *et al*., 2013). Previous work measuring calcification on the Florida Reef Tract is limited. A benthic chamber system (SHARQ) was deployed by Yates and Halley (2003) ~10-20 km from our Pennecamp Park transect. Averaging and converting the rates of Yates and Halley (2003) for comparative purposes results in an annual rate that ranges from 0.5 to 6.15 mmol m^{-2} d^{-1}. The higher average rate likely stems from the inclusion of SHARQ incubations (2 of 13 total) in higher than average coral cover (>10%). Our annual NEC rates are comparable (-1.82 to 5.0 mmol m^{-2} d^{-1}), though slightly lower, which we attribute to the lack of winter (n=1) SHARQ deployments by Yates and Halley (2003) or the larger scale of the current study. While Yates and Halley (2003) also observed dissolution, their nighttime dissolution never exceeded daytime calcification in summer deployments (n=12) or winter deployments (n=1) of the SHARQ system. The satellite-based calculations of Moses *et al*. (2009), which included the *in situ* metabolic measures by Yates and Halley (2003) estimate that the reef tract could also be undergoing net dissolution (-0.02 mmol m^{-2} d^{-1}), and further supports our findings that the reef tract is very close to a reef accretion tipping point.

Our study is unique in that it uses large-scale hydrochemical methods that measure calcification and dissolution over large time scales. Perry *et al*. (2013) also estimated calcification and dissolution rates over the scale of the Caribbean, but instead

used a scaling up technique that combined estimates of benthic species composition and cover, and limited published growth rate data. Interestingly, they predict net dissolution when coral cover in the Caribbean region drops below 10%. The percent coral cover on the Florida Reef Tract is currently about 5.3% (Burman *et al*., 2012), and our observations that show that strongly corroborates the prediction of Perry *et al*. (2013).

2.5.5 Comparison to other Reef Systems

Coral reefs in other regions tend to have low summer NCP rates (e.g., Kaneohe Bay, HI: -14.2 mmol m^{-2} h^{-1}; Tiahura Reef, Moorea: 0.1 mmol m^{-2} h^{-1}; and Yonge Reef Australia: 1.4 mmol m^{-2} h^{-1}; see Shamberger *et al*., 2012). This compares to the summertime NCP on the Florida Reef Tract of 3.7 mmol m^{-2} h^{-1} (converted from mmol m^{-2} d^{-1}) which is considerably higher. In winter, the Florida Reef Tract shows an NCP of -4.0 mmol m^{-2} h^{-1} whereas reefs in Moorea (Gattuso *et al*., 1996) and the Red Sea (Silverman *et al*., 2007a, b) range between 3.1 and 3.3 mmol m^{-2} h^{-1}. However most of these studies occur over short time scales and on small reefs, in contrast to the reef tract scale in this study. Thus while direct comparisons have less utility, our data indicates the FRT is a highly productive system in the summer that then switches to being dominated by net respiration in the winter.

Compared to other reef systems, the average summer and winter net ecosystem calcification (NEC) rates on the Florida Reef Tract are relatively low. Converting our daily rates to hourly rates as done in Shamberger *et al*., (2012) results in a summer calcification rate of 1.3 mmol m^{-2} h^{-1} and a winter dissolution rate of -0.6 ± 0.3 mmol m^{-2} h^{-1} (± standard deviation). Generally, the calcification rate on the Florida Reef Tract is

10 fold lower than reefs in the major reef tracts from Hawaii to the Great Barrier Reef (See Shamberger *et al* 2012 for review table). Rates of calcification in the 10-11 mmol m^{-2} h^{-1} range (Shamberger *et al*., 2012) occur in Kaneohe Bay, HI (Kinsey, 1985), Tiahura Reef, Moorea (Gattuso *et al*, 1993) and Yonge Reef, Australia (Gattuso *et al*., 1996). One of the few reefs with comparable calcification rates occurs in the Red Sea at Eliat reef which exhibits summer calcification rates of 2.5 mmol m^{-2} h^{-1} (Silverman *et al*., 2007a,b). Of the reef sites mentioned above, none were reported to undergo dissolution in winter (Shamberger *et al*., 2012). Nighttime dissolution makes up the majority of observations in the coral reef ecosystem (e.g. Barnes and Devereux, 1984; Yates and Halley, 2003; Silverman *et al*., 2007a, b, Shamberger *et al*., 2011). In rare occurrences, nighttime dissolution has been observed to outpace daytime calcification. Specifically, Réunion Island exhibited nighttime dissolution rates strongly exceeded daytime rates, producing net dissolution rates of -3.8 mmol m^{-2} h^{-1} (Conand *et al*., 1997). The data presented here contrasts most other reef studies as we report dissolution over a very broad spatial scale (200 km) that was collected repeatedly over a longer time frame, thereby allowing us to connect seasonal declines in calcification and production to reoccurring net dissolution.

2.5.6 Relationships between Net Ecosystem Calcification (NEC), Aragonite Saturation State (Ω) and Net Community Production (NCP)

The relationship between net ecosystem calcification (NEC) and net community production (NCP) is linear and may involve a positive feedback system. Averaging over both 2009 and 2010 showed that high NCP was significantly correlated with high

NEC, whereas low rates of NCP occurred with low NEC ($r^2 = 0.54$, Figure 2.8). These findings are consistent with several other studies from Australia (Shaw *et al*., 2012) to Hawaii (Kinsey, 1985; Gattuso *et al*., 1999). The correlation here (r^2=0.54) is higher than those reported by Shaw *et al*., (2012) and Gattuso *et al*., (1999) indicating the strong influence that NCP may have on NEC on the Florida Reef Tract. In the Florida Reef Tract, the stronger linear relationship between NCP and NEC may be attributable to the large amounts of seagrass derived organic matter. While dissolution rates are arguably contributed to by a range of factors such as bioerosion and bioirrigation, our system shows evidence of metabolic dissolution. Evidence for metabolic dissolution comes from the TA-DIC relationship that in winter was close to 1:1, indicating a link to organic matter decay (Andersson and Gledhill, 2012).

The relationship between Ω and NEC shows a weaker correlation ($r^2 = 0.31$, Figure 2.9). Over both years, NEC along the five transects trended higher in summer when Ω was high and lower (including dissolution) in winter when Ω was low (Table 2.2). We also observed, however, one instance of decoupling between Ω and season. This occurred at Looe key where the Ω was 3.4 during both the summer and winter cruise and showed similar NEC (10 ± 2 mmol m^{-2} d^{-1} and 8 ± 10 mmol m^{-2} d^{-1}) in summer and winter, respectively. The relationship of Ω and NEC measured in other studies have also been linear, such as the reef flat of Lady Eliot Island, Australia (r^2 = 0.32; Shaw *et al*., 2012) and the barrier reef in Kaneohe Bay, Hawaii ($r^2 = 0.48$; Shamberger *et al*., 2011).

The relationships between NEC, NCP and Ω can be disrupted by both physical and biological factors. For example, the positive correlation between NEC and NCP is

logical given that photosynthesis and calcification both increase with increases in light and temperature (Gattuso, 1999; LeClerq *et al*., 2002; Kleypas *et al*., 2011), but this relationship can be disrupted if stressful conditions differentially impact photosynthesis and calcification. The correlation between NEC and Ω may also vary due to different physical and biological processes that differentially impact either calcification or carbonate chemistry (e.g. Falter *et al*., 2012). While both NEC and Ω are affected by temperature and salinity, NEC is additionally strongly influenced by light, nutrients, coral cover and dissolution (Andersson *et al*., 2007). In our system, when the summer NCP and NEC are high the community metabolism leads to an increase in Ω, whereas in winter the reverse is true. This is an example of a positive feedback system where an increase in NCP elevates Ω that in turn enhances NEC; and a decrease in NCP reduces Ω that in turn depresses NEC. However this feedback does not occur across all reef systems similarly. In systems dominated by calcifiers (e.g., work done by Suzuki and Kawahata, 2004 in the southern Great Barrier Reef) the elevated calcification rates lead to an increase in pCO_2 that reduces Ω. Thus the ratio of NCP to NEC is important in determining the behavior of the carbonate chemistry on a reef system (Kleypas *et al*., 2011; Anthony *et al*., 2011).

Here we show that calcification at the community level is complex, with feedbacks that vary between reef systems. The variation between reef systems is due to the balance between production, calcification and dissolution that is a function of parameters such as carbonate chemistry, light, temperature, hydrography, nutrients and benthic community composition. The strength of local production can act to amplify oscillations in Ω as in a highly productive system such as observed here, or could have

relatively little effect in a system with lower productivity. By describing the benthic productivity of the system in unison with calcification and carbonate chemistry, we can develop a much stronger understanding of the feedbacks that control calcification and carbonate chemistry in coastal ecosystems (Andersson and Gledhill, 2012). As ocean acidification increases, utilizing measurements of net community production estimates in reef environments could aid in the interpretation of NEC to Ω relationships in different reef systems. The impact of net community production on Ω means the utility of Ω as a predictor of calcification rates may be dependant on local rates of net community production and is vital to predicting how NEC and Ω relationships differ by ecosystem and may shift differently under ocean acidification.

2.5.7 Future Implications

Our results show that dissolution occurs yearly and across a large regional scale on the Florida Reef Tract. The large scale hydrochemical approach used here uses drawdowns in alkalinity and inorganic carbon to measure the seasonal oscillations of calcification and photosynthesis on the reef. The resulting data set highlights the utility of TA:DIC diagrams to resolve the net effect of total reef metabolism on seawater Ω and the significant productivity and respiration effects on coastal Ω and community calcification. The strong impact of community production on dissolution in this system is evidence of the limits of using estimates of oceanic Ω to predict OA induced declines of calcification in coastal systems.

The threshold for calcium carbonate formation on the Florida Reef Tract as evidenced by the regression analysis of Ω to net community calcification, crosses from

calcification to dissolution at a Ω of 3.63 ± 0.16 (standard error), indicating that 3.63 is a threshold level for reef growth in this system. Strikingly, the average of Ω over 2 years of data and 7 cruises on the Florida Reef Tract is also 3.63 ± 0.33 (± standard deviation, n=173), thus the Florida Reef Tract is currently straddling it's biogeochemical tipping point. Although recent organismal studies have shown some corals can maintain calcification in undersaturated waters, this may not translate into net reef building in a natural setting where bioerosion and organic matter decomposition can actively affect the geomorphologic complexity if the reef and the Ω of the surrounding waters. The net loss of calcium carbonate represents a physical tipping point at which reefs can no longer be maintained, as the long scale persistence of corals reefs is dependent on the net production of calcium carbonate being greater than the net loss. While a longer study with increased sampling effort would be advantageous, this data set of carbonate chemistry and the biological feedbacks of the Florida Reef Tract identifies this reef region may be the first to reach a biogeochemical tipping point under ocean acidification.

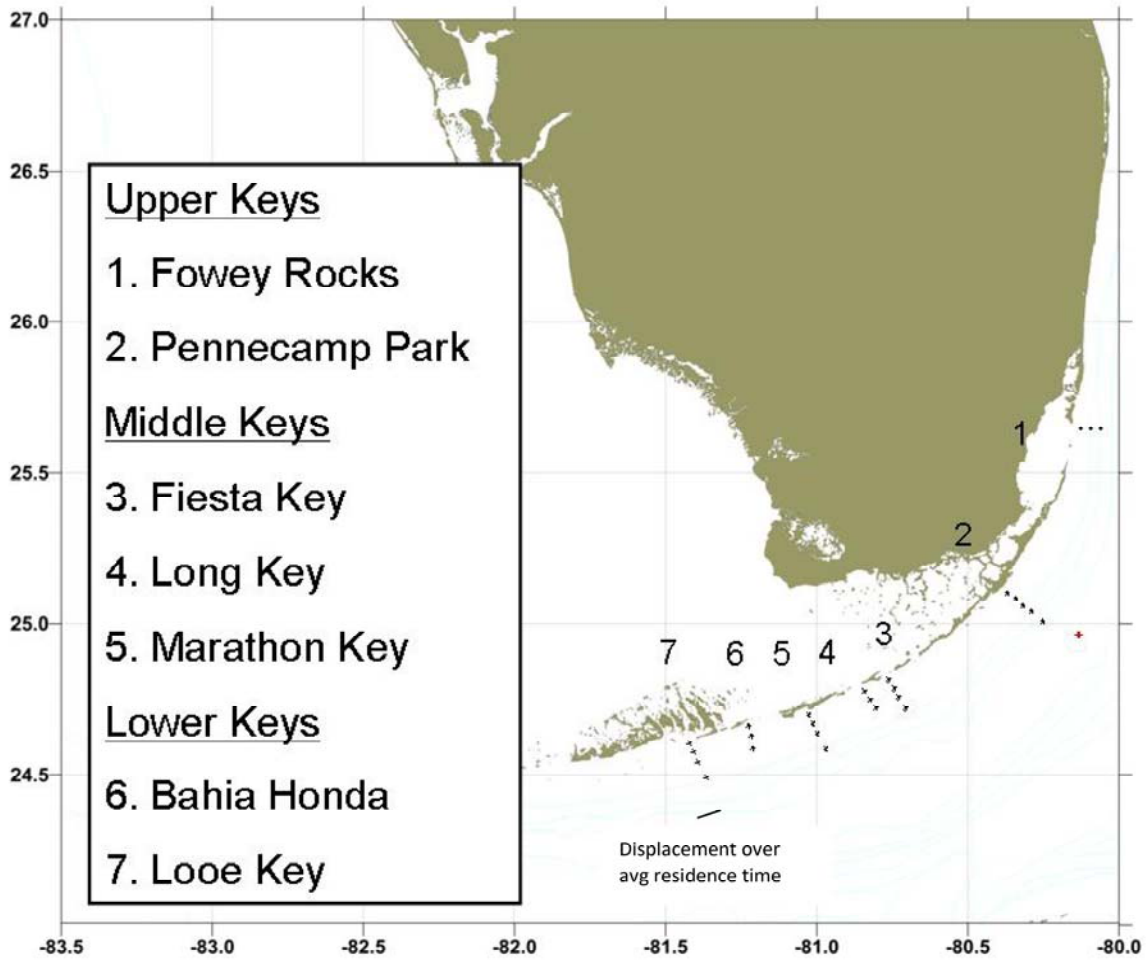

Figure 2.1. Location of the Florida Reef Tract (FRT) off the eastern coast of the southern United States. Cruises surveyed ~ 210 km from station 1 to 21.5 on 7 cruises occurring in 5/09, 8/09, 10/09, 12/09, 5/10, 10/10 and 12/10. Oceanic sample is demarcated by the red mark extending out from transect 2 where water from the Gulf Stream was collected (longitude -80.230, latitude 24.994). The chemical signal of the source water in the Gulf Stream is used to assess changes in carbonate chemistry due to coastal metabolism.

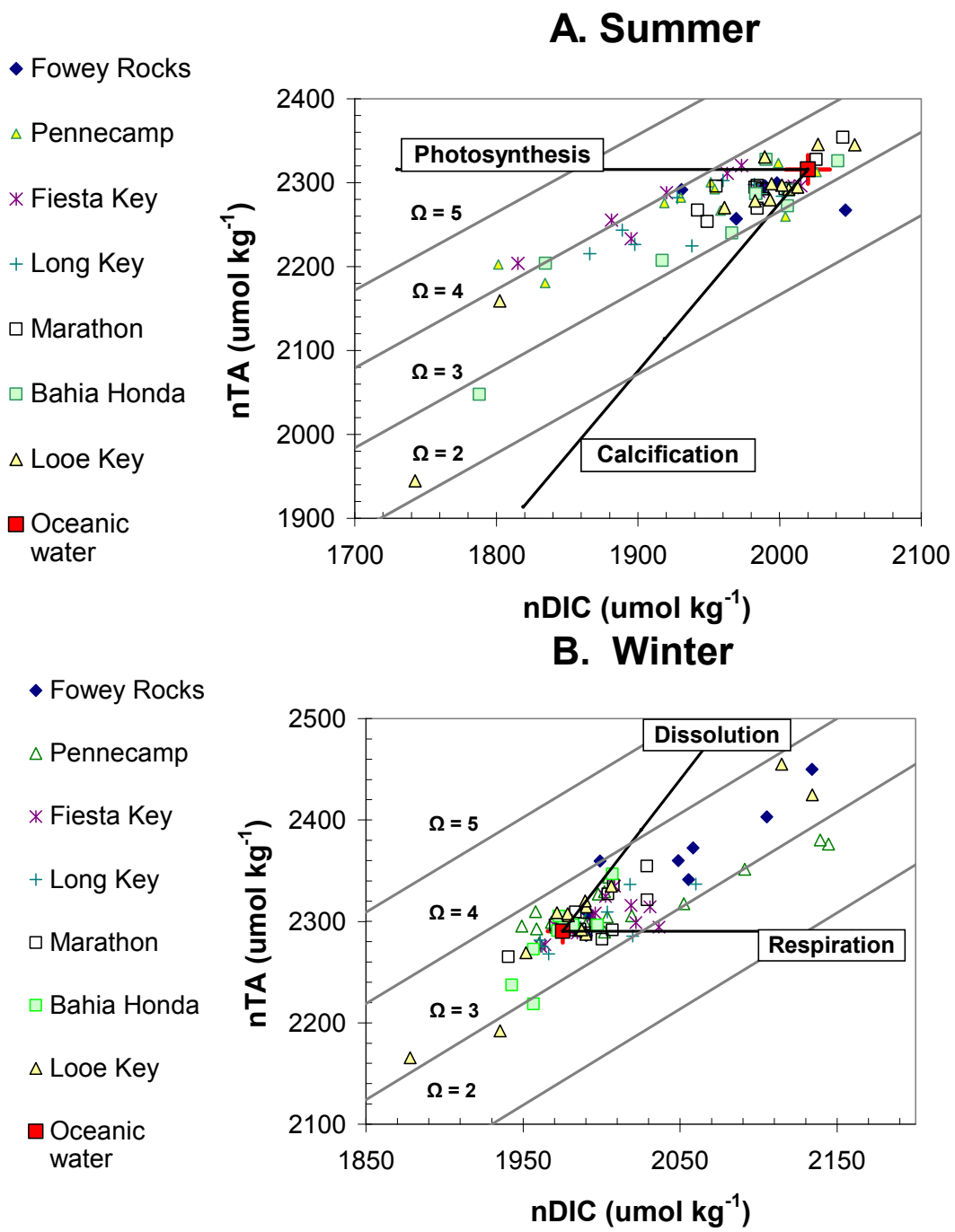

Figure 2.2. Scatterplot of salinity normalized Total Alkalinity (nTA) and salinity normalized dissolved inorganic carbon (nDIC) for each transect and the average oceanic source water (red squares) for the reef in A. summer and B. winter. Error bars on the source water are standard error of oceanic water averaged by season. Summer source water was nTA 2316 ± 17 μmol kg^{-1} and nDIC 2020 ± 16 units μmol kg^{-1}. Winter source water was nTA 2290 ± 11 μmol kg^{-1} and nDIC 1975 ± 10 μmol kg^{-1}. Legend shows transects from northernmost to southernmost.

	Salinity (psu)	Temp (°C)	Ω average	Ω inshore	Ω offshore	Ω oceanic	Δ Ω
April '09 WS0906	36.7 (n=26)	25.4 (n=26)	3.44	3.61	3.38	3.32	-0.29
Aug. '09 WS0914	36.1 (n=26)	27.4 (n=26)	3.58	3.17	3.69	3.54	0.37
Oct. '09 WS0919	**36.1 (n=30)**	**28.1 (n=30)**	**3.73**	**3.57**	**3.81**	**3.83**	**0.27**
Dec. '09 WS0923	**36.3 (n=27)**	**26.1 (n=27)**	**3.72**	**3.52**	**3.77**	**3.84**	**0.32**
May '10 WS1007	35.5 (n=26)	26.8 (n=26)	3.85	4.10	3.75	3.69	-0.41
Oct. '10 WS1018	**35.2 (n=27)**	**26.9 (n=27)**	**3.48**	**3.11**	**3.58**	**3.72**	**0.61**
Dec. '10 WS1022	**36.2 (n=16)**	**24.6 (n=16)**	**3.59**	**3.31**	**3.71**	**3.73**	**0.42**
Grand Average	**36.2 (n=178)**	**26.4 (n=178)**	**3.63**	**3.48**	**3.67**	**3.67**	**0.18**

Table 2.1. Comparison of seasonal shifts in aragonite saturation state at inshore (<1.6 km from coast), offshore (>3.0 km from coast) and oceanic (an average of 12.7 km from coast) stations. Values in bold are cruises that occurred in fall and winter months during a 2 year period (2009-2010). Average Ω for inshore and offshore columns is computed from all stations that stretch over the 7 transect measured on each of 7 cruises on the Florida Keys (See Figure 1). Oceanic Ω is the average Ω of source waters from the Gulf Stream and some of the outermost stations (See methods). Δ Ω is the oceanic Ω minus the inshore Ω per cruise.

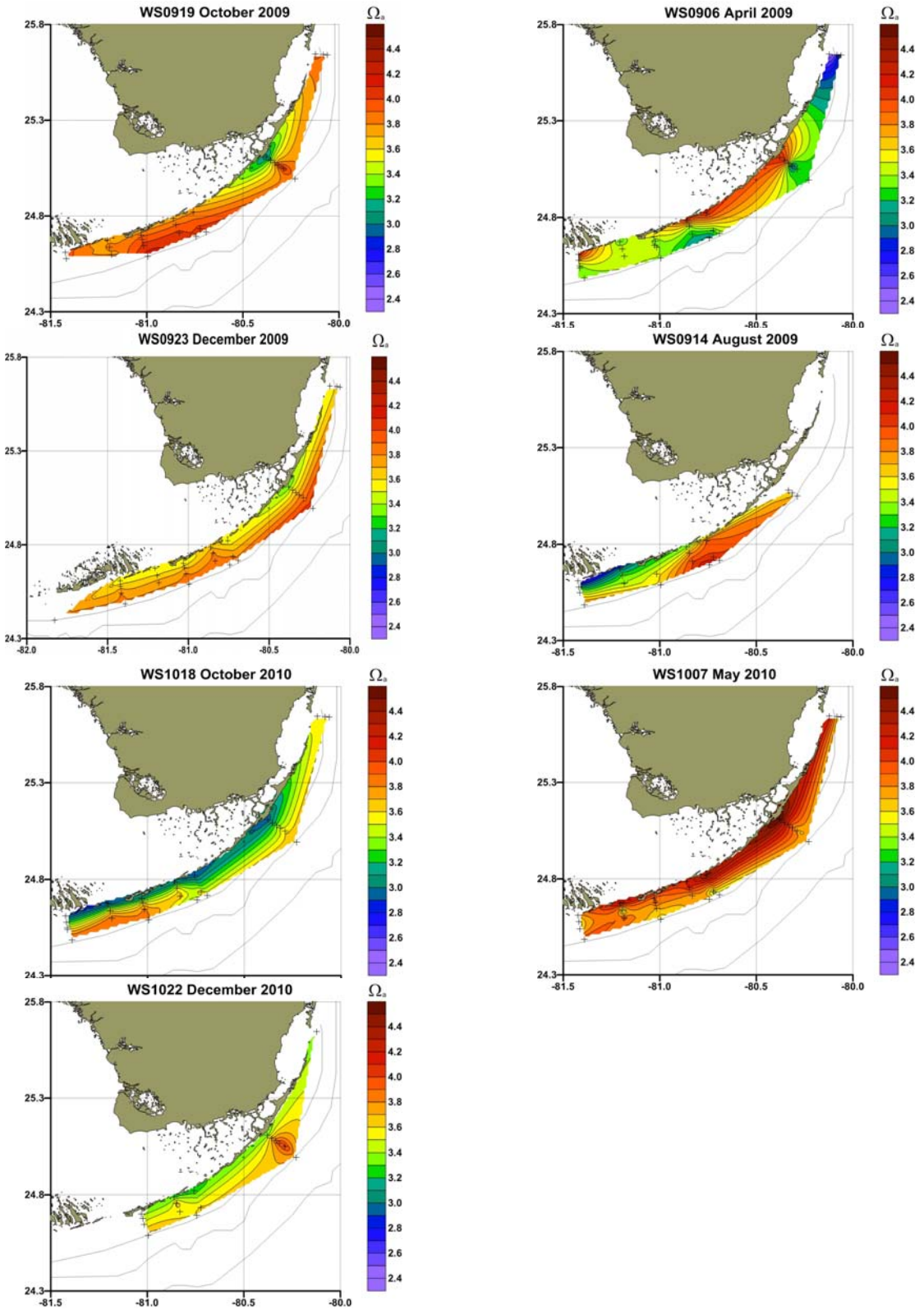

Figure 2.3. Maps of the Ω for the 7 cruises from 2009 to 2010 with the fall and winter cruises on the left and spring and summer cruises on the right

Transect	**τ (day)**	**Temp. (°C)**		**pCO_2 (ppm)**		**Ω_{rag}**		**NEC (mmol m^{-2} d^{-1})**		**NCP (mmol m^{-2} d^{-1})**	
		S	**W**	S	**W**	S	**W**	S	**W**	S	**W**
Fowey Rocks	5.0 (1.0)	26.0 (0.3)	**25.8 nd**	383 (49)	**452 nd**	3.9 (0.3)	**3.5 nd**	6 (3)	**-78 nd**	40 (47)	**-151 (3)**
Penne-camp	6.3 (2.4)	27.2 (0.7)	**25.4 (0.3)**	332 (58)	**443 (40)**	4.2 (0.4)	**3.4 (0.3)**	15 (8)	**-17 (5)**	50 (16)	**-35 (29)**
Fiesta Key	4.4 (2.4)	25.8 (0.5)	**26.1 (0.2)**	387 (56)	**464 (4)**	3.8 (0.3)	**3.2 (.01)**	12 (15)	**-12 (7)**	24 (16)	**-20 (25)**
Long Key	5.3 (1.1)	28.1 nd	**25.6 (0.6)**	357 nd	**425 (4)**	4.1 nd	**3.5 (0.2)**	40 nd	**-1 (3)**	78 nd	**-29 (8)**
Mara-thon Key	6.8 (2.8)	27.6 (nd)	**25.3 (0.3)**	412 (nd)	**434 (5)**	3.9 (nd)	**3.4 (0.1)**	12 (nd)	**-12 (9)**	24 (nd)	**-37 (.04)**
Looe Key	6.5 (2.4)	25.3 (0.2)	**26.8 (0.9)**	448 (5)	**594 (48)**	3.4 (.04)	**3.4 (0.2)**	10 (2)	**8 (10)**	45 (20)	**-14 (10)**
Average	5.7 (2.5)	26.2 (0.2)	**25.8 (0.2)**	387 (62)	**469 (26)**	3.87 (.12)	**3.41 (.04)**	16 (5)	**-19 (12)**	44 (8)	**-48 (21)**
Annual average:						***3.63***		***-1 ± 8***		***-2 ± 18***	

Table 2.2. Seasonal (S for summer and W for winter) and spatial trends of calcification (NEC) and net community production (NCP) in 2009 and 2010 by transect. Transects are listed from north to south in the Florida Keys and NEC and NCP were measured on a subset of stations in Figure 1. The average pCO2 and Ω , temperature and salinity reported in this table are a subset of the total carbonate chemistry, and represent values only for transects where residence time, NEC and NCP were calculated. Standard error is shown in parentheses while "nd" indicates no error data due minimal sampling. Samples were averaged first by station and then by transect to control for variable sampling intensity. Annual calcification and net production for the FRT excluding Fowey Rocks is 5 ± 4.8 (mmol m^{-2} d^{-1}) and 9 ± 12 (mmol m^{-2} d^{-1}).

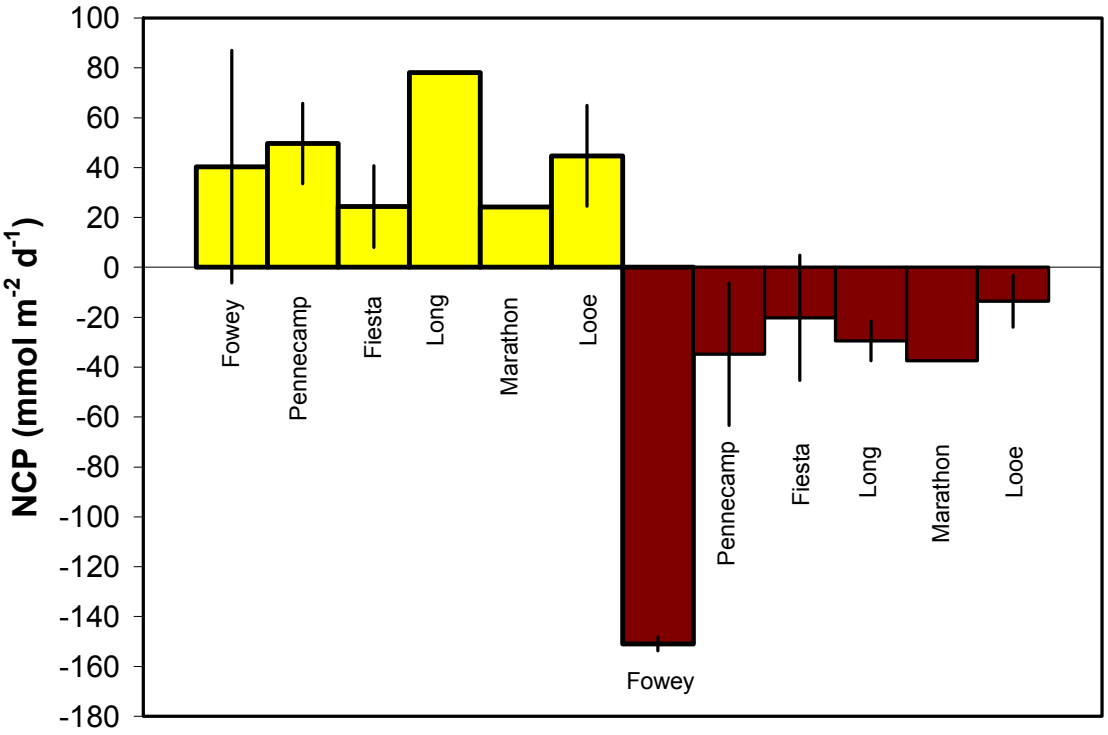

Figure 2.4. Net community production (NCP), measured using changes in dissolved inorganic carbon, and averaged for each transect for summer months (yellow bars) and winter months (red bars) over the years 2009-2010. Positive values indicate net production while negative values indicate net respiration. Data are arranged by transect north to south, from Fowey Rocks to Looe Key. Error bars are standard error and are absent at transects containing only 1 observation.

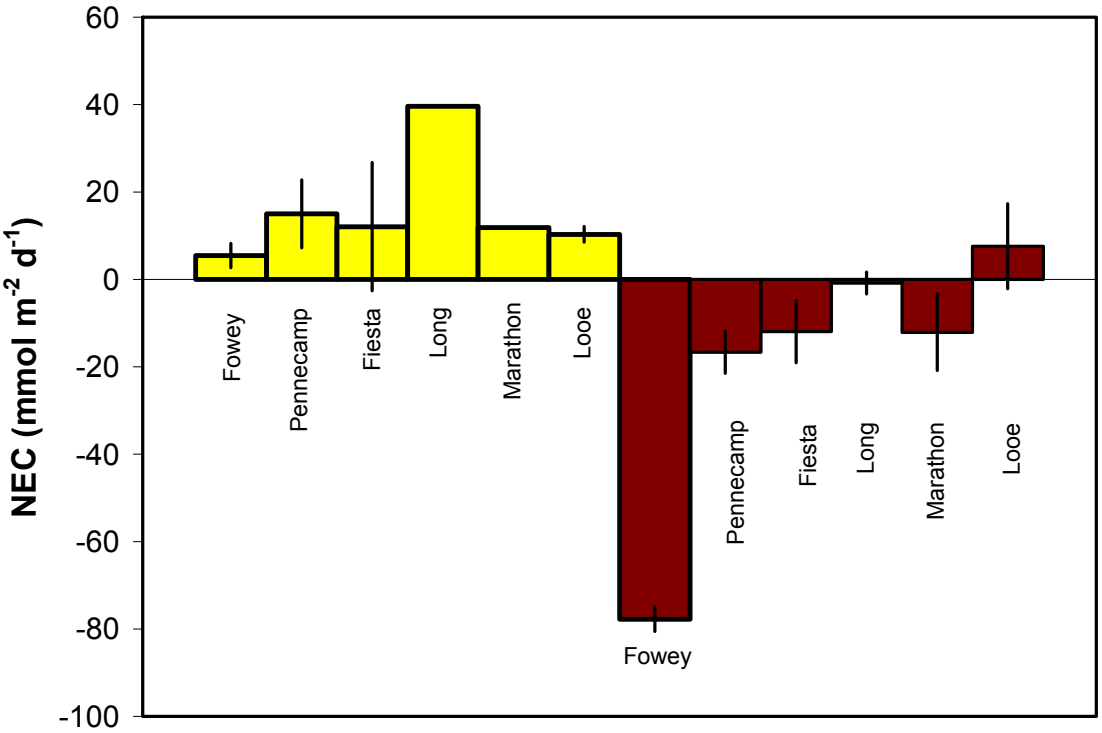

Figure 2.5. Net ecosystem calcification (NEC) measured using fluxes in salinity normalized total alkalinity, and averaged for each transect for summer months (yellow bars) and winter months (red bars) over the years 2009-2010. Positive valued indicate net calcification while negative values indicate net dissolution. Data are arranged by transect from north to south from Fowey Rocks to Looe Key. Error bars are standard error and are absent at transects containing only 1 observation.

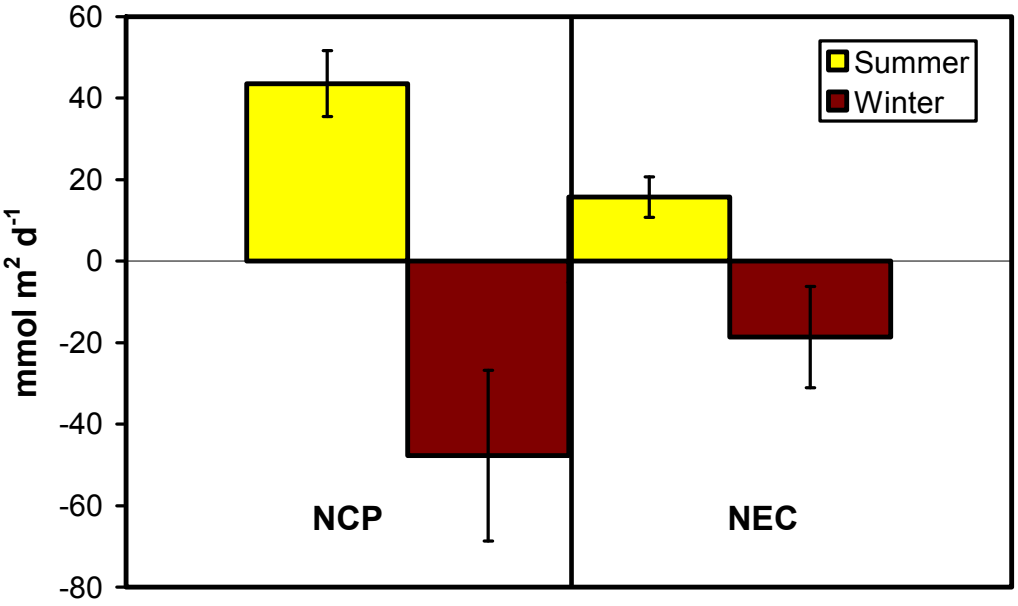

Figure 2.6. Average summer (yellow bars) and winter (red bars) net community production (NCP) and net ecosystem calcification (NEC) ever the years 2009-2010. Error bars are standard error.

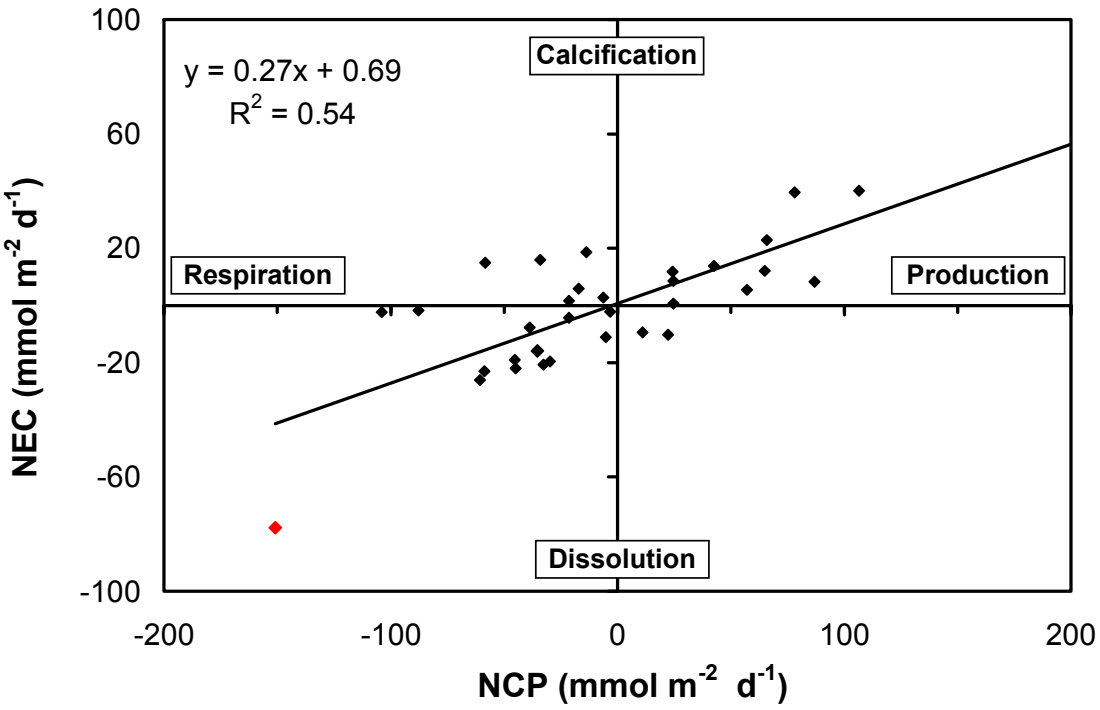

Figure 2.7. Linear regression of net community production (NCP), and net ecosystem calcification (NEC) in the years 2009-2010. Data points in the upper right quadrant represent net production and net calcification, while those that fall in the bottom left quadrat represent net respiration and carbonate dissolution on the reef. An outlier left in the analysis is marked in red, and represents observations at Fowey Rocks (See Table 2).

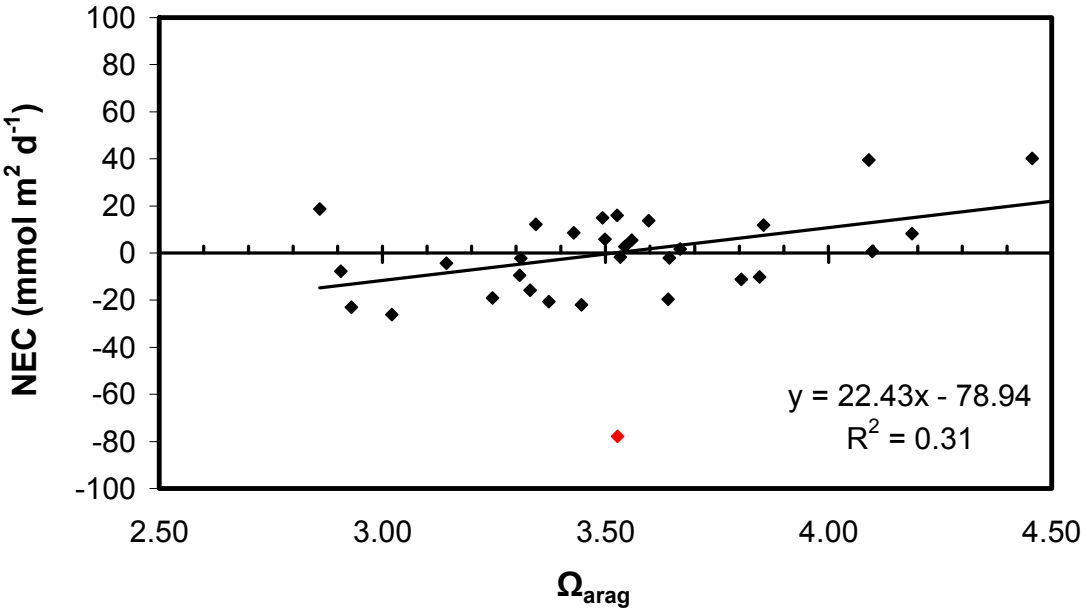

Figure 2.8. Net ecosystem calcification (NEC) is plotted as a function of aragonite saturation state, showing that NEC scales linearly with Ω with an r^2 of 0.31. One outlier, (NEC -77 mmol m^{-2} d^{-1}, Ω 3.53) is demarcated in red. This outlier was excluded because it represents the only strong decoupling of Ω and NEC, reflecting an unequal influence on these two factors occurring at Fowey Rocks (see Table 2), which is not representative of the reef tract as a whole.

Date	St.	$^{7}Be_{SW}$ dpm m^{-3}	$^{7}Be_{P}$ dpm m^{-3}	$^{234}Th_{SW}$ dpm m^{-3}	$^{234}Th_{P}$ dpm m^{-3}	F_{rain} dpm m^{-2} d^{-1}
4/09	5.5	295 (±21)	128 (± 75)	21 (± 4)	135 (± 19)	62.5 (± 12)
	8	262 (± 44)	48 (± 37)	563 (± 63)	467 (± 23)	
	9.5	245 (± 49)	32 (± 31)	690 (± 49)	441 (± 35)	
	20.5	411 (± 31)	135 (± 88)	1414 (± 102)	366 (± 24)	
	21.5	195 (± 38)	249 (± 82)	1082 (± 51)	612 (± 49)	
	6.75	134 (± 32)	15 (± 11)	822 (± 68)	406 (± 47)	
12/09	1	426 (± 30)	227 (± 33)	449 (± 129)	172 (± 8)	256 (± 89)
	4	240 (± 20)	161 (± 33)	136 (± 22)	83 (± 4)	
	7	262 (± 26)	60 (± 27)	629 (± 56)	150 (± 6)	
	10	328 (± 17)	166 (± 39)	339 (± 41)	174 (± 6)	
	13	310 (± 16)	70 (± 37)	249 (± 94)	115 (± 4)	
	19	271 (± 15)	32 (± 10)	373 (± 66)	200 (± 6)	
	6.75	43 (± 13)	96 (± 25)	1282 (± 131)	369 (± 14)	
5/10	1	288 (± 28)	105 (± 13)	118 (± 38)	217 (± 4)	27.8 (± 16)
	2	278 (± 29)	37 (± 18)	546 (± 55)	245 (± 4)	
	4	384 (± 30)	104 (± 18)	249 (± 54)	91 (± 5)	
	5.5	295 (± 35)	195 (± 23)	150 (± 53)	142 (± 2)	
	7	328 (± 45)	109 (± 38)	169 (± 42)	181 (± 3)	
	8	267 (± 41)	185 (± 40)	348 (± 50)	395 (± 3)	
	10	349 (± 32)	339 (± 53)	296 (± 42)	293 (± 7)	
	13	239 (± 30)	239 (± 25)	315 (± 44)	287 (± 5)	
	19	272 (± 48)	117 (± 36)	346 (± 46)	186 (± 8)	
	20	185 (± 38)	130 (± 24)	262 (± 34)	208 (± 2)	
	21.5	370 (± 35)	142 (± 17)	924 (± 54)	395 (± 8)	
	6.75	109 (± 29)	45 (± 28)	1007 (± 65)	460 (± 6)	
10/10	4	705 (± 36)	277 (± 34)	280 (± 147)	69 (± 7)	428 (± 78)
	5	1042 (± 45)	387 (± 32)	105 (± 70)	119 (± 3)	
	7	1241 (± 54)	735 (± 48)	38 (± 14)	126 (± 3)	
	8	1333 (± 52)	888 (± 67)	589 (± 134)	402 (± 6)	
	13	936 (± 50)	571 (± 42)	106 (± 47)	127 (± 3)	
	14	756 (± 40)	355 (± 38)	296 (± 45)	357 (± 7)	
	19	1485 (± 54)	340 (± 20)	786 (± 110)	126 (± 3)	
	20.5	1314 (± 49)	489 (± 22)	914 (± 94)	357 (± 7)	
	6.75	356 (± 28)	42 (± 17)	1426 (± 76)	472 (± 9)	
12/10	4	324 (± 18)	54 (± 17)	379 (± 135)	139 (± 4)	91 (± 23)
	5.5	375 (± 25)	74 (± 18)	44 (± 36)	221 (± 4)	
	13	324 (± 22)	137 (± 16)	203 (± 33)	162 (± 3)	
	14	378 (± 22)	47 (± 11)	239 (± 23)	156 (± 2)	
	6.74	325 (± 24)	64 (± 10)	2086 (± 77)	646 (± 8)	

Table 2.3. Summary of total alkalinity data and the ^{7}Be and ^{234}Th activity in sea water (SW) and on particles (P). Station is indicated by "St."

Date	station	Residence time (d)	Kp (d^{-1})	^{7}Be response time (d)	^{234}Th response time (d)
Apr-09	5.5	4	0.24	4	3.7
	8	2.5	0.22	4.3	4
	9.5	2	0.26	3.7	3.5
	20.5	6	0.24	4	3.7
	21.5	3	0.14	6.5	5.9
Dec-09	1	5	0.7	1.4	1.4
	4	3	0.66	1.5	1.5
	7	2	0.86	1.1	1.1
	10	6	0.84	1.2	1.2
	13	4	0.7	1.4	1.4
	19	4	0.44	2.2	2.1
May-10	1	6	0.26	3.7	3.5
	2	4	0.94	1.0	1.0
	4	9	0.14	6.5	5.9
	5.5	7	0.12	7.5	6.7
	7	5	0.24	4.0	3.7
	8	4	0.18	5.2	4.8
	10	4.5	0.04	18.9	14.5
	13	8	0.36	2.7	2.6
	19	9	0.14	6.5	5.9
	20	6.5	0.84	1.2	1.2
Oct-10	4	10	0.88	1.1	1.1
	5	10	0.9	1.1	1.1
	7	8	0.3	3.2	3.0
	8	7	0.14	6.5	5.9
	13	11	0.16	5.8	5.3
	14	8	0.72	1.4	1.3
	19	9	0.16	5.8	5.3
	20.5	8	0.9	1.1	1.1
Dec-10	4	4	0.44	2.2	2.1
	5.5	3.5	0.32	3.0	2.9
	13	6	0.18	5.2	4.8
	14	3.5	0.66	1.5	1.5

Table 2.4. Summary of residence times, particle scavenging rates (Kp) and tracer response times for each sampling date and station. If the tracer response time is within the same order of magnitude as the estimated residence time than the tracers are responding at a rate appropriate to estimate local reef water residence times.

Transect	Station	Average	Standard deviation	Individual observations
Fowey Rocks	1	5.5	0.7	(6.0, 5.0)
	2	4.0	n/a	(4.0)
Pennecamp Park	4	6.5	3.5	(9.0,3.0,10.0,9.0)
	5	10.0	n/a	(10.0)
	5.5	5.5	2.1	(4.0, 7.0)
Fiesta Key	7	5.0	3.0	(5.0, 2.0, 8.0)
	8	4.8	3.2	(2.5,7.0)
	9.25	2.0	n/a	(2.0)
Long Key	10	5.3	1.1	(4.5, 6.0)
Marathon	13	7.3	3.0	(8.0, 4.0, 11.0, 6.0)
	14	9.0	1.4	(8.0, 10.0)
Looe Key	19	7.3	2.8	(4.0, 9.0, 9.0)
	20.5	7.0	1.4	(8.0, 6.0)
	21	3.0	n/a	(3.0)

Table 2.5. Residence time by station and transect over the years 2009-2010.

Chapter 3: Shifting the Slope of Decline: The Systematic Alleviation of Ocean Acidification by Heterotrophy in *A. cervicornis* in Ω from 0.5 to 3.6

3.1 Summary

Predicting the effects of ocean acidification on corals rests on our ability to robustly describe the aragonite saturation state and calcification (Ω-G) relationship, and to quantify the modifiers of the Ω-G relationship. Heterotrophy has been shown to be important in helping some corals survive thermal stress and has been suggested to alleviate ocean acidification in coral and coral larvae, though it is unknown to what degree this alleviation occurs across a range of future saturation states. Here, we report the results of experiments that looked at the calcification of fed and unfed *Acropora cervicornis* corals. The corals were preconditioned for one month, grown at six different levels of aragonite saturation state (0.5, 0.9, 1.2, 1.8, 2.2 and 3.6) under natural light, and near optimal temperature (27°C). Calcification rates of both fed and unfed corals declined linearly with decreasing saturation state. The calcification rate of fed corals declined at a modest 8% per unit change in saturation state, while the calcification rate of unfed corals declined by 13% per unit change in saturation state. It is noteworthy that both fed and unfed corals were able to sustain a reduced, but still positive, rate of calcification even when the water was significantly undersaturated with respect to aragonite (Ω=0.9 and 0.5). These results indicate that the response of the calcification of *Acropora cervicornis* to ocean acidification is a steady decline over a broad range of saturation states, suggesting that the Ω-G relationship is best described by a linear model, but not one that reaches dissolution in undersaturation. Heterotrophy significantly alleviated the impact of ocean acidification in every pCO_2 level, but did not negate the effect of the ocean acidification on calcification rates in coral.

3.2. Background

Reefs are the foundation of complex marine coastal communities with considerable aesthetic and socioeconomic value as one of the most productive marine ecosystems (Costanza *et al*., 1997). Although geographically restricted to tropical seas and occupying only 0.1% of the earth surface, coral reefs have globally important roles as sustainable fisheries, coastal buffer zones, tourism dollars and this. The foundations of tropical reefs rely on the prodigious capacity of symbiotic scleractinians to calcify and to fix large amounts of carbon (Hoegh-Guldberg 2005). Rapid calcification by corals plays a critical role in coral reef function, because it leads to the formation of a massive, wave resistant framework that provides habitat for many taxa (Idjadi and Edmunds 2006). Understanding the factors controlling coral calcification is critical to understand how coral reef communities will be impacted by rising atmospheric pCO_2 and the resulting ocean acidification (OA) (Pandolfi *et al*., 2011).

Already, many coral reefs are in a state of decline (Hoegh-Guldberg *et al.,* 2007), due in large part to the effects of multiple anthropogenic disturbances acting on local (Jackson *et al*., 2001) and regional scales (Hoegh-Guldberg *et al.,* 2007). Current pCO_2 levels of 380 μatm were predicted to easily exceed 700 μatm by the year 2100, if "business-as-usual" CO_2 emissions are maintained (IPCC 2007) however high emission scenarios such as RCP8.5 (Riahi *et al*., 2007) result in end of century pCO_2 levels of over 900 μatm. Some reef systems may show amplifications of atmospheric pCO_2 levels that are non-linear, leading to reef flat pCO_2 levels up to 3 times higher than the predicted end of the century pCO_2 levels (Shaw *et al*., 2013). Increases in atmospheric pCO_2will cause substantial declines in the pH, aragonite saturation state (Ω), and

carbonate (CO_3^{2-}) concentrations of seawater, which in turn inhibits coral calcification (Hoegh-Guldberg *et al.,* 2007). Multiple studies have shown a strong and positive relationship between coral calcification and Ω (e.g. Langdon *et al*., 2000), with declines in Ω depressing coral calcification by 20-40% for a doubling of pCO_2 from current levels (Hoegh-Guldberg, 2005).

Predictions of how coral calcification will change under ocean acidification tend to report a summary of percent declines in calcification across a range of experimental conditions (e.g. 40% Hoegh-Guldberg *et al.,* 2007). However, the decline in calcification has been found to vary from 15% to 54%, between studies and species (Kleypas and Langdon, 2006). This variability contributes to an emerging difficulty in creating predictions for coral calcification and carbonate chemistry or reduces the perceived threat of ocean acidification. For instance, the results of field studies of calcification rates from coral cores (e.g. Cooper *et al.,* 2008, De'ath *et al.,* 2009) do not closely enough match the predicted declines from lab studies which can lead to a general lack of confidence in our predictive ability (Pandolfi *et al.,* 2011) and the conclusion that ocean acidification may not play as substantial a role in decreasing calcification rates in the field (e.g. Cantin *et al.,* 2010).

While coral calcification is known to decrease under ocean acidification (Langdon *et al.,* 2000), there are multiple interacting factors that can modulate the calcification response, such as nutrients (Langdon and Atkinson, 2005), gender (Holcomb *et al.,* 2011), temperature (Anthony *et al.,* 2008), metabolic regulation (Wood *et al.,* 2008) and the coral-symbiont community (Brading *et al.,* 2011).

One emerging source of variability between OA studies on coral calcification is what can be loosely coined the coral energy budget (Lesser *et al*., 2012), and which may directly affect the corals ability to regulate its internal pH as the seawater ph declines due to ocean acidification (Venn *et al*., 2009; 2013). The coral energy budget can be shifted by multiple factors such as the energetic costs of reproduction (Holcomb *et al.,* 2011), mucus production (Crossland *et al.,* 1980), and bleaching (Grottoli *et al.,* 2006). Some species of corals have been found to be able to use heterotrophy to increase their energy budgets when faced with bleaching stress (Grottoli *et al.,* 2006) and shifts between heterotrophy and autotrophy have been shown to occur in response to light and dark adaptation (Hoogenboom *et al*., 2010). Thus the question arises as to what degree heterotrophy can play a role in the calcification response, and whether it can confer some type of resistance to acidification effects on coral growth.

In this study we use higher number of pCO_2 levels (n=6, 320-4570 μatm) to fully explore and demonstrate the nature of the aragonite saturation state to calcification (Ω-G) relationship in an endangered Atlantic coral, *Acropora cervicornis*. The sensitivity of the Ω-G relationship to heterotrophy was examined by creating subsets (n=57) of all corals (n=122) after 6 weeks of growth to form a fed and unfed contingent. Additionally we examine the effect of heterotrophy on calcification using a broad spectrum of prey size classes (2–450 μm) to better mimic the type of heterotrophic inputs that are available to corals in the natural setting.

3.3. Methods

3.3.1 Coral Collection

Three colonies of *Acropora cervicornis* were sourced from the Smithsonian Marine Station at Fort Pierce, in February of 2011. Corals were continually submerged and affixed in an upright position in coolers, during transport to the University of Miami's Experimental Hatchery (UMEH) on Virginia Key. Upon arrival, polyps were extended on many branches; evidence of the delicate handling used to reduce stress during collection and transport. After 12 hours in incubation tanks, all branches had emerged polyps and exhibited no additional signs of stress (e.g., mucus production, tissue loss). Specimens were shaded to ~ 200 μmol photons m^{-2} s^{-1} during a 2-week recovery period, after which time they were fragmented into branches of similar sizes (4.5-6.5 cm) to reduce the influence of branch length on overall growth (Bucher *et al*., 1998). Branches were affixed with underwater epoxy (Z-Spar A788 Splash Zone compound) to plastic bases (Birkeland, 1976). Branches were allowed to recover from fragmentation for 1 week, followed by growth measured weekly over a 3-week period to assess recovery before experimentation. Stable growth rates were used as an indication that corals had recovered from the fragmenting process.

3.3.2 Incubation

For a full description of the carbon dioxide system used at UMEH to maintain experimental aquaria, and the carbonate chemistry methods used for seawater analyses, please refer to Chapter 1 of this thesis. Coral branches were distributed across 12 tanks and 6 pCO_2 levels; control (318 μatm) and five high pCO_2 levels (611, 915, 1540, 2379

and 4567 µatm). In the remainder of this chapter, CO_2 levels will be rounded to the nearest 10. The lower two pCO_2 levels were chosen to represent levels that are predicted to occur in the next 100 years (610 µatm and 920 µatm), according to the IPCC scenarios A2 and A1B (Caldeira and Wickett, 2005). The highest pCO_2 levels (2380 and 4570 µatm) were chosen to create two levels with saturations states < 1.

Coral branches were randomly distributed among 12 tanks, with 2 tanks per treatment and 9-11 corals per tank, resulting in a total n per pCO_2 treatment of ~20. Bases were cleaned weekly with a toothbrush to remove any organisms that might influence coral growth. The tanks were illuminated with natural sunlight; light levels were measured and logged continuously by a light logger suspended ~ 0.5 m above the tanks in a central location. Temperature was monitored continuously with alarms that sent text messages and emails when the temperature departed from the set temperature by 0.5°C. Salinity was measured 3-5 times a week. Water samples were taken three times per week, in PET bottles (see Chapter 1, Section 3), from each of the 12 tanks to measure pH and total alkalinity for calculation of the carbonate system parameters.

3.3.3 Feeding Regime

Corals were fed weekly by transferring corals into a submerged feeding bin that was then slowly raised and secured at the edge of then tank. This maintained the temperature control in the feeding bin and allowed for the seawater, enriched with the feed diet, to be discarded afterwards. Corals were exposed to the food mixture for 6 hours, in the late afternoon and evening, when polyps are extended as corals are known to feed in natural settings (Houlbréque *et al*., 2009). Similar to other studies that

investigated the role of feeding on coral growth response to CO_2 (Comeau *et al*., 2012; Drenkard *et al*., 2013), the corals were assumed to have an ample supply of food, and the particle capture or removal rates were not monitored.

The diet was composed of a combination of commercially available products (Table 2.6) and was designed with two major considerations in mind. First, although the majority of feeding studies target the use of *Artemia* (~ 450 µm) or copepods (~ 800 µm), much of the coral diet consists of very small particles (< 20 um) such as pico- and nanoplankton and cyanobacteria (Bak *et al*., 1998; Houlbréque *et al*., 2004). Second, feeding rates are considered to be concentration dependent (Ferrier-Pages *et al*., 2010; Houlbréque *et al*., 2004). To account for these two factors, a diet was created that encompassed both smaller and larger size classes, including live phytoplankton (2-20 µm), oyster eggs (40-50 µm), and fish larval feed ranging from 100-450 µm (see Table 3.6). To create a concentration-dependent diet we utilized methodology used to calculate the feeding quantities in other marine invertebrates (Espinosa and Allam, 2006), and adapted it for use in corals. The concentration-based diet, by Espinosa and Allam (2006), uses the dry weight content (g 100 mL^{-1}) of prey/food, provided at a rate of 15% of the dry animal weight per day (Epifano and Ewart, 1997). This was reduced by half to 7%, based on the estimate that heterotrophic input accounts for ~50% of the fixed carbon (Houlbréque and Ferrier-Pages, 2009). The dry tissue weight of 2 mg cm^{-2} of *A. palmata* (Fitt *et al*., 2000) was used as a proxy for *A. cervicornis,* and a surface area of ~10 cm^{-2} was estimated from prior surface area to height regressions for *A. cervicornis*.

3.3.4 Buoyant Weighting

Calcification was assessed as the change in mass of the carbonate skeleton, as determined by buoyant weighing (based on Davies, 1989), using a Mettler-Toledo balance (accurate to 0.001 g), calibrated weekly. Salinity was kept constant (35) for all weighing, using freshwater or saltwater (36, from incubation tanks), as needed. Temperature was monitored throughout weighing sessions (5-7 hours) and maintained within ± 0.1°C. A glass reference weight was used to calculate water density and monitor scale performance, before and after each weighing session. Mass changes were then assumed to reflect changes in the mass of aragonite as the contribution by the thin tissue layer is considered to be negligible in seawater (Davies 1989).

3.3.5 Surface Area

Calcification was assessed as the change in mass of the carbonate skeleton and was normalized by time and by the coral surface area (mg cm^{-2} d^{-1}). Tissue was removed from the coral skeleton using an airbrush and filtered seawater in a process referred to as "blasting." Blastate was homogenized for a standard time period (15 seconds). Aliquots for symbiont cell counts (1.5 ml) and chlorophyll *a* (1 ml) were removed from the total blastate for analysis (see Chapter 4), while the skeleton was saved to assess surface area as determined by wax dipping (Stimson and Kinzie, 1991). This method uses objects of known surface area (wood dowels) and weight to create a correlation between wax weight and surface area. Corals are then weighed, before and after dipping in wax, to back calculate the surface area. The r^2 of wax weight on dowels

to surface area attained was 0.98, thereby allowing for a highly precise back calculation. This method was chosen for its accuracy for branching coral species (Veal *et al*., 2011).

3.3.6 Statistics

To test for effects of pCO_2 on coral calcification we used linear regression analysis with pCO_2 as an explanatory variable. Normality was tested using a goodness of fit test and Welch's test was used to assess homoscedasticity as well as visually assessing the plot of residuals versus predicted residuals. The factor "tank" was nested in the pCO_2 treatment and found to be insignificant ($p > 0.05$); therefore, data from replicate tanks were pooled before analysis. All statistical analyses were performed using JMP statistical software (SAS Institute, Version 10, Cary, NC). To examine if the slopes were significantly different from one another, we compared the standard error of the slope, which showed overlap of the error margins and precluded further analysis. To examine if feeding had a significant effect on the calcification while exposed to pCO_2 we used a two factor ANOVA with feeding and Ω as fixed categorical factors.

3.4. Results

3.4.1 Tank Conditions

Twelve tanks were maintained at pCO_2 levels consisting of a control and 5 elevated pCO_2 levels providing replication at the tank level. There was no significant difference between tanks of the same pCO_2 level ($p<0.05$; Table3.4). Temperature and salinity were not significantly different between tanks and averaged 27.1 ± 0.4°C and

36.5. The average maximum light intensity at noon was 331 μmol photon m^{-2} s^{-1} while the overall total average over the course of the day was 247 μmol photon m^{-2} s^{-1}.

3.4.2 Fed Corals: Test of Linearity

Regression analysis showed a significant effect of pCO_2 on calcification rates in fed corals (Table 3.2). The slope of the decline was 0.27 ± 0.09 (standard error) with an R^2 of 0.89 (Figure 3.1). The average percent reduction per 1 unit drop in Ω was 8 ± 0.5% (average ± standard error). In the highest pCO_2 level (4570 μatm), coral calcification declined by 30% compared to control conditions. Both feeding ($P < 0.0001$) and Ω ($P = 0.0001$) were found to be significant with no interaction ($P = 0.15$) between the factors (Table 3.1).

3.4.3 Fed and Unfed Corals: Test of Effect

Regression analysis showed a significant effect of pCO_2 on calcification rate of both fed and unfed corals (Table 2). The slope of the decline of fed corals was 0.32 ± 0.13 (standard error), with an R^2 of 0.88, while unfed corals displayed a slope of 0.48 ± 0.16 (standard error) with an R^2 of 0.83 (Figure 2). The overlapping standard error of the slopes indicated they are not significantly different between fed and unfed corals. The average percent reduction for unfed corals per 1 unit drop in Ω was 13 ± 1.3 % (average ± standard error), and ranged from 9.5 to 17.5% decline per Ω.

3.5. Discussion

The relationship between aragonite saturation state (Ω) and coral calcification rate (G) in *Acropora cervicornis* is linear across the full spectrum of pCO_2 levels, indicating that there is no observable tipping point at which these corals physiologically alter their response to pCO_2. Positive net calcification was observed in all pCO_2 levels, including the two levels where Ω was undersaturated (Ω = 0.9 and 0.5). This study also provides a robust test of the sensitivity of the Ω -G relationship to heterotrophy in *A. cervicornis*, by examining the responses of both fed and unfed corals to a broad range of pCO_2 values (n=6; 320-4570 µatm). We observed that corals provided with opportunities to supplement their energetic budget with a broad size spectrum of live plankton and organic particulates were better able to calcify (average 22% higher) in saturated and undersaturated seawater. Although heterotrophic feeding was found to alleviate the affect of ocean acidification, it does not completely negate declines in calcification nor does it appear to alter the linearity of the Ω-G relationship in acidified seawater.

3.5.1 Linearity of the Ω-G Relationship

The broad range of Ω used serves to clearly define the Ω-G relationship, and helps overcome the growth variability naturally exhibited by corals (Pandolfi *et al*., 2011). The largest decline in growth observed was 30%, from an average of 3.22 ± 0.57 mg cm^{-2} d^{-1} (±SD) in control conditions (320 µatm) to 1.32 ± 0.31 mg cm^{-2} d^{-1} in the highest pCO_2 (4570 µatm). The correlation between the average growth rate and Ω (R^2=0.89), and the slope of 0.27 clearly display the gradual, but steady, decline of coral

calcification under ocean acidification. Compared to other studies, the average decline in calcification per unit Ω was 8% (Figure 1), which is only slightly lower than the 10% average in a recent meta-analysis of studies that used the buoyant weighing method (Chan and Connolly, 2012). Chan and Connolly (2012) make a valuable differentiation between the greater (25%) decline in calcification per unit Ω in studies using the alkalinity anomaly technique, which is often measured over hours, versus those utilizing buoyant weighing (10%), which measures calcification rates integrated over both day and night. These quantifications of the ways in which feeding regimes and measurement techniques can impact the decline in calcification rate in high pCO_2 are important steps in understanding the variability reported across ocean acidification studies.

Non-linear responses to pCO_2 have also recently been reported, however they could be related to the use of temperate corals (Reis *et al*., 2010) or early life history stages (Cohen *et al*., 2009; de Putron *et al*., 2011). The temperate coral, *Oculina arbuscula*, used by Reis et al. (2010) is uniquely different from tropical corals in that the symbiosis with the photosynthetic zooxanthellae is not obligate, and the energetic source of growth appears to be primarily heterotrophy (Piniak, 2002). Non-linear Ω-G relationships have been reported in larvae of two coral species, specifically in *Favia fragum* (Cohen *et al*., 2009; de Putron *et al*., 2011) and *Porites astreoides* (de Putron *et al*., 2011), indicating that coral spat that may respond differently to extreme levels of Ω during early life history stages. By using numerous CO_2 levels (6) over a broader range of Ω (3.5 to 0.5), we illustrate a strongly linear relationship between Ω and G; however, had we used fewer levels or a narrower range of values, such as from Ω 2 to 0.5 (Figure

1), the trend may have appeared non-linear. Our results thus underscore the importance of robust tests of the Ω-G relationship to accurately describe coral calcification under ocean acidification. While we only report the results for *A. cervicornis*, species-specific differences in the linearity/non-linearity have not been observed within multi-species studies, such as Comeau *et al*. (2013) who examined 4 species of scleractinian corals and found a consistent linear decline, nor do they emerge from large meta-analyses (Chan and Connolly, 2011; Pandolfi *et al*., 2011).

Heterotrophy was not observed to change the shape of the Ω-G relationship in our study. Approximately 50% of the meta-analysis data used in a review of calcification under OA, by Chan and Connolly (2011), is taken from corals that were fed to some degree, yet all showed linear declines with decreasing Ω. However, comparing across studies in the future may be challenging due to the great differences between feeding regimes utilized. Feeding regimes across experiments have varied in the past, but typically use large prey such as adult copepods (~ 800 μm) and brine shrimp/*Artemia* (~ 450 μm). Large prey have advantages, as they allow for feeding rates to be assessed by removal of particles from incubation water or counting of prey in dissected polyps. However using solely large prey may not be sufficient to assess the role of heterotrophy in relieving ocean acidification. Recent research highlights the full complement of nutrient sources that corals utilize (Houlbréque *et al*., 2009) and the importance of different size classes such as picoplankton (0.2 – 2 μm) and nanoplankton (2-20 μm; Houlbréque *et al*., 2004). Pico and nanoplankton have been shown to be depleted by 30-45% during passage over coral reefs due to heterotrophic feeding on the reef (Houlbréque *et al*., 2004; Patten *et al*., 2011). Corals also prey on < 100 μm small

particles (DiSalvo, 1971; Sorokin, 1973; Bak *et al*., 1998; Houlbréque *et al*., 2004b). Experiments that examining coral polyp contents on the reef found that even corals with large polyps (1-3 mm diameter) fed preferentially on prey only 200-400 um in length and were not observed to prey on copepods (Palardy *et al*., 2006). Experimental systems in lab settings typically cannot simulate natural diurnal prey oscillations, high flow rates and particle delivery on the reef (Yahel *et al*., 2005). Lab settings may therefore be underestimating the role of heterotrophy in coral calcification responses. This study attempts to resolve some of these issues by adjusting feedings to include late day and evening hours (2 pm until 9 pm) and using live prey, eggs and particulate food in the 2-450 μm size classes, thereby providing a closer comparative diet to that found in the natural reef setting (Lewis and Price, 1975; Houlbréque *et al*., 2009). Therefore, the growth rates of corals in this study, compared to fed and unfed corals in other studies, may represent an example of the best-case scenario for coral growth under ocean acidification.

3.5.2 Calcification in Ω <1

Our inclusion of two undersaturated levels serves to ground the saturation state to calcification (Ω-G) relationship and explore the ability of corals to maintain net calcification in undersaturated seawater. All *A. cervicornis* whether fed or unfed, maintained positive net calcification in undersaturated water (Figure 3.1 and 3.2). Corals in the control calcified at 3.22 ± 0.57 mg cm^{-2} d^{-1} (± standard deviation). After the first 6 weeks, fed corals still calcified in undersaturated Ω of 0.5 (n = 21), with an average net calcification rate of > 2.24 ± 0.56 mg cm^{-2} d^{-1} (± standard deviation; Figure

3.1). After an additional 3 weeks, corals which were no longer given weekly feeding regimes maintained lower, but still positive calcification rates in all Ω levels (Figure 3.2). Calcification in unfed corals growing in undersaturated seawater (0.5) was 1.32 ± 0.31 mg d^{-1} cm^{-2} and averaged 57% lower than calcification in the unfed control tanks at the same Ω (3.06 ± 0.9 mg d^{-1} cm^{-1}; Table 3.5).

Undersaturated waters (Ω < 1) have been assumed to not be able to support coral calcification, either because it was energetically no longer possible, or because the rate of dissolution would overcome the rate of calcification. For instance, earlier OA studies such as Schneider and Erez (2006) found such observed nighttime dissolution at a Ω of 2, while Fine and Tchernov (2007) were able to create skeleton-less corals in undersaturated waters. The tissue covering the skeletal surface has been found to be the key determinant of the occurrence of dissolution in undersaturated seawater (Cohen and Fine, 2012), thus inadvertent portions of exposed skeleton could contribute to a small part of the observed dissolution. Additionally, lab settings with reduced light may alter the OA response (Suggett *et al*., 2013) or the heterotrophic conditions could have resulted in a differential allocation of energy towards tissue rather than skeleton (Anthony *et al*., 2000). More recently, net calcification in undersaturated seawater has been found in multiple instances, from coral larva (Cohen *et al*., 2009) to temperate corals (Ries *et al*., 2010), and more recently, in different species tropical corals (Krief *et al*., 2010; Venn *et al*., 2013).

While many aspects of biomineralization in corals are not mechanistically understood, the process of calcification is considered to be energetically costly. The energetic cost of calcification has been calculated as 13-30% of the total energetic

budget for *Porites porites* (Edmund and Davies, 1986), with ion transport comprising an important portion of the total cost (Palmer *et al*., 1992). Increases in the energetic budget of corals may increase rates of ion transport to the site of calcification or allow corals to better compensate for the stress induced by low pH conditions (Vidal-Dupiol *et al*., 2013).

3.5.3 Comparing between Studies

Ocean acidification studies have utilized a broad range of pCO_2 levels (200-4500 μatm) and typically report calcification declines as percentages of the original coral weight or percent decline from the control. While the metrics are useful for discussing the results within a study, it hampers easy comparisons between studies due to the wide differences in treatment levels used. Reporting declines per unit saturation state and calculating the decline compared to preindustrial Ω (4.6) can provide a common currency for communication purposes. In Figure 4 we add the growth for *A. cervicornis* to a data set compiled data from numerous calcification studies by Chris Langdon (Andersson *et al*., 2011) and expresses calcification as a percent of pre-industrial Ω of 4.6 using the following equation:

Equation 1: 100 * Current G / 4.6

Compared to other studies (Figure 4), our study displays noticeably lower calcification response per unit Ω. The relatively milder decline in calcification may be partially attributable to the coral husbandry and feeding regime used here. High growth

rates were observed in this study, averaging 3.22 ± 0.57 mg cm^{-2} d^{-1} (± SD) and are approximately 1.5-2x faster than observed in other studies. *A. cervicornis* growth by Renegar and Riegl (2005) exhibited growth rates of 1.42 - 2.09 mg d^{-1} though normalized to weight rather than surface area. Corals in this study were given a month to acclimate to the UMEH incubation tanks before experimentation, thus were unlikely to exhibit any residual collection or fragmenting stress (Tentori and Allemand, 2006). In addition, corals were rarely exposed to air and any algal growth along the base or near polyps was removed almost daily. Transfers to coral feeding bins were done keeping the coral submerged to ensure the polyps remained extended. Feeding also occurred at ecologically relevant times of day, during late afternoon and evening, and provided corals with important food size classes that are normally omitted in most feeding and OA studies (Table 3.6; Houlbréque *et al*., 2004b). These efforts increase the chance that changes in calcification due to heterotrophy would be detectable and that variable capture rates of large live prey would not influence growth rates

The use of fed or unfed corals in ocean acidification studies could help explain a large amount of the variability in the calcification declines reported between studies. Using the 490-1250 µatm IPCC predicted range of pCO_2 levels in 2100 translates into 14% decline in calcification rate of fed corals whereas unfed corals decline by 20%. In the highest pCO_2 levels, fed corals showed a 34% decline compared to the controls, while unfed corals showed a 54% decline, thus we observe a maximum 20% difference reduction in growth, in response to ocean acidification, when unfed. Thus, depending on the level of pCO_2 used in a study, providing corals with an environmentally relevant feeding regime can cause a 6 to 20% change in the reported decline in calcification due

to ocean acidification. The declines in calcification due to ocean acidification have ranged from 15-54% (Kleypas *et al*., 2006) and understanding this variability is an important task to increase our predictive abilities.

3.5.4 Comparison of Fed and Unfed Coral Growth to Ocean Acidification

Feeding has a strong and significant ($p<0.0001$) effect on coral calcification under increasing pCO2, indicating that the energetic budget of corals could play an important role in the response to ocean acidification. Both fed and unfed corals displayed significant calcification declines in response to pCO_2 ($p < 0.05$), with a linear response across Ω from 0.5 to 3.6 (Figure 3.2). Fed corals grew an average 22% faster than unfed corals across all pCO_2 levels. The average decline in calcification of unfed corals (13 ± 1.3 % per unit Ω) versus fed corals (8 ± 0.5%; average ± standard error) is almost the same proportional change (8 and 14%) in calcification under feeding and Ω manipulations as found by Drenkard *et al*. (2013) using larvae of *Favia fragum*. While Drenkard *et al*. (2013) uses only one pCO_2 treatment (1311 μatm), their results using corals in different developmental stages provides additional evidence that heterotrophy could alleviate the effects of ocean acidification.

Prior to studies using high pCO_2, the enhancement of calcification due to heterotrophy is widely known. While increased heterotrophy impacts multiple processes, the effect on calcification is likely due to the increase in the coral energetic budget (Anthony *et al*., 2009). The energetic cost of calcification is in part attributed to the delivery of calcium and inorganic carbon to the site of calcification along with the removal of hydrogen ions. In addition, increases in coral biomass from feeding

(Houlbréque *et al*., 2003) could stimulate calcification by increasing the delivery of seawater to the site of calcification or increasing the production of organic matrix. The importance of the organic matrix lies in its position as the biological substrate within which calcium carbonate is deposited (Barnes and Crossland, 1980) and it is both energetically costly to build and has already been shown to be enhanced during heterotrophy (Allemand *et al*., 1998). Thus the increased calcification due to feeding is likely to be from a combination of organic matrix production and the delivery of ions to the site of calcification.

Other studies examining both heterotrophy and ocean acidification have reported mixed results. For instance, changes in biomass-normalized calcification rates enable *Porites* spp. to calcify better under ~800 ppm (Edmunds 2011); however, no feeding effect was reported for *Porites rus* (Comeau *et al*., 2013). The lack of effect in Comeau *et al*., (2013) may be due to the lack of carryover time allowed, and the pooling of all data (3 weeks) during the starvation period. Houlbréque *et al*. (2003) reports a minimum of 2 weeks may be needed to observe differences in calcification rates, thus experiments with longer carryover periods (>2 weeks) and longer observation times are important. The study by Comeau *et al*. (2013) does include some additional methods that moves beyond those employed here, specifically by creating a true "starvation" treatment ($\leq$ 2 μm filtration). In this study, corals in the unfed treatment were not truly starved, as they were still exposed to particles < 10 μm in size, and could have attained nutrition through dissolved and particulate organic matter (Lasker, 1981; Anthony, 1999), bacteria (Sorokin, 1973), free amino acid uptake (Grover *et al*., 2008), and the occasional copepod (Sorokin, 1991; Ferrier-Pagés *et al*., 1998) in the incubation tanks

we used. In addition, because our carryover period was only 11 days long, it is possible that the regression of unfed calcification to Ω still slightly underestimates the effect of reduced feeding. .

Comparing the slope of the fed and unfed corals under different Ω treatments, suggests that feeding may be more important in undersaturated water. Evidence for this can be found in the comparison between the average decline between fed and unfed corals in oversaturated water (4%) versus an average 10% decline in undersaturated water. However since the slope of the linear regression for fed corals (0.31 ± 0.15, standard error) was close to that of unfed corals (0.47 ± 0.29, standard error), and the lack of significant difference in the slopes indicates this trend is not very strong. Further research is needed to tease apart whether corals can alter the portion of the energetic budget allocated towards calcification in undersaturated waters. However overall, the effect of feeding has a strong and significant ($p<0.0001$) effect on coral calcification under increasing pCO_2, indicating that the nutritional status of coral could play an important role in their response to ocean acidification.

3.5.5 Conclusion

This study highlights the compounding difficulties that corals will face as they strive to build their skeleton in the high-CO_2 world. In the ideal lab setting where food is replete, light is high and corals are protected from temperature swings, the decline in calcification may be as modest as 8% per unit drop in saturation state for species such as *A. cervicornis*. However, changes in the corals energetic budget due to different heterotrophic inputs can amplify the calcification response to ocean acidification almost

2 - fold. The quantification of the role of heterotrophy in the calcification response to OA brings increased clarity to the variable declines observed between studies. While we observe that feeding can alleviate the effects of ocean acidification even in undersaturated water, it does not negate the decline in calcification due to ocean acidification. By using robust tests of the calcification to saturation state relationship (Ω-G) we create an important tool for our predictive ability regarding coral declines in an acidifying ocean.

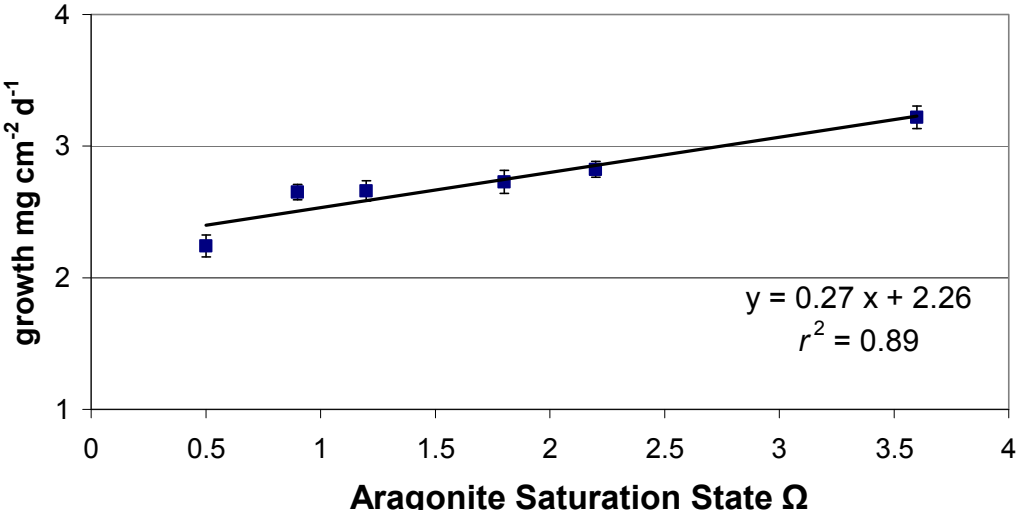

Figure 3.1. Growth (G) of *A. cervicornis* (n=122) over 6 weeks with the sample sizes per Ω level as follows: 3.6 (n=20), 2.2 (n=21), 1.8 (n=19), 1.2 (n=21), 0.9 (n=20), 0.5 (n=21). Error bars are 95% confidence intervals. R^2 reported on graph is for averaged growth rates per Ω. Linear regression equations were G = Ω * 0.27 (± 0.09) + 2.26 (± 0.09) (adj. r^2=0.22, n=122, p<0.0001).

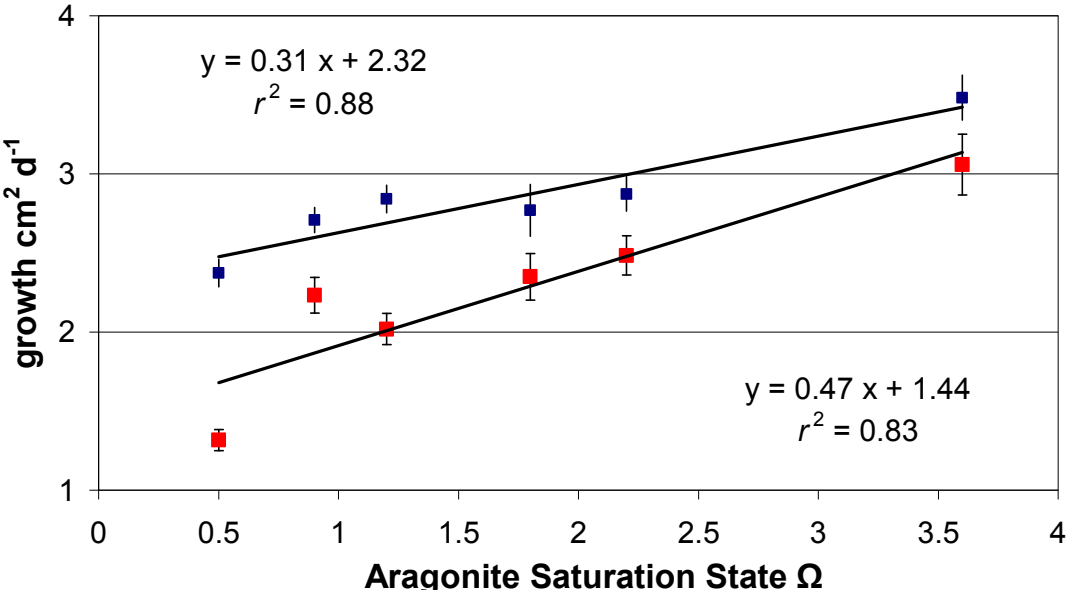

Figure 3.2. Growth of a subset (n=57) of the total (n=122) *A. cervicornis* that were fed for 6 weeks (black squares), and subsequently unfed (red squares) for 2 weeks. Corals were given a carryover period of 11 days before collecting data for the unfed period. Corals were incubated in Ω of 3.6 (n=10), 2.2 (n=10), 1.8 (n=9), 1.2 (n=10), 0.9 (n=8), 0.5 (n=10). Error bars are 95% confidence intervals. R^2 reported on graph is for averaged growth rates per Ω. Linear regression equations for fed corals were G = Ω * 0.31 (± 0.13) + 2.28 (± 0.13) (adj. r^2=0.29, n=57, p<0.0001). Linear regression equations for unfed corals were G = Ω * 0.48 (± 0.16) + 1.41 (± 0.16) (adj. r^2=0.39, n=57, p<0.0001).

Categorization criteria Variable	df	SS	F	P
Ω	5	21.3329	13.3402	<0.0001
Feeding	1	5.5762	10.6033	<0.0001
pCO_2 x Feeding	5	2.683	1.6780	0.1465
Residual	103	32.9423		
Total	114	65.3794		

Table 3.1. Summary of 2-factor ANOVA based on categorized environmental data (Ω) and feeding regime (fed or unfed) on the calcification rate (mg cm^{-2} d^{-1}) of *A. cervicornis*.

	Fed (n=122)	Fed Subset (n=57)	Unfed Subset (n=57)
Beta	0.27 (±0.09)	0.31 (±0.13)	0.47 (±0.16)
r^2	0.89	0.88	0.83
t statistic	25.4	17.2	8.93
Intercept	2.27	2.32	1.44
Significance (p)	<0.0001	<0.0001	<0.0001
Standard error of regression	0.51	0.51	0.61

Table 3.2. Output from Linear Regression for growth rate and saturation state for the six treatment (pCO_2) levels. Beta values are followed by the standard error.

	Salinity	T (°C)	pH_T	pCO_2 (µatm)	$\Omega_{aragonite}$	Light (µmol photons m^{-2} s^{-1})
Control 1	36.3 ± 0.4	27.1 ± 0.3	8.08 ± 0.04	318 ± 33.8	3.62 ± 0.31	326 ± 126
Level 2	36.6 ± 0.4	27.1 ± 0.4	7.82 ± 0.05	611 ± 76	2.23 ± 0.31	340 ± 123
Level 3	36.2 ±0.8	27 ± 0.3	7.68 ± 0.08	915 ±172	1.75 ± 0.27	338 ± 140
Level 4	36.6 ± 0.5	27.2 ± 0.5	7.53 ± 0.13	1549 ± 212	1.20 ± 0.13	303 ± 112
Level 5	36.6 ± 0.4	27.1 ± 0.4	7.33 ± 0.07	2379 ± 333	0.89 ± 0.10	333 ± 137
Level 6	36.7 ± 0.4	27.2 ± 0.4	7.08 ± 0.05	4567 ± 574	0.52 ± 0.06	304 ± 126

Table 3.4. Physical and chemical conditions of aquaria during growth experiment with *A. cervicornis*. All chemical measurements are based upon duplicate or triplicate analyses for each sample. pH_T, pCO_2, HCO^{3-}, CO_3^{2-}, CO_2, TCO_2, and Ω_a were calculated using CO2SYS. Average ± standard deviation. Replicate tanks were not significantly different ($p<0.05$). Light per tank was measured 18 times at approximately noon.

Title: Acropora cervicornis calcification rates			
	Time period 1	*Time period 1*	*Time period 2*
pCO_2 level	Fed corals rate (n=122) (mg d^{-1} cm^{-2}	Subset of Fed corals (n=57) (mg d^{-1} cm^{-2})	Subset subsequently Unfed (n=57) (mg d^{-1} cm^{-2})
Control Level 1 318 ppm, Ω 3.62	3.22 ± 0.13 (20)	3.48 ± 0.21 (10)	3.06 ± 0.28 (10)
Level 2 611 ppm, Ω 2.23	2.82 ± 0.09 (21)	2.87 ± 0.16 (10)	2.48 ± 0.18 (10)
Level 3 915 ppm, Ω 1.75	2.73 ± 0.13 (19)	2.77 ± 0.24 (9)	2.35 ± 0.22 (9)
Level 4 1549 ppm, Ω 1.20	2.66 ± 0.11 (21)	2.84 ± 0.13 (10)	2.02 ± 0.15 (10)
Level 5 2379 ppm, Ω 0.89	2.65 ± 0.09 (20)	2.71 ± 0.12 (10)	2.23 ± 0.17 (8)
Level 6 4567 ppm, Ω 0.52	2.24 ±0.12 (21)	2.37 ± 0.13 (10)	1.32 ± 0.10 (10)

Table 3.5. . Average ± standard error (sample size) of growth rates in fed versus unfed *A. cervicornis* across 6 levels carbon dioxide.

Content	Size	Content
Dried Feed (Larval AP100)	250-450um	Protein Minimum 50.0 %, Fat Minimum 15.0 %, Fiber Maximum 2.5 %, Moisture Maximum 10.0 %, Ash Maximum 9.5 %
Dried Feed (Larval AP100)	100-150um	Protein Minimum 50.0 %, Fat Minimum 15.0 %, Fiber Maximum 2.5 %, Moisture Maximum 10.0 %, Ash Maximum 9.5 %
Oyster eggs (Brand)	40-50 um	Moisture: 80 % Protein: 7 % Total Fat: 2.49% EPA: 14.8 % of total fat DHA: 9.64 % of total fat Fiber: < 0.2% Ash: 2 %, 8 % carbohydrates
DT's Live Marine Phytoplankton	2-20 um	*Nannochloropsis oculata, Phaeodactylum tricornutum, Chlorella*

Table 3.6. Size classes and content of food particles provided to *A. cervicornis* on a weekly basis.

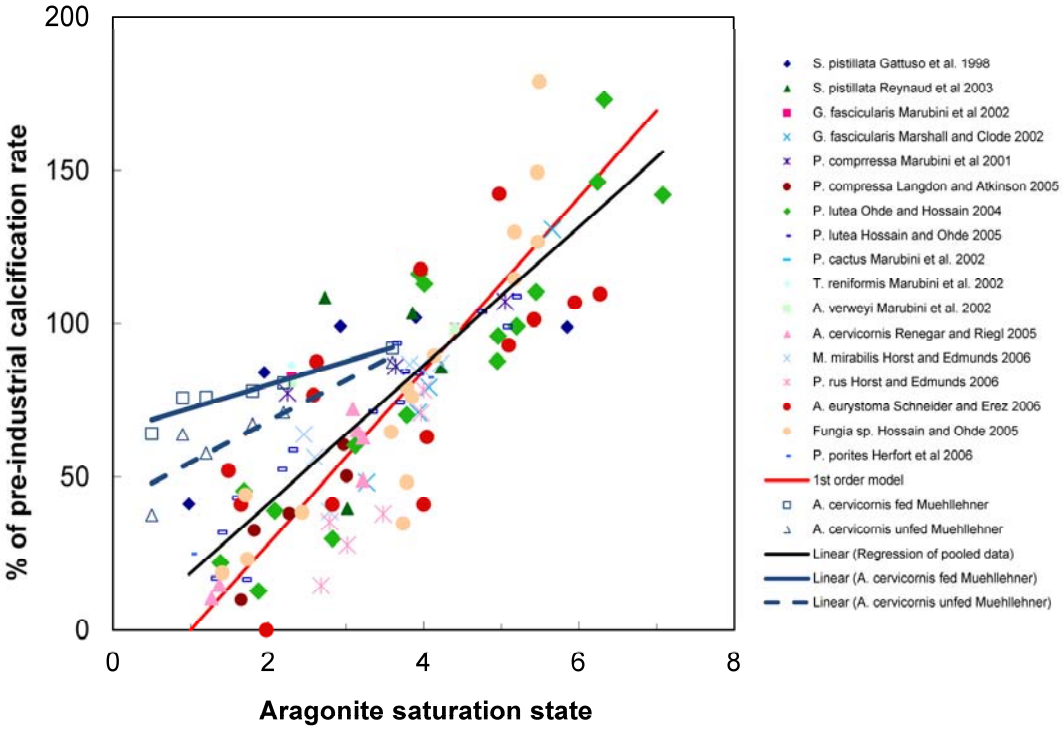

Figure 3.3. Effect of Ω on calcification rate (G) expressed as a percentage of the preindustrial rate. Data are from published studies on a range of coral species (Andersson *et al*., 2011). *A. cervicornis* from this study are average rates per treatment level and shown in blue (solid line is fed, n=57; dotted line is unfed, n=57). Linear regression equations on averaged data were Fed G = Ω * 8.25 +62.7 (r^2=0.88, n=57, p<0.011) and Unfed G = Ω * 12.98 + 39.9 (r^2=0.83 n=57, p<0.005).

	Beta (slope)	y intercept	Standard error of regression	r^2	P value
Fed (n=122)	0.27	2.27	0.4	0.89	0.004
Fed subset n=57	0.31	2.32	0.5	0.88	0.005
Unfed subset n=57	0.47	1.44	0.5	0.83	0.011
Converted Fed, n=122	7.65	64.7	3.3	0.89	0.004
Converted Fed, n=57	8.25	62.7	7.2	0.88	0.011
Converted Unfed, n=57	12.98	39.9	7.2	0.83	0.005

Table 3.7. Output from linear regression for saturation state and growth of the original data and data converted to the growth rate normalized to percentage of growth at preindustrial Ω (Ω=4.6). Cells contain the value followed by the standard error where appropriate. There are 6 treatments (pCO_2) levels. The r^2 is on the averaged data per Ω.

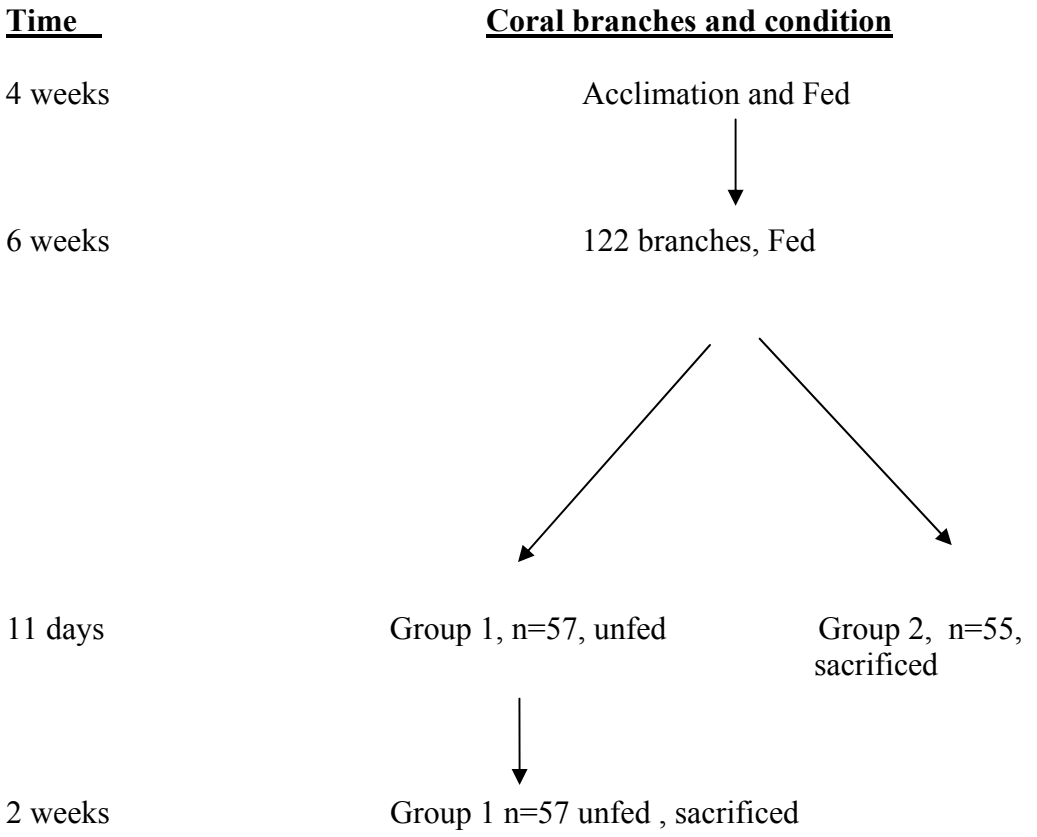

Figure 3.4. Experimental design – colonies of *Acropora cervicornis* were fragments and branches were divided into 12 tanks with 6 replicate pCO_2 levels. After 6 weeks, ½ of the branches were sacrificed and the remaining half became an unfed group.

Chapter 4: Elevated CO_2 Causes Declines in Symbiont Density in Laboratory and Field Studies

4.1 Summary

Coral fitness is strongly influenced by the obligate symbiosis with *Symbiodinium microadriacticum*, yet predicting the response of symbionts to increasing pCO_2 relies on few lab studies, which provide little basis for predicting the symbiont response in the natural environment. The array of differences between the laboratory and *in situ* conditions could modify the symbiont response to increasing pCO_2, thereby changing our predictions for the effects of ocean acidification. The goal of this research is to examine changes in symbiont density and chlorophyll *a* concentration in response to ocean acidification, both *in situ* and in experimental settings. The long-term effect of pCO_2 on the symbiont community was assessed in 2 coral species (*Pocillopora damicornis* and *Acropora millepora*) from volcanic vents in the tropical Pacific. *In situ*, corals exposed to high pCO_2 (~850 μatm) had significantly less symbionts than at control sites and displayed an average 48% decline in the symbiont to host cell ratio. In the lab, *Acropora cervicornis* were exposed to 7 weeks of pCO_2 levels stretching from 320 to 4570 μatm to fully explore symbiont response to increasing the pCO_2. Symbiont density in the lab significantly declined in response to pCO_2, with the greatest decline (26%) under 4570 μatm. Future studies are needed to explore factors inherent in the natural setting that can modify the symbiotic response to high pCO_2 for us to understand how results from laboratory setting will translate into the natural environment.

4.2. Background

Atmospheric CO_2 levels are rapidly rising due to anthropogenic influences such as construction, deforestation and fuel combustion (Raupach *et al*., 2007). As atmospheric pCO_2 has risen, approximately one third has dissolved in our oceans since the industrial revolution (Sabine *et al*., 2004) leading to a decline in pH of ~0.1 pH units (Caldeira and Wickett, 2005). While the absolute value of the pH decline appears small, it represents a 30% increase in acidity, which has been shown to impact multiple marine organisms (Kroeker *et al*., 2010).

Coral reefs are likely to be particularly vulnerable to ocean acidification due to the dependence of corals on favorable carbonate chemistry for calcification (Langdon et al., 2000; Langdon *et al*., 2005; Kleypas and Yates, 2009). Skeletal records suggest that coral growth has already declined across broad spatial areas in recent decades (De'ath *et al*., 2009). A growing number of experiments have quantified the reduction in coral calcification due to ocean acidification (OA), yet broad ranges in the observed and predicted declines in calcification persist in the literature. The most recent IPCC report projects a 20%–60% reduction in coral calcification when pCO_2 reaches 700 μatm and by 2070 many reefs could be in rapid decline (Veron *et al*., 2009). Several hypotheses have been proposed to explain the variability in coral calcification to ocean acidification, such as the influence of nutrients (Langdon and Atkinson, 2005), light (Marubini *et al*., 2001; Langdon and Atkinson, 2005, Suggett *et al*., 2013), temperature (Reynaud *et al*., 2003; Langdon and Atkinson, 2005), study duration (Krief *et al*., 2010) and energetic status (Cohen and Holcomb, 2009). Yet inherent in the host response is the interplay with the independent/interconnected response of the symbiont

(*Symbiodinium microadriacticum*). The obligate symbiont, *Symbiodinium*, is vital for coral fitness and survival due to its influence on calcification and carbon acquisition for the host (Muscatine *et al*., 1981). Calcification during day-light hours, when *Symbiodinium* are photosynthesizing, is 3–4 times greater than in the dark (Gattuso *et al*., 1999a; Furla *et al*., 2000). The large role that *Symbiodinium* plays in carbon acquisition for the growth of the host has long been known (Muscatine; 1977, 1990), along with the tendency for symbiont density to vary with depth and light (Rowan and Knowlton, 1995; Iglesias-Prieto *et al*., 2004), season (Fitt *et al*., 2000) and heterotrophy in the coral host (Rodolfo-Metalpa *et al*., 2008). Thus changes in the symbiont can play a strong role in the host response in virtually every environment. Understanding how the coral response to OA is mediated by the coral-algal symbiosis is vitally important for improving our predictive ability in OA research.

Our current understanding of the *Symbiodinium* response to ocean acidification is limited to lab settings (Reynaud *et al*., 2003; Crawley *et al*., 2010; Krief *et al*., 2010; Kaniewska *et al*., 2012; Tremblay *et al*., 2013) or mesocosm settings (Anthony *et al*., 2008). Lab experiments are typically performed under constant temperature, light and regular feeding. While they allow for the precise relating of a response variable to a specific or a specific set of environmental parameters, they can be poor analogues of the naturally complex environment. Natural settings by definition are variable with multiple physical factors undergoing diurnal oscillations. Thus they hold great potential for representing how the coral and symbiont will respond to natural environmental variability over long time scales. Recently, volcanic vent systems have been used to augment lab studies by examining the response of organisms acclimated to long-term

CO_2 exposure (Fabricius *et al*., 2011; Kroeker *et al*., 2011; Hall-Spencer *et al*., 2008). Unlike lab experiments, vent systems provide unique opportunities to examine the effect of high pCO_2 in natural multifactor settings that accounts for the adaptive capability of the symbiont and its host.

Here we evaluate the effect of pCO_2 on symbiont responses both in the field, using *Acropora millepora* and *Pocillopora damicornis* growing *in situ* in a volcanic vent region, and the symbiont response in *Acropora cervicornis* grown in a controlled lab setting. The objective of the lab study was to use pCO_2 levels representing both the predicted scenarios for the end of this century (IPCC 2007) in addition to levels 2-4x higher to develop more robust estimates of the physiological response to pCO_2. The objective of the field portion of this study was to document the symbiont response in corals acclimated to decades of high pCO_2 in the natural environment. This paper presents the first assessment of changing symbiont density to elevated CO_2 *in situ* with the goal of advancing our understanding of how ocean acidification may impact coral-algal symbioses.

4.3. Methods

4.3.1 Field Methods

The study was conducted at volcanic sites at Normanby Island, D'Entrecasteaux Island group, Milne Bay Province, Papua new Guinea (Figure 4.1). At each reef, a control site and a high CO_2 site, were investigated. The results presented here are from Upa-Upasina Reef located on the north-western side of Normanby Island. At this site

the CO_2 emerges from thousands of bubble streams interspersed between bare substrate, seagrass beds and coral. Bubbling extends from <0.5 m – 5 m depth, with higher intensity in shallow regions. Village elders have confirmed that these seeps have been active in this location for the duration of their life spans, a fact that is reflected in the local site name "Illi Illi Bua Bua" which translates to "Blowing Bubbles". Currents are weak, longshore and tidal, with a range from 2-4 cm s^{-1} during the time of this study. The Upa-Upasina control site was located 500 m south of the seep site and contained similar depths and topography.

A small boat was used with a real-time pCO_2 monitoring system composed of a LiCor 820 Infrared Gas Analyzer, submersible pump and showerhead equilibrator to sample water ~ 1 m above the benthos. The site CO_2 levels were mapped prior to taking coral samples, and discrete water samples for later analysis were also taken. For discrete samples, a Niskin bottle or divers were used. Temperature and salinity were assessed immediately using a YSI model 30 Portable Conductivity, Salinity and Temperature Meter. Two aliquots were fixed with mercuric chloride and stored in 125 ml PET bottles for determination of total alkalinity using an open-cell Gran titration and analysis of dissolved inorganic carbon using an UIC Coulometer system. Other seawater parameters such as Ω and pCO_2 were calculated from pH, total alkalinity, salinity and temperature using CO2SYS. For more details, please refer to Carbonate Chemistry section in Chapter 1 of this thesis. For more details on volcanic gas sampling methodology, please refer to Fabricius *et al.* (2011).

Coral samples were collected (Figure 4.2) using scuba from a depth of ~3 m and placed in small ziplock bags. One branch per colony was collected from Upa-Upasina

reef for a total of 29 samples of *Acropora millepora* (n=15 control site, n=14 high CO_2 site) and 56 samples of *Pocillopora damicornis* (n=29 control site, n=27 high CO_2 site). Samples were stored submersed at *in situ* temperatures for a maximum of 3-5 hours before preservation in 90% ethanol using 1.5 ml Eppendorf tubes. Ethanol was replaced after 24 hours to ensure sufficient preservative to tissue volume proportions.

DNA from *A. millepora* and *P. damicornis* from high and control pCO_2 sites at Upa-Upasina were analyzed with real-time PCR (rtPCR) assays targeting the actin gene to provide an estimate of symbiont density in the form of symbiont to host cell ratios (Mieog *et al*., 2009). *P. damicornis* samples were analyzed following the methods of Cunning *et al*., (2012). *A. millepora* samples were analyzed using the same *Symbiodinium* clades C and D assays and a new assay for quantifying an actin locus in *A. millepora*. All qPCR reactions were performed using a StepOnePlus Real-Time PCR system (Applied Biosystems) in 10 µl reactions containing 5 µl Taqman Genotyping Master Mix and 1 µl genomic DNA template. The *P. damicornis* assay included 100nM forward primer (PdActF, 5´-GAGAAGCTCTGCTATGTTGCCA-3´), 200 nM reverse primer (PdActR, 5´-TCCACGGAATCGCTCGTT-3´) and 100nM Taqman probe (PdActProbe, 5´-NED-AGACTGCTGCCTCAAC-MGB-3´). The *A. millepora* assay included 900 nM forward primer (5'-CGCTGACAGAATGCAGAAAGAA-3'), 1 µM reverse primer (5'-GGACCCTCCAATCCATACAGAGT-3'), and 250 nM probe (5'-NED-TGAAGATCAAGATCATTGCCC-MGB-3'). The multiplexed Symbiodinium clade C and D assay included 50 nM clade C forward primer (CActF, 5´-CCAGGTGCGATGTCGATATTC-3´), 75 nM clade C reverse primer (CActR, 5´-TGGTCATTCGCTCACCAATG-3´), 100nM clade C probe (CActProbe, 50-VIC-

AGGATCTCTATGCCAACG-MGB'3′), 50 nM clade D forward primer (DActF, 50-GGCATGGGGTAAGCACTTCTT-3′), 75 nM clade D reverse primer (DActR, 5′-GATCCTTGAACTAGCCTTGGAAAC-3′) and 100 nM clade D probe (DActProbe, 5′-6FAM-CAAGAACGATACCGCC-MGB-3′).

4.3.2 Lab Methods

Large branches of *Acropora cervicornis* were transported from the Smithsonian Laboratory in Fort Pierce, FL to the outdoor seawater facility at the University of Miami's Experimental Hatchery (UMEH) in January 2011. All branches came from 3 neighboring colonies that aquarists believed were a single genotype; however this was not verified through genetic analysis. Polyps were seen to open upon transfer to tanks, thus the stress during transport was likely to be low. After 1 week, large branches were divided into 5-7 cm tall individual branches and affixed to plastic tiles (35 x 37 mm) using Zspar underwater epoxy as described in Davies (1995). All branches had tissue enclosed tips and were affixed so that no bare skeleton was exposed. Corals were lightly shaded after transport and breaking into branches. Shading was reduced over 3 weeks to allow for acclimation to the normal diurnal light cycle. No visible bleaching was observed during the acclimation period.

Natural light was provided in the UM Experimental Hatchery which is fitted with a transparent roof providing UV filtration and shelter from rain. Salinity was measured every 2-3 days using a YSI model 30 Portable Conductivity, Salinity and Temperature Meter while temperature was monitored remotely and checked manually biweekly. A full description of the experimental system for manipulating carbonate

chemistry and the analysis of carbonate is detailed in Chapter 1. Corals were fed weekly using smaller plastic bins suspended within the larger growth tanks, ensuring constant temperatures during the 5-6 hr feeding interval. The weekly feeding consisted of food particles from 20 μm to 500 μm in size with the total volume of food normalized to the estimated tissue biomass of the coral (Epstein *et al*., 2001). For a full discussion of the diet used, please refer to Chapter 3.

Branches of *Acropora cervicornis* were grown for 6 weeks. Twelve tanks with 9-11 branches per tank were maintained. Treatment levels were replicated using two tanks per CO_2 level to create a control and 5 levels of pCO_2, however only the results for 3 levels are presented here due to mechanical failure in a water pump that resulted in areal exposure of corals in some of the tanks.

After 7 weeks, coral branches where brought to the lab and tissue was removed from coral branches using an airbrush and filtered seawater in a process referred to as "blasting". Blastate was homogenized for a standard time period (15 seconds). Aliquots for symbiont cell counts (1.5 ml) and chlorophyll *a* (1 ml) were removed from the total blastate for analysis while the skeleton was used to assess surface area.

Aliquots for symbiont cell count were stored in Eppendorf tubes with 0.5 ml Lugols solution for preservation and stored in the dark until analysis. Before counting cells, samples were vortexed thoroughly and visually assessed for clumps of cells. A haemocytometer was used to make triplicate counts of each sample with over 100 cells counted per loading of the haemocytometer. The absolute magnitude of cells per coral varied by treatment level, however the standard deviation of replicate counts of the same coral averaged only 14% of the total. For example, a sample counted in triplicate has an

average of 371 ± 51 cells per loading of the haemocytometer. Cell counts were normalized to surface area measured using the wax dipping technique (Stimson and Kinzie, 1991). This method uses objects of known surface area (wood dowels) and weight to create a correlation between wax weight and surface area. Corals are then weighed before and after dipping in wax to back calculate the surface area. The r^2 of wax weight on dowels to surface area attained was 0.98, thereby allowing for a highly precise back calculation. This method was chosen for its accuracy specifically for branching coral species (Veal *et al*., 2010).

Aliquots for chlorophyll *a* analysis (1ml) were placed in glass vials with 9 ml of 90% acetone and extracted in a -80°C for 28-30 hours. Time of extraction was carefully maintained to vary only by 2 hours per set of samples extracted to avoid introducing variability. After extraction, samples were brought to room temperature (20 minutes), kept out of direct sunlight and vortexed, before being further diluted with acetone to bring the fluorescence into the range of the fluorometer being used. Fluorescence was measured using a Fluorometer TD-700 (Turner Designs) before and after acidification with 1 drop of 10% HCl. The follow equation was used to calculate the concentration of chlorophyll *a*.

Equation 4.1 $$Chla = (1*10^{-3}) * D * (K * T) * (Fo-Fa)$$

where Chla is the amount of the pigment in the coral tissue sample in μg, the factor 10^{-3} converts from liters to milliliters, D is the overall dilution with acetone, K is the calibration constant (K = 0.0000892904 μg mL^{-1}), T is the maximum ratio of

chlorophyll *a* fluorescence before and after adding acid (T = 1.885908293), Fo is the first fluorescence reading, Fa is the second fluorescence reading after acidifying the sample. Sensitivity analyses of the fluorescence reading for the amount of HCl added and the time between removal from the -80 C were completed and found to be negligible (<1%). Chlorophyll *a* methodology was adapted from Jones *et al.* (1997) and Hitchcock *et al.* (1993).

4.3.3 Statistical Methods

To test for the effects of pCO_2 on symbiont density and chlorophyll *a*, we used linear regression analysis with pCO_2 as an explanatory variable. Normality was tested using a goodness of fit test and equal variance was assessed by plotting the residuals versus. predicted residuals. For lab experiments, the variable of incubation tank was nested in the pCO_2 treatment and found to be insignificant ($p<0.05$); therefore data from replicate tanks was pooled for statistical analysis.

Field data were log transformed to approximate normality. Normality was tested using a goodness of fit test and equal variance was assessed by plotting the residuals versus predicted residuals. Linear regression analysis was used to asses the effect of pCO_2 on symbiont to host cell ratio. All statistical analyses were performed using Microsoft Excel and JMP statistical software (SAS institute, Version 10, Cary, NC).

4.4. Results

4.4.1 Field Results

The gas composition emitted from the volcanic vents was analyzed and found to have no detectable hydrogen sulfide (H_2S_2), nitrous oxide (N_20) or (C_2H_4) ethylene. Carbon dioxide made up > 99% of the composition, with minor amounts of oxygen (0.5%), nitrogen (0.1%) and methane (CH_4, 87 μatm, < 0.4%). Carbonate chemistry in the field is most strongly affected in waters closest to a bubble stream and reaches ambient levels within <0.1 m of a gentle bubble stream and at < 5 m near vigorous bubble streams. The seep sites tend to be a mosaic of high pCO_2 sites surrounded by normal pCO_2. At the seep site of Upa-Upasina, median pH was 7.77 however the reductions in pH were less on windy than on calm days, due to mixing. Carbonate chemistry for the site is reported in Table 4.1 and mapped in Figure 4.2.

Symbiont to host cell ratio was significantly reduced in both species at the high CO_2 site (846 μatm). In *A. millepora* the symbiont to host cell ratio was reduced significantly ($F_{1,27}$=9.962; *P*=0.0039, Table 4.2) with an average percent reduction of 54% between control and high pCO_2 (Figure 4.3). In *P. damicornis* the ratio was similarly reduced by 32% which was significantly different ($F_{1,55}$=5.7310; *P*=0.0201, Table 4.3) between the high (n=26) and control (n=29) pCO_2 sites (Figure 4.4). Neither clade C nor clade D was found to be consistently associated with high pCO_2 conditions in the field. In the lab *A. cervicornis* contained only clade A, thus variation in the clade community due to pCO_2 could not be tested.

4.4.2 Lab Results

Salinity and temperature were not significantly different between tanks receiving replicate pCO_2 levels nor between tanks receiving different pCO_2 levels ($p<0.05$). Average salinity and temperature for all corals averaged across tanks was 36.6 and 27.1 ° C, respectively. Carbonate chemistry maintained in replicate tanks (n=8) was not statistically different within pCO_2 levels (n=4). Average pCO_2 data is provided in Table 4.4.

Average symbiont density per pCO_2 level is provided in Table 4.5. Elevated pCO_2 exhibited a significant treatment effect on the density of symbionts in *Acropora cervicornis* ($F_{3,34}$ =4.1931, P = 0.0125) (Table 4.6). Symbiont density data from replicate tanks were not significantly different (P = 0.10) thus tanks receiving the same pCO_2 were pooled and the total data set analyzed using simple linear regression. Symbiont density decreased by 26% from the control pCO_2 (318 µatm) to the highest pCO_2 at 4567µatm (Figure 4.5). Normalizing the drop in symbiont density to pCO_2 shows a decline of 3% for every 500 µatm rise in pCO_2.

Elevated pCO_2 did not exhibit a significant treatment effect on the chlorophyll *a* concentration per symbiont in *A. cervicornis* ($F_{3,34}$ =2.165, P < 0.279) (Table 4.7). Data from replicate tanks were not significantly different (P = 0.45) thus tanks receiving the same pCO_2 were pooled and analyzed using simple linear regression. Symbiont chlorophyll *a* concentration and cell counts are provided in Table 4.5. Chlorophyll *a* decreased by 51% from the control pCO_2 to the highest pCO_2 (318 to 4567 µatm; Figure 4.6). Normalizing the drop in chlorophyll *a* to pCO_2 shows a decline of 7% for every 500 µatm rise in pCO_2.

4.5. Discussion

4.5.1 Lab

Our current understanding of the impacts of ocean acidification (OA) on coral symbioses is still in its infancy due to a limited number of laboratory experiments and a lack of research carried out *in situ*. Other short-term experimental studies have yielded contradictory responses (increases and decreases) in chlorophyll *a* concentration, while symbiont density declines to varying degrees under high CO_2 (Table 4.8). Symbiont density declined significantly in this study, though the magnitude of the decline was variable between different pCO_2 levels. The largest decline in symbiont density observed was a 26% reduction between the control pCO_2 (318 µatm) to the highest pCO_2 at 4567µatm (Figure 4.5).

Lab experiments are an effective tool for isolating the effect of specific variables applied in increasing intensities, in order to display the nature of the relationship between a predictor and response variable. Here we use 4 levels of pCO_2 ranging from 318 µatm to 4567 µatm to create a robust test of the symbiont response to ocean acidification. In the laboratory setting, we found that increasing pCO_2 caused a gradual decline in symbiont density in *Acropora cervicornis*. There was 20% decline from control conditions (318 µatm) to a pCO_2 of 611 µatm for both symbiont density and chlorophyll *a*, implying that symbionts are sensitive to mild changes in pCO_2. As pCO_2 increased further, the magnitude of the decline shows variability and may indicate acclimation processes and/or host-symbiont mediation such as changes in gene

expresses in response to increased pCO_2 (Kaniewska *et al*., 2012). In the highest level of 4567 µatm, both the density of the symbionts and the chlorophyll *a* concentration within each symbiont was substanually depressed (Figure 4.5 and Figure 4.6) indicating that the overarching relationship between OA and symbionts is one of decline.

Incorporating higher pCO_2 levels in experimental settings may also have more environmental application than previously thought; as recent modeling by Shaw *et al*. (2013) shows that the diurnal metabolism of the benthic community can greatly alter the diurnal pCO_2 fluctuations. Shaw *et al*. (2013) predict that diurnal exposures as high as 2100 µatm may be reached within 100 years in shallow reef flat areas due to biological CO_2 metabolism in coastal areas. The diurnal fluctuations are also predicted to increase further due to changes in the buffering capacity of coastal water, thus the high pCO_2 levels (>3000; Table 4.8) used in many recent experiments (e.g. Krief *et al*., 2010, Tremblay *et al*., 2013) both allow us to overcome some of the inherent variability in the organismal response and may be more realistic that previously assumed.

Other lab studies have also found reductions in symbiont density under high pCO_2 but with a wide range in the degree of symbiont loss. A number of other varying factors, such as light, temperature, experimental ranges in pCO_2 levels, make direct comparisons between the studies challenging, however parsing their results by the broad categories of the pCO_2 level used provides a framework for comparison (Table 4.8). An increasing number of lab studies have utilized pCO_2 levels >2000 µatm, perhaps as a method of coping with the inherently high variability in the organismal response. Tremblay *et al*. (2013) utilized levels of 3898 µatm, only ~600 µatm lower than in this study and found symbiont declines 2 fold larger (48%). We show a 26% decline in

symbiont density at 4567 µatm, comparable to the 20% decline found by Krief *et al*.,. (2010) in 3976 µatm and 1908 µatm pCO_2 levels. While pCO_2 levels > ~3000 µatm are not expected to occur in the next century, including them in experimental simulations can help clarify the relationship between physical and organism parameters when variability in the degree of the response occurs (see Table 4.8). While the degree of decline may be variable, the existing literature typically shows symbiont declines of 20-50% in pCO_2 levels >2500 µatm.

Symbiont density in response to lower experimental pCO_2 levels (<2500 µatm) seem to show higher variability across experiments. For instance, Crawley *et al*. (2010) show no effect of pCO_2 on symbiont density at 600-790 µatm, although the experimental incubation time of four days may have been too short for the symbiont and host to fully respond. Using pCO_2 levels in the range of 760-1500 µatm, symbiont declines have been reported to decrease strongly by 40-50% (Kaniewska *et al*., 2012), to decrease minimally (10%, this study) or even display increases in symbiont density (Reynaud *et al*., 2003). However it should be noted that the later study normalized in a unique manner (cell specific density) that is not commonly used and may complicate direct comparisons.

Chlorophyll *a* levels of *A. cervicornis* grown in the lab declined broadly but with variable magnitudes as pCO_2 increased. The maximum depression in chlorophyll *a* was 51% at 4567 µatm (Figure 4.6). Similar to this study, Tremblay found a decline of 42% in chlorophyll *a* per cm^{-2} under a pCO_2 of 3898 µatm. However other researchers have found no change in chlorophyll *a* in response to lower levels pCO_2 such under 1908 µatm (Krief *et al*., 2010) or 760 µatm (Reynaud *et al*., 2003). Additional, reports of

increased chlorophyll *a* has also been found under pCO_2 levels of 3976 µatm (Krief *et al*., 2010) and 1160-1500 µatm (Crawley *et al*., 2010). While our findings are inconsistent with those of Crawley *et al*. (2010), who finds CO_2 enrichment can increase chlorophyll *a* per cell and enhances photoacclimation, we note that the time frame of the two experiments (4 days versus the 6 weeks used here) may preclude direct comparison. Changes in gene expression may also play a role in longer term experiments, as Kaniewska *et al*. (2012) found evidence of changes to respiration, photosynthesis and symbiosis after 28 days of increased pCO_2.

When considering declining symbiont density under increasing pCO_2, two viewpoints emerge from the literature. First, the decline in symbionts can be viewed as a stress response, due to a breakdown in the symbiotic relationship in response to changes in carbon-concentrating mechanisms, photorespiration, and/or the impacts of acidosis (Anthony *et al*., 2008; Kaniewska *et al*., 2012). Examples of this have been found in the lab under sub-saturating light levels combined with high pCO_2, resulting in decreased productivity (Crawley *et al*., 2010), while studies using *in situ* light with increased pCO_2 resulted in synergistic effects on symbiont decline (Anthony *et al*., 2008). Using this perspective, the changes in symbiont density observed here would be considered evidence of additional stress on the host and evidence of the breakdown of symbiosis in response to pCO_2. Alternatively, the decline in symbiont density can be viewed less as a stress response, and more as an acclimation to changing physical parameters. This occurs in response to other physical parameters, such as the response to normal seasonal differences in light and temperature (Stimson, 1997; Fitt *et al*., 2000; Fagoonee *et al*., 1999). Seasonal differences in optimal temperature creates time

periods for optimal growth and photosynthetic rates while adjustments in carbon fixation in the symbiont responds to seasonal light changes (Fitt *et al*., 2000). These fluctuations provoke significant changes in symbiont density on an annual cycle, leading to theories about the impact on host fitness throughout the year (Fitt *et al*., 2000). While seasonal fluctuations in symbiont density have been correlated to seasonality in host tissue biomass, they do not necessarily cause a change in autotrophic energy acquisition by the host (Hoogenboom *et al*., 2010). In addition, recent research on autotrophic energy acquisition under increasing pCO_2 indicates that the host carbon budget may be unchanged by declines in symbiont density (Tremblay *et al*., 2013). Tremblay *et al*. (2013) found that symbionts exposed to low pH (7.2; 3898 μatm) translocated more of the photosynthetic carbon they produced, thus retaining less for their own growth and reproduction. The 10% reduction in photosynthate translocation was associated with a 48% decline in symbiont density in *Stylophora pistillata*. This suggests that the greater percentage of carbon translocated from the symbiont to the host, then reduces the carbon available to the symbiont for growth and cell division; potentially providing a mechanism for the reduction in symbiont density. Whether the symbiont response to increasing pCO_2 represents a strong stress response or more of an adjustment to the changing physical conditions is beyond the scope of this research, but is a theoretical perspective that plays an important role in how we view the effects of ocean acidification on corals.

4.5.2 Field

While laboratory experiments provide a critical tool for our understanding of specific relationships, naturally occurring CO_2 vents can provide an important and complementary system to examine the impact of ocean acidification acting in conjunction fluctuating parameters in the natural environment. Symbiont density in response to long-term ocean acidification in the field declined an average of 48% under an 846 μatm average pCO_2. Both species showed similar declines (42% and 53%, *Pocillopora damicornis* and *Acropora millepora*, respectively), thus there is no indication that the effect of pCO_2 on symbiont density is coral species specific.

There is a contrast between the field and laboratory results presented here, as pCO_2 in the lab provoked a more muted symbiont decline compared to high CO_2 levels at natural venting sites. In the laboratory setting we measured a maximum of a 26% decline in symbiont under pCO_2 of 4567 μatm, but also variable declines of 10% under 2309 μatm and 20% under 611 μatm. However all of these are substantially less than the 48% decline in symbiont density in the field exposed to pCO_2 levels with an average of only 846 μatm. The decline in the field is also larger than most existing lab studies. Only 2 lab studies showed similar declines, and either used high light (maximum of 1000 (μmol photons m^{-2} s^{-1}, Kaniewska *et al*., 2012) or 4-fold higher pCO_2 (Tremblay *et al*., 2013; Table 4.8). Part of the contrast between laboratory and *in situ* observations may be due to temporal factors that can impact perturbation experiments, but would be absent from organisms growing near natural vents. First, short-term perturbation experiments such as those performed here may not represent a fully acclimated organismal response, since increased pCO_2 seems to result in a cascade of altered gene

expression (Kaniewska *et al*., 2012). Second, organisms in perturbation experiments can be stressed and may undergo behavioral modifications that can shift their response to ocean acidification. Some coral species that are artificially stressed and lose their symbiont populations in lab have shown increased heterotrophy and subsequently recover their symbionts more quickly after bleaching stress (Grottoli *et al*.,. 2006). It's possible that the corals in this experiment which were exposed to ample prey during weekly feeding, may have altered their heterotrophic effort under high pCO_2, leading to increased symbiont density. Increased heterotrophic input may provide an ecological advantage both to the host as well as increasing nitrogen for symbionts (Piniak & Lipschultz, 2004), chlorophyll *a* and symbiont density (Grottoli, 2002; Titlyanov *et al*., 2000a,b, 2001). *Recent research suggests that a greater percentage of carbon is translocated from the symbiont to the host under increased pCO_2, reducing the carbon available to the symbiont for growth and cell division and potentially providing a mechanism for the reduction in symbiont density.* While lab conditions are created to be as realistic as possible, the differences between the lab and the field underscores the importance of utilizing *in situ* data as an important complementary system for modeling the impact of changes in pCO_2 in the natural environment.

While the clade of symbiont hosted has been shown to vary in response to factors such as temperature (Baker *et al*., 2004) and nutrients (Baker *et al*., 2013), we do not see significantly more of one particular clade (C or D) at high CO_2 sites. *A. cervicornis* in the lab hosted only clade A, thus shifts in the proportion of clades could not be assessed. To fully assess the potential of clade community shifts under OA *in*

situ may require incorporating more intensive sampling along with environmental monitoring (e.g. pCO_2, temperature and light) at the vent site (Fabricius *et al*.,. in prep).

This study utilizes recent advances in molecular biology to assess symbiont density, which uses the number of host cells as a normalization factor (See Cunning *et al*., 2012). Changes in the number of host cells between high and low pCO_2 sites could therefore influence the S/H cell ratio observed in the field. The magnitude of the decline in symbiont density observed in the field was 2 fold larger (26% versus 48%) at pCO_2 levels ~4 fold less than those in the lab, thus it is highly unlikely that changes to this degree could be caused by changes in host cell number. In addition, as host cells are lost, symbionts are expelled as a regulatory mechanism to maintain cell ratio densities below a critical threshold (Cunning *et al*., 2012). Overall, normalization of symbiont density to host cell number may be a more physiological meaningful metric than normalizing to surface area (Cunning *et al*., 2012).

While the field setting is inherently more variable than the lab, there is no indication of strong physical differences between the high and control CO_2 field sites or strong physical site factor occurring in this system (See Fabricius *et al*., 2012). Physical factors potentially affecting symbiont density in the field include factors such as salinity, nutrients and temperature. No anomalous salinities were recorded during our short duration (7 days) at field sites in Papua New Guinea, however the yearly oscillations in salinity or freshwater input from land is unknown. Fortunately, tropical cycles are rare at this latitude and the nearly 100% vegetation cover on the island would minimize terrestrial runoff (Fabricius *et al*., 2011). Prior environmental data for this extremely remote location are sparse, thus it is also unknown if corals experienced high

temperature prior to collection, however no visible bleaching was observed. Severe coral bleaching did occur in the Milne Bay region in 1996 as well as minor bleaching in 1998 and 2000-2001. Aside from these events, the relatively high coral cover and information from by the local native community suggests that reefs in this island region have had relatively low mass bleaching events since the 1996 event.

Perturbation studies in the lab are useful to reveal the specific relationship between pCO_2 and an organism; however a missing link in our understanding lies in the long-term *in situ* response to increased ocean acidification. Coastal ecosystems can have strong pCO_2 oscillations (100-300 μatm) on a seasonal (Chapter 2) and diurnal scales (Manzello, 2010, Ohde & van Woesik, 1999, Shamberger *et al*., 2011, Shaw *et al*., 2012, Yates & Halley, 2006), thus organisms in the field may be exposed to and already adapted to intermittently high pCO_2 (Hofmann *et al*., 2011). Simultaneous oscillations in other environmental factors such as light and temperature are known to have important impacts on the physiological response of marine organisms (Somero *et al*., 2012) and could interact with increased pCO_2 levels. The *in situ* light and temperature changes on an annual scale already create seasonal oscillations in symbiont density (Fitt *et al*., 2000) and photosynthetic capacity (Warner *et al*., 2002). Thus, the natural oscillations of light and temperature could contribute the higher decline of *in situ* symbionts observed in this study.

4.5.3 Conclusion

This study found that symbiont densities declined in 3 different species in response to increased pCO_2, in both the laboratory setting, and *in situ*. The use of

volcanic vent sites to provide a natural proxy for ocean acidification allows us to examine the long-term response in the field (decades) versus the comparable short term (weeks) response in the laboratory. While we observe a 2-3 fold greater effect of pCO_2 in the field with declines in symbiont density that was consistent in both species; further study is needed to understand the factors that contribute to the amplification of the CO_2 effect *in situ*. Ocean acidification research is only beginning to be augmented with *in situ* experiments, thus naturally occurring CO_2 vent sites like the ones studied here provide unique systems to evaluate coral and symbiont responses to long-term changes in pCO_2 and serve as an important complement to experimental work in the lab setting. The observed symbiont declines under high pCO_2 are robust in that they occur across species and in very different settings (lab versus field), supporting the idea that the effect of ocean acidification on symbionts needs to be part of our predictive models.

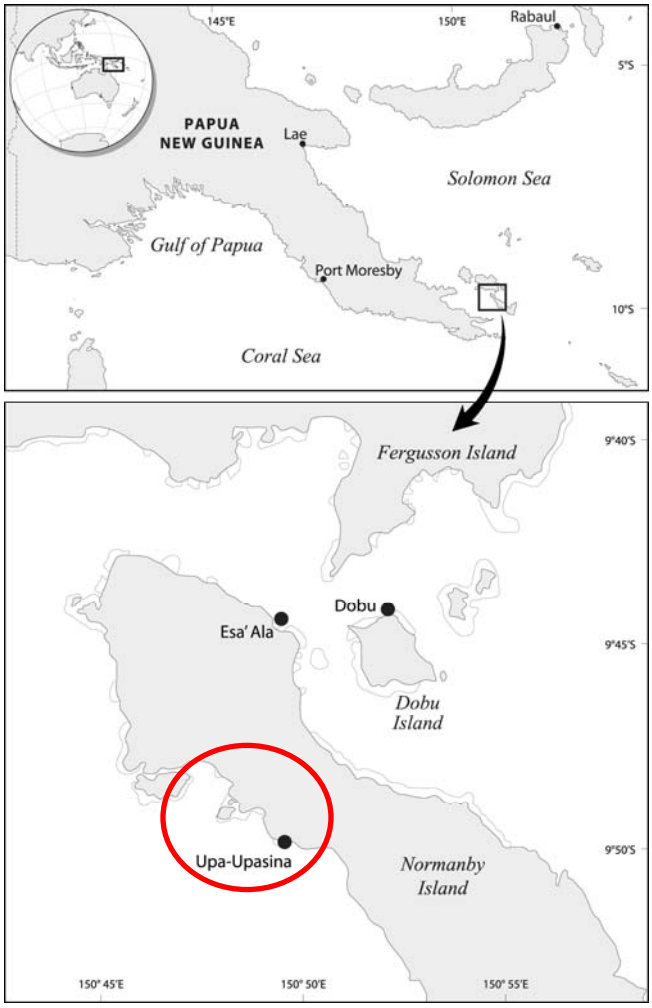

Figure 4.1. Location of volcanic vents releasing CO_2 into the local reef ecosystem in the Central Pacific, Papua New Guinea. Results presented here are from the site Upa-Upasina.

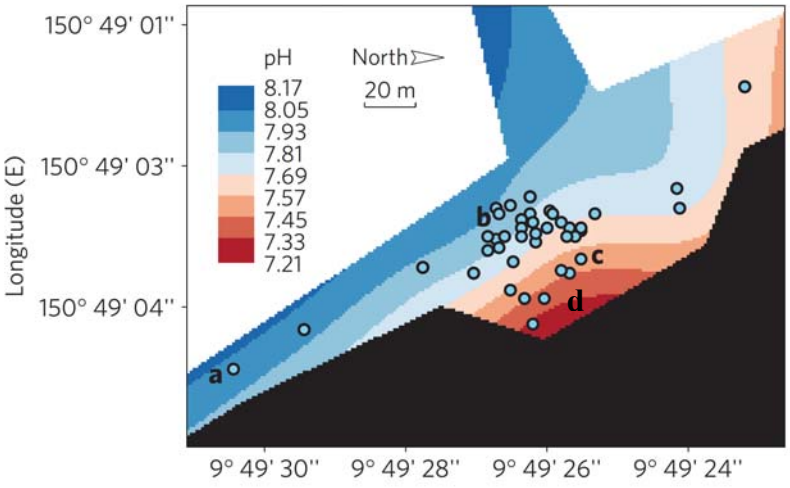

Figure 4.2. Map of the pH conditions at the Upa-Upasina site in Papua New Guinea. Dots represent sites where collaborative work was completed and coral samples were taken from “a” and “d”.

	Salinity	T (°C)	pH_T	pCO_2 (μatm)	Ω
Control (N=6)	34.5 (34.5, 34.6)	27.7 (27.4, 28.6)	8.01 (7.99, 8.02)	443 (416, 456)	3.48 (3.35, 3.66)
Vent site (N=31)	34.5 (34.4, 34.6)	27.6 (27.4, 28.1)	7.77 (7.02, 7.99)	846 (454, 5737)	2.28 (0.49, 3.37)

Table 4.1. Median values of the physical and chemical conditions at volcanic vents in Papua New Guinea at Upa-Upasina reef. Values in parentheses are the 5th and 95th percentile, respectively. Samples of coral symbionts were obtained from *Acropora millepora* and *Pocillopora damicornis*. All chemical measurements are based upon duplicate or triplicate analyses for each sample. pH_T, pCO_2, HCO^{3-}, CO_3^{2-} CO_2, TCO_2, and Ω_a were calculated using CO2SYS. For full data set please refer to Fabricius *et al*., 2011, supplemental materials.

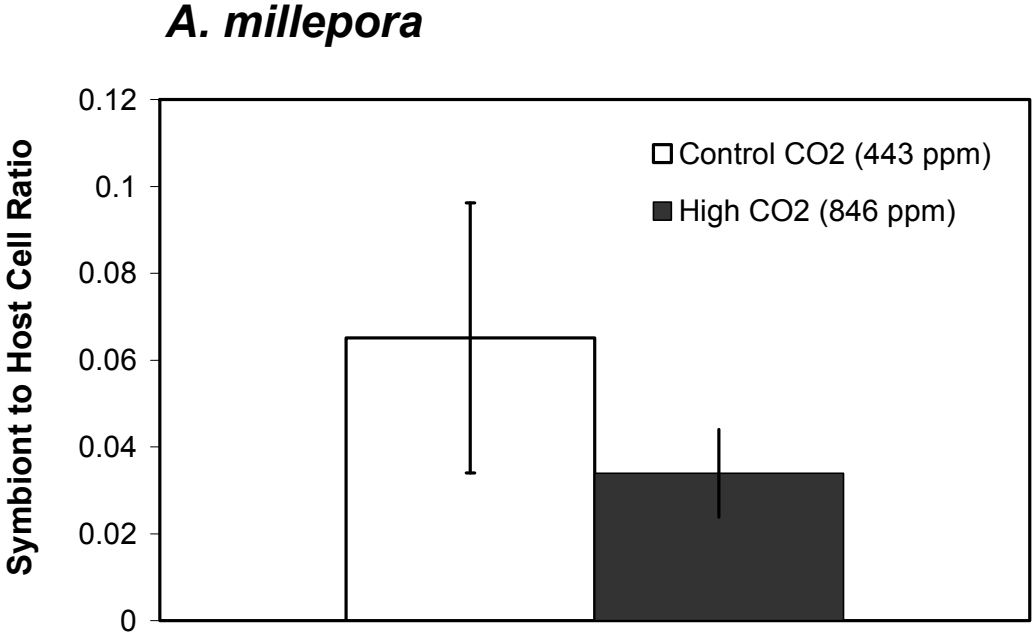

Figure 4.3. *Acropora millepora* quantitative PCR results show reduced symbiont to host cell ratios of 54% at high CO_2 site (Upa-Upasina) at Papua New Guinea. Error bars are the 95% confidence intervals calculated from the standard deviation of non-log transformed data. High pCO_2 site has an n=14 and control site has an n=13.

Title					
ANOVA	DF	SS	MS	F ratio	P
Treatment	1	0.5782	0.5782	9.962	0.0039
Residual	27	1.5670	0.0580		
Total	28	2.1452			

Table 4.2. Analysis of variance table of the symbiont to host cell ratio in *Acropora millepora* from the control and high pCO_2 volcanic vent site Upa-Upasina in Papua New Guinea.

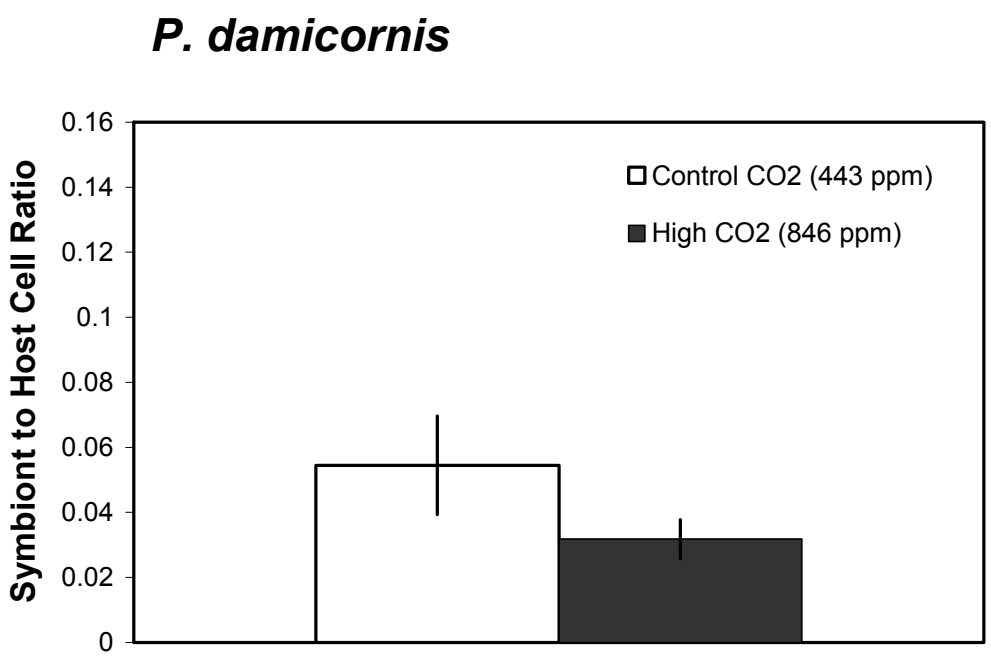

Figure 4.4. *Pocillopora damicornis* quantitative PCR results show reduced symbiont to host cell ratios at high CO_2 sites at Upa-Upasina site in Papua New Guinea. Error bars are the 95% confidence intervals calculated from the standard deviation of non-log transformed data. High pCO_2 site represents an n=27 and the control site has an n=29.

Title					
ANOVA	DF	SS	MS	F ratio	P
Treatment	1	0.6150	0.6150	5.7310	0.0201
Residual	55	5.9029	0.1073		
Total	56	6.5179			

Table 4.3. Analysis of variance table of the symbiont to host cell ratio in *Pocillopora damicornis* from the control and high pCO_2 volcanic vent site Upa-Upasina in Papua New Guinea.

	Salinity	T (°C)	pH_T	pCO_2 (ppm)	Ω
Control	36.3 ± 0.4	27.1 ± 0.3	8.08 ± 0.04	318 ± 33.8	3.62 ± 0.31
Level 1	36.6 ± 0.4	27.1 ± 0.4	7.82 ± 0.05	611 ± 76	2.23 ± 0.31
Level 2	36.6 ± 0.4	27.1 ± 0.4	7.33 ± 0.07	2379 ± 333	0.89 ± 0.10
Level 3	36.7 ± 0.4	27.2 ± 0.4	7.08 ± 0.05	4567 ± 574	0.52 ± 0.06

Table 4.4. Physical and chemical conditions of aquaria during growth experiment with *Acropora cervicornis*. All chemical measurements are based upon duplicate or triplicate analyses for each sample. pH_T, pCO_2, HCO^{3-}, CO_3^{2-}, CO_2, TCO_2, and Ω_a were calculated using CO2SYS. Average ± standard deviation. Replicate tanks were not significantly different ($p<0.05$). Light in the lab was an average of 331 μmol photons m^{-2} s^{-1} at noon, 247 μmol photons m^{-2} s^{-1} averaged over the day and maximum of 756 μmol photons m^{-2} s^{-1}.

Acropora cervicornis grown in the Laboratory				
pCO_2 level	Control	Level 1	Level 2	Level 3
	318 ppm	611 ppm	2379 ppm	4567 ppm
Symbiont density ($*10^6$ cm^{-2})	19 ± 1 (9)	15 ± 1 (11)	18 ± 1 (9)	15 ± 1 (9)
Chlorophyll *a*	0.79 ± 0.04	0.55 ± 0.03	0.76 ± 0.04	0.30 ± 0.04
(pg per cell)	(9)	(11)	(9)	(9)

Table 4.5. Average ± standard error (sample size) of symbiont density and chlorophyll *a* per symbiont in *Acropora cervicornis* across 4 levels of carbon dioxide for six weeks.

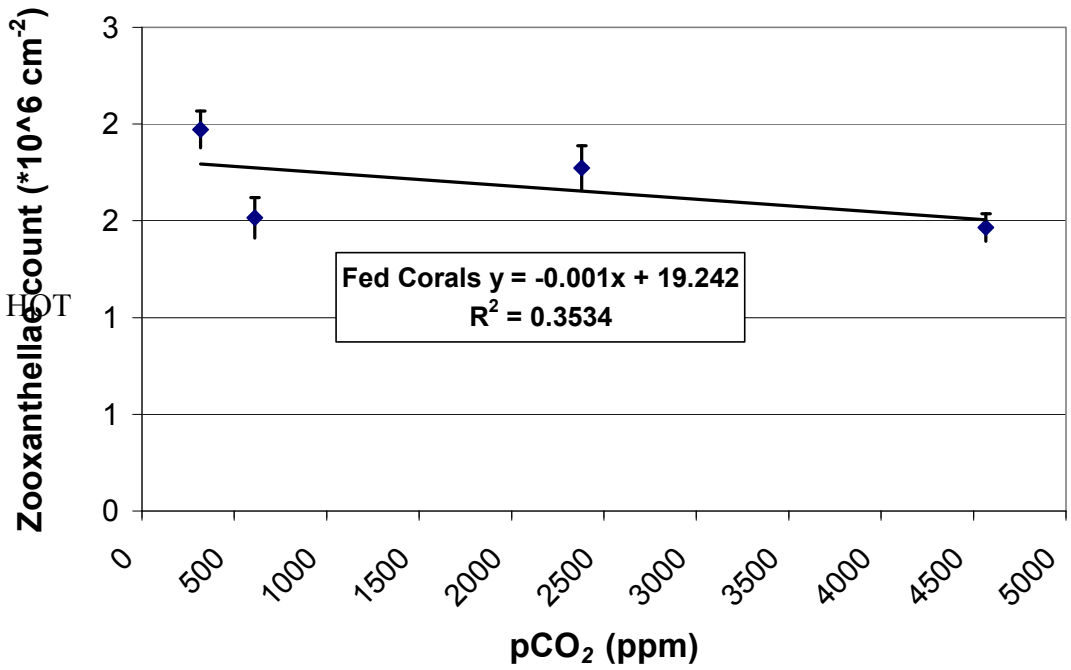

Figure 4.5. Symbiont density in *Acropora cervicornis* as measured by cell counts. Error bars are standard error. Sample sizes were as follows: N=9 (4567 ppm), N=9 (2379 ppm), N=11 (611 ppm), N=9 (318 ppm).

Linear Regression Analysis					
	DF	SS	MS	F ratio	P
Treatment	3	155.4207	51.8069	4.1931	0.0125
Residual	34	420.0775	12.3552		
Total	37	575.4982			

Table 4.6. Results of simple linear regression analysis with predictor factor pCO_2 and response variable as symbiont density (p= 0.10). The assumptions of a normality and homoscedasticity (equal variances) were met. Analysis done on average values per treatment. Slope of the regression was -0.000084 ± 0.0024. R^2 reported by regression statistic using excel was 0.35.

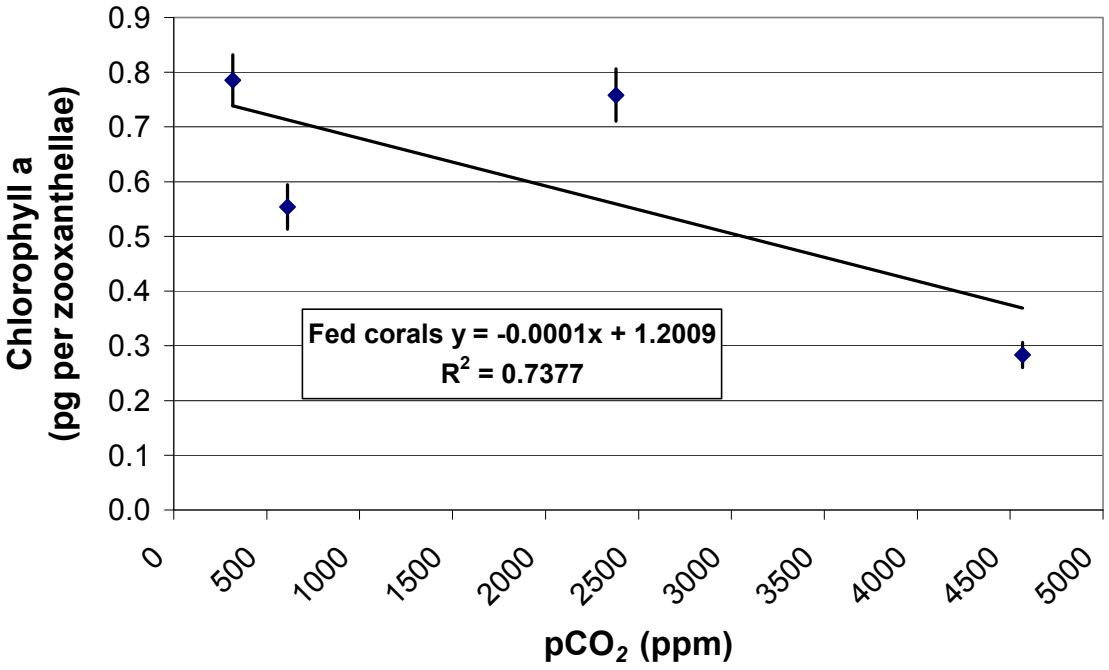

Figure 4.6. Chlorophyll *a* concentration in *Acropora cervicornis* Fed corals. Error bars are standard error. Sample sizes were as follows: N=9 (4567 ppm), N=9 (2379 ppm), N=11 (611 ppm), N=9 (318 ppm).

Linear regression Analysis					
	DF	SS	MS	F ratio	P
Treatment	1	0.0801	0.0816	2.165	0.279
Residual	2	0.0740	0.03702		
Total	3	0.1542			

Table 4.7. Results of simple linear regression analysis with predictor factor pCO_2 and response variable as chlorophyll *a* . The assumptions of a normality and homoscedasticity (equal variances) were met. Analysis done on average values per treatment.

Table 4.8. Comparisons of symbiont density and chlorophyll *a* responses to increased pCO_2 across recent studies. Light is in units of (μmol photons m^{-2} s^{-1}). NS is not significant.

pCO_2 level μatm	Source of light	Light	Time	Species	Symbiont density per cm^{-2}	Chloro. *a* cm^{-2} or symbiont	Source
520-700	natural	1000	8 wks	*Acropora intermedia Porites lobata*	↓10-20% (luminance)	n/a	Anthony *et al*. (2008)
611	natural	331	7 wks	*Acropora cervicornis*	↓ 23%	↓ 29%	this study
600-790	lab	110	4 days	*Acropora formosa*	NS	↑	Crawley *et al*. (2010)
760	lab	350	5 wks	*Stylophora pistillata*	↑ (normalized to host cells)	NS	Reynaud *et al*. (2003)
1000 - 1300	natural	1000	8 wks	*Acropora intermedia Porites lobata*	↓ (luminance)	n/a	Anthony *et al*., (2008)
1010 - 1350	lab	443 av. 1000 max	28 dys	*Acropora millepora*	↓ 50%	n/a	Kaniewska *et al*. (2012)
1160 - 1500	lab	110	4 dys	*Acropora formosa*	NS	↑	Crawley *et al*. (2010)
1908	lab	200	6-14 mths	*Stylophora pistillata & Porites sp.*	↓ 20%	NS	Krief *et al*. (2010)
2369	natural	331	7 wks	*Acropora cervicornis*	↓ 10%	↓ 3%	this study
3898	lab	140	6 mths	*Stylophora pistillata*	↓ 48%	↓ 42%	Tremblay *et al*. (2013)
3976	lab	200	6-14 mths	*Stylophora pistillata & Porites sp.*	↓ 20% same as 1908 ppm	↑	Krief *et al*. (2010)
4567	natural	331 av. 756 max	7 wks	*Acropora cervicornis*	↓ 26%	↓ 61%	this study

Chapter 5: The Relationship between Calcification and Aragonite Saturation State (Ω) on Symbiotic Corals and on the Coral Reef Tract

5.1 Summary

The studies described in this dissertation demonstrate, for both corals and coral reefs, the relationship between changing seawater chemistry and calcification is directly proportional. However, the degree of decline in calcification per unit aragonite saturation state (Ω) differs greatly between the coral reef and corals in the laboratory. In addition, the threshold for calcification in the lab can be alleviated by heterotrophy. Thus, our evidence shows the Ω thresholds for coral growth versus coral reef growth are vastly different, and that using experimental evidence of coral calcification declines to predict reef loss, may seriously underestimate when reefs will transition from reef growth to a net reef loss. For example, results of yearly surveys of the Florida Reef Tract show that calcification rates decline proportionally with aragonite saturation state (Ω) and shift from net reef growth in summer months, to net reef loss in winter months. In winter months, dissolution occurs at a Ω of 3.63, indicating that the Florida Reef is seasonally crossing the threshold for net carbonate production at a relatively high saturation state. Comparatively, in the laboratory we observe calcification in scleractinian coral to also decline linearly with Ω, however we did not detect dissolution despite 2 levels of Ω undersaturation. The calcification of *Acropora cervicornis* in undersaturated water occurred despite declining amounts of the symbionts and was strongly dependent on heterotrophy in the coral host. Heterotrophy in the host resulted in a 3% to 7% increase in growth rates in each Ω level, indicating the potential for

heterotrophy to alleviate, but not erase, the declines in calcification due to ocean acidification. The strong difference in the thresholds for coral reef calcification *in situ*, versus those in the laboratory indicate that using experimental studies to predict reef growth may grossly underestimate the risks due to ocean acidification. The implications of these findings are discussed below.

5.2. Coral Reef Calcification

Field surveys encompassing 210 km of the Florida Reef Tract over 2 years indicate that the processes of calcification and dissolution are closely tied to seasonal production and respiration rates of the benthic community. Seasonal oscillations over both years were observed, with strong correlations between production and calcification in summer, and respiration and dissolution occurring in winter. The combined ecosystem metabolism, meaning both the processes of calcification and production, has an strong impact on coastal carbonate chemistry as oceanic waters move over the reef. In summer, the slope (0.56) of the coastal metabolism line on TA-DIC property-property plots crosses the isopleths of aragonite saturations state (Ω) and results in an elevation of the Ω. Conversely, in winter the coastal metabolism results in the net production of carbon dioxide which depresses Ω, resulting in a difference between average summer and winter Ω of 0.46. Temporally, Ω shows seasonal trends across the entirety of the Florida Reef Tract, but also displays additional spatial trends that occur within seasons. In the summer, the inshore waters show bands of higher Ω, due to the high summer primary productivity that draw down carbon dioxide and elevates Ω in coastal waters. The spatial trend reverses in winter, with inshore regions showing lower

Ω than offshore waters due to carbon dioxide released during net respiration, consequently depressing Ω in winter months.

The net effect of these biological processes alters the carbonate chemistry of oceanic waters and results in seasonal net dissolution. The mechanism for dissolution on the reef may stem from multiple processes acting in conjunction, including bioerosion, microbial remineralization and hydraulically driven pore water. Background levels of dissolution may be high due to bioerosion, as up 23% of all corals on the Florida Reef Tract are colonized by encrusting and excavating sponges (Chiappone *et al*., 2007). Microbial remineralization also contributes the seasonal increase in dissolution, as it can occur strongly in winter when the build up of organic matter from seagrasses and macroalgae decomposes (Zieman *et al*., 1999). Seagrasses, which cover ~56% of the reef tract (Lidz *et al*., 2007) also contribute to year round dissolution through their enhancement of microbial respiration in the sediment (Burdige *et al*., 2010). Below ground dynamics, such as the oxidation of organic matter, creates undersaturated conditions in porewaters of the reef, thereby enhancing dissolution of calcium carbonate in the substrate (Entsch *et al*., 1983). It is likely that the dissolution observed on the Florida Reef Tract occurs via multiple mechanisms that vary in their intensity on seasonal scales. Regardless of the mechanism driving the observed dissolution, the Florida Reef Tract appears to be straddling the threshold for net reef growth, and may switch to net reef loss on an annual scale in the near future.

The effect of biological processes (i.e. calcification and photosynthesis) on seawater carbon chemistry are well known in other systems, such as the barrier reef in Moorea, French Polynesia (Frankignoulle *et al*., 1996; Gattuso *et al*., 1997; Boucher *et*

al., 1998; Kleypas *et al*., 2011). However evidence of dissolution on other coral reefs is relatively rare and generally restricted to nighttime observations (Anderson and Gledhill, 2012). While calcification on the Florida Reef Tract is generally 10 fold lower than other reef systems (See Shamberger *et al*., 2011 for review), reefs with similar calcification rates in the Red Sea (Silverman *et al*., 2007a,b) have not been observed to experience seasonal dissolution. These differences have been attributed to the benthic community, and highlight the importance of the benthos in determining coastal carbonate chemistry. We hypothesize that the ratio of photosynthesizing organisms to calcifying organisms (Kleypas *et al* 2011) may be a key determinant in net reef growth the occurrence of dissolution in reef systems.

The net dissolution observed seasonally in this reef system is of increasing concern, as it occurs in addition to other destructive processes such as hurricanes, disease outbreaks, and bleaching events, all of which result in reef loss. Reef systems need strong and continued calcification to recover from episodic loss events that can severely degrade the existing reef structure and result in the net loss of calcium carbonate on the reef. This work demonstrates that the Florida Reef Tract is no longer strongly calcifying and instead appears to be straddling a tipping point for reef growth. The repeated seasonal dissolution observed holds implications for the reef tracts ability to recover from episodic degradation and to sustain in the face of sea level rise in the future. If the factors contributing to the seasonal dissolution observed here, also apply to other reef systems, then many reef systems may be experiencing net seasonal loss of calcium carbonate despite existing in over-saturated waters. As ocean acidification continues, reef calcification rates are predicted to further decrease (Silverman *et al*.,

2009) while rates of dissolution may simultaneously increase (Andersson and Gledhill, 2012), thereby driving many reef systems to their threshold for net accretion.

5.3 Coral Calcification

Calcification and heterotrophy experiments conducted with *Acropora cervicornis* indicate that decreasing aragonite saturation state (Ω) significantly affects calcification rates. In both fed and unfed corals, the effect of declining Ω caused a linear decline in calcification. Fed corals displayed significantly higher rates of calcification than unfed corals at all Ω levels. Interestingly, corals were able to calcify in undersaturated seawater in levels as low as 0.5, with rates depressed only by 10% in fed corals and 20% in unfed corals relative to the control (Ω 3.63).

Ocean acidification (OA) may strongly depress coral growth, thus the heterotrophic enhancement of calcification in corals exposed to OA represents the organismal ability to compensate for changing seawater chemistry. The degree of compensation and the nature of that compensation has not been thoroughly quantified prior to this study. While much has been learned about calcification, many of the mechanistic underpinnings and the energetic costs of these different processes are still debated or unknown. Proton removal from the extracellular fluid at the site of calcification is performed by the calicoblastic cells (McCulloch *et al*, 2012; Cohen *et al*., 2009) and may involve direct proton pumping, a Ca^{2+}-proton ATPase and/or transcellular proton-solute shuttling (McConnaughey and Whelan, 1997; Al-Horani *et al*., 2003; Cohen and McConnaughey, 2003). Regardless of the locus of control, ion

transport in response to acidified seawater is a new and active area of research (Venn *et al*., 2013).

Ion pumping is recognized as an energetically costly process, yet we have little understanding of how the coral allocates and shifts its allocation of energy towards this process. The results presented here, which indicate calcification declines linearly with Ω, support a model of calcification where the mechanism driving calcification, such as proton pumping rates (Ries *et al*., 2011), is unchanged across Ω levels. As the pH of the external seawater changes, calcification is theorized to become more energetically costly, as more hydrogen ions must be removed from the site of calcification to elevate the pH under the calcifying tissue (Venn *et al*., 2011). We show that while heterotrophy may increase calcification by increasing the energetic budget of the coral, it does not seem to result in a change in the proportion of the energetic budget allocated towards calcification in *A. cervicornis*. The total proportion of the energetic budget attributed toward calcification ranges from estimates as low as 13% (Edmunds and Davies, 1986) to mid ranges of 20% (Cohen *et al*., 2009) to as high as 30% (Allemand *et al*., 2011), thus there may be species or environmentally dependent effects occurring that could impact the coral calcification response to ocean acidification.

If we assume that the proportion of energy allocated towards calcification does not change based on the external changes in carbonate chemistry, then it suggests that changes in calcification due to OA are caused by changes in the functional capacity for calcification at the cellular levels. One mechanism by which this could occur may be disruptions in cell pH homeostasis. As Ω and pH decline, there are steady declines in the pH of the calcifying fluid as well as pH declines in overlying cells of the

calicoblastic epithelium (Venn *et al*., 2013). Changes in the internal cellular pH in response to OA may be 0.1-0.2 (Venn *et al*., 2013) and have been linked to reduced cellular metabolism in other marine invertebrates (Reipschlager and Portner, 1996). Reductions in the internal pH in coral cells of the calicoblastic layer could alter the activity of enzymes and proteins involved in biomineralization, such as secretory carbonic anhydrase (Moya *et al*., 2008) or proteins involved in the formation of the organic matrix (Zoccola *et al*., 2009). There is also evidence from gene expression research that ocean acidification creates a cascade of effects, resulting in classic acidosis responses that include changes in calcium homeostasis, cytoskeletal remodeling and metabolic depression (Kaniewska *et al*., 2012).

Research on other marine invertebrates has found that deviations in the environment, such as increased CO_2, can create sub-optimal conditions that consequently create additional metabolic energy demands (Somero, 2012). This can overwhelm the cellular capacity to provide enough ATP for routine metabolism, and may result in an organism increasing metabolic flux to cover ATP demands, or becoming metabolically depressed to conserve energy. Corals have shown both reductions in protein under ocean acidification (Krief *et al*., 2010; Edmunds *et al*., 2013; Tremblay *et al*., 2013) and gene expression evidence of metabolic depression (Kaniewska *et al*., 2012), indicating the increased pCO_2 could create additional metabolic energy demands in corals. Studies of the metabolic cost of OA in other marine invertebrates have used metabolic profiling and estimates of the fraction of cellular energy used for ion regulation in order to gauge the shift in metabolic pathways in response of high CO_2 (Lannig *et al*., 2010). Lannig *et al*. (2010) found that ion

regulation was not affected in the oyster, *Crassostrea gigas*, but that ATP was reduced in many tissues, indicating that heterotrophy in similar organisms could alleviate the effects of OA without impacting ion regulation. Future studies of this kind are needed to understand the energetic budget for coral calcification, and examine how it shifts in response to OA due to increased heterotrophy.

5.4 Coral Symbioses

Consistent declines in symbiont density were found in response to increased pCO_2 in the laboratory, in *Acropora cervicornis*, and *in situ,* in *Acropora millepora* and *Pocillopora damicornis*, growing near natural CO_2 vent systems. Symbiont declines of 26% to 48% were found respectively, in response to pCO_2 using traditional cell counting techniques in the lab and novel quantitative PCR (qPCR) methods to track changes in symbiont to host cell ratios. These results suggest that the obligate symbiont, *Symbiodinium microadriacticum*, will decline in response to pCO_2 across species and across a range of physical environments. Symbiont communities did not seem to display shifts in clade composition due to increasing pCO_2, however the small sample size and factors such as thermal history and light history in the field may preclude our ability to detect community shifts. Analyses of the clade community should be repeated in the lab using coral species known to host multiple clades, in order to tease apart how rising pCO_2 could influence this aspect of symbiosis.

The declines in symbiont density in the lab were less than those observed in the field, which may be attributable to differences in other physical factors in the lab and field (e.g. light, temperature), or attributable to oscillations of physical factors in the

field are typically held constant in the lab. Specifically, thermal history *in situ* could have affected symbiont density (Middlebrook *et al*., 2008), along with different light environments over time (Iglesias-Prieto *et al*., 2004). These factors could either independently affect symbiont density, or could interact or act synergistically with increased pCO_2 (Anthony *et al*., 2008; Suggett *et al*., 2013). Future *in situ* studies would benefit from including the following: a) light logger to gather light history, b) nutrients and zooplankton quantification *in situ*, c) comparison of pH fluctuations around natural vents versus the laboratory, in order to better constrain the mechanism(s) contributing the symbiont density changes.

The persistent trend of declining symbiont density under increased pCO_2 can be mechanistically explained in 1 of 2 ways, that may not mutually exclusive: 1) symbiont declines could represent a reduction in the symbiont energetic budget for growth *in hospite* and/or 2) physiological stress could contribute to the breakdown in the symbiotic relationship.

Each of these potential mechanisms is addressed separately: 1) Recent research by Tremblay *et al*. (2013) indicates that symbionts under increasing pCO_2 retain less carbon and translocate more of the carbon fixed during photosynthesis. The reduction of carbon available to the symbiont could lead to slower cell growth and division, thereby resulting in lower symbiont density observed (Tremblay *et al*., 2013). Tremblay *et al*. (2013) also observed lower rates of photosynthesis, as has also been shown by other researchers (Anthony *et al*., 2008; Kaniewska *et al*., 2012). However, as interesting as these results seem, they have only been shown to occur in one species (*Stylophora pistillata*), and in response to very high pCO_2 levels (3898 ppm) that may

incur other cellular affects in both the host and symbiont, contributing an additional affect on symbiont cell growth.

2) A second, though not mutually exclusive, explanation for the observed trend in symbiont density, is that increasing pCO_2 represents a physiological stress on the coral-algal symbiosis. While the process by which high pCO_2 induces bleaching loss is unknown, it could involved a number of mechanisms. The direct impacts of acidosis could alter carbon concentration mechanisms, particularly if the concentration mechanism was biochemical in nature, utilizing enzymes such as carbonic anhydrase (Leggat *et al*., 1999). Other evidence for physiological stress lays in the molecular studies of gene expression in response to increased pCO_2. Changes in the gene expression of PGPase, an enzyme that converts the product of oxygen photorespiration, could result in reduced photorespiration, as has been found in *Acropora formosa* (Crawley *et al*., 2010). Additional research on *Acropora millepora* indicate that increases in pCO_2 could affect a wide range genes associated with physiological stress in both the host and symbiont (Kaniewska *et al*., 2012). Changes in gene expression for processes specifically related to symbiosis include oxidative stress, apoptosis and symbiont loss (Kaniewska *et al*., 2012). Interestingly, Kaniewska *et al*., (2012) did not find changes in calcification rates despite using pCO_2 levels of 1000 ppm, suggesting that although a stress response occurs, the symbiosis may still function adequately enough to support calcification in the host. Alternatively, the host could be compensating for the physiological stress experienced by the symbiont, however this is unlikely as different phylotypes (clades) of free-living symbionts have exhibited no change in respiration rates in response to pCO_2 along with increased or steady growth

rates depending on phylotypes (Brading *et al*., 2011). Other marine autotrophs have shown the ability to increase their photosynthetic rates in carbon and nutrient replete conditions (Rost and Riebesell, 2004; Riebesell *et al*., 2007), suggesting that high pCO_2 is not necessarily a source of stress, but may instead be impacting the mechanisms in the host which serve to maintain the symbiosis. Overall, the factors leading to symbiont density declines as observed here may represent a combination of non-stressful adaptation to pCO_2, along with some stress induced reactions, and requires further study to clarify the mechanistic underpinnings of the patterns we observe.

5.5 Conclusion

This work demonstrates that the relationship between calcification and carbonate chemistry, specifically Ω, appears to be linear, both on the coral reef, and in laboratory setting. Additionally, we found that increasing pCO_2 prompted symbiont declines in areal density and in relation to the number of host cells. Heterotrophic opportunities for the host alleviated a significant portion of the calcification decline due to OA. While we cannot differentiate between the direct effects of heterotrophy on calcification versus the indirect effects on the symbiont and subsequent calcification, the combine effects represent the total scope for the heterotrophic alleviation in the future ocean. While heterotrophy in scleractinian corals exhibits the ability to enhance calcification rates in the acidified ocean, it does not completely negate the decline in calcification. Therefore the ability of corals to build reef structures in the natural environment under ocean acidification will still be reduced over time, along with rates of reef growth in the face of natural degradation. Based on our study of calcification rates on the Florida Reef

Tract, we see that current rates of reef growth are near a threshold, and the processes that drive dissolution on the reef are already creating net dissolution on a seasonal basis. As ocean acidification continues, we predict that calcification of a coral colony may decline as little as 8-13% per unit saturation state. However, a decline in one unit Ω on the reef tract would translate into ~90% of our reef observations exhibiting net dissolution. Thus, extrapolating from experimental relationships to reef predictions can lead to gross underestimation of reef growth under ocean acidification, a factor that needs to be incorporated into future predictive scenarios. The ability to predict a particular coral reef's trajectory cannot be done through Ω alone, and may require both the consideration of the processes that driving dissolution rates in reef system, as well as the spatial and temporal variation in calcification and dissolution.

Works Cited

Albright, R., and C. Langdon (2011), Ocean acidification impacts multiple early life history processes of the Caribbean coral *Porites astreoides*, *Global Change Biology*, *17*, 2478-2487.

Al-Horani, F.A., S.M. Al-Moghrabi, and D. de Beer (2003), Microsensor study of photosynthesis and calcification in the scleractinian coral, *Galaxea fascicularis*: active internal carbon cycle, *Journal of Experimental Marine Biology and Ecology*, *288*, 1-15.

Allemand, D., E. Tambutte, J.-P. Girard, and J. Jaubert (1998), Organic matrix synthesis in the scleractinian coral *Stylophora pistillata*: role in biomineralization and potential target of the organotin tributyltin, *Journal of Experimental Biology*, *201*, 2001-2009.

Allemand, D., É. Tambutté, D. Zoccola, and S. Tambutté (2011). Coral calcification, cells to reefs, in *Coral reefs: an ecosystem in transition*, vol., edited by Z. Dubinsky, and N. Stambler, pp. 119-150, Springer. New York.

Andersson, A., N. Bates, and F. Mackenzie (2007), Dissolution of carbonate sediments under rising pCO_2 and ocean acidification: observations from Devil's Hole, Bermuda, *Aquatic Geochemistry*, *13*, 237-264.

Andersson, A., I. Kuffner, F. Mackenzie, P. Jokiel, K. Rodgers, and A. Tan (2009), Net loss of $CaCO_3$ from a subtropical calcifying community due to seawater acidification: mesocosm-scale experimental evidence, *Biogeosciences*, *6*, 1811-1823.

Andersson, A., F.T. Mackenzie, and J.P. Gattuso (2011). Effects of ocean acidification on benthic processes, organisms, and ecosystems, in *Ocean Acidification*, vol., edited by J.P. Gattuso, and L. Hansson, Oxford University Press. New York.

Andersson, A.J., and D. Gledhill (2012), Ocean acidification and coral reefs: effects on breakdown, dissolution, and net ecosystem calcification, *Annual Review of Marine Science*, *5*, 321-348.

Andersson, A.J., and F.T. Mackenzie (2012), Revisiting four scientific debates in ocean acidification research, *Biogeosciences*, *9*, 893-905.

Andersson, A.J., F.T. Mackenzie, and A. Lerman (2005), Coastal ocean and carbonate systems in the high CO_2 world of the Anthropocene, *American Journal of Science*, *305*, 875-918.

Andersson, A.J., F.T. Mackenzie, and A. Lerman (2006), Coastal ocean CO_2–carbonic acid–carbonate sediment system of the Anthropocene, *Global Biogeochemical Cycles*, *20*.

Andersson, A.J., F.T. Mackenzie, and L.M. Ver (2003), Solution of shallow-water carbonates: An insignificant buffer against rising atmospheric CO_2, *Geology*, *31*, 513-516.

Anthony, K. (1999), Coral suspension feeding on fine particulate matter, *Journal of Experimental Marine Biology and Ecology*, *232*, 85-106.

Anthony, K., J. A Kleypas, and J.P. Gattuso (2011), Coral reefs modify their seawater carbon chemistry; Implications for impacts of ocean acidification, *Global Change Biology*, *17*, 3655-3666.

Anthony, K., M.O. Hoogenboom, J.A. Maynard, A.G. Grottoli, and R. Middlebrook (2009), Energetics approach to predicting mortality risk from environmental stress: A case study of coral bleaching, *Functional Ecology*, *23*, 539-550.

Anthony, K., D. Kline, G. Diaz-Pulido, S. Dove, and O. Hoegh-Guldberg (2008), Ocean acidification causes bleaching and productivity loss in coral reef builders, *Proceedings of the National Academy of Sciences*, *105*, 17442-17446.

Anthony, K.R.N., and K.E. Fabricius (2000), Shifting roles of heterotrophy and autotrophy in coral energetics under varying turbidity, *Journal of Experimental Marine Biology and Ecology*, *252*, 221-253.

Anthony, K.R.N., D.I. Kline, G. Diaz-Pulido, S. Dove, and O. Hoegh-Guldberg (2008), Ocean acidification causes bleaching and productivity loss in coral reef builders, *Proceedings of the National Academy of Sciences*, *105*, 17442-17446.

Atkinson, M., and J. Falter (2003). Coral reefs, in *Biogeochemistry of Marine Systems*, vol., edited by S.G. Black K, pp. 40-64, CRC Press. Boca Raton, FL.

Atkinson, M.J., and P. Cuet (2008), Possible effects of ocean acidification on coral reef biogeochemistry: topics for research, *Marine Ecology Progress Series*, *373*, 249-256.

Bak, R.P., and E.H. Meesters (1998), Coral population structure: the hidden information of colony size-frequency distributions, *Marine Ecology Progress Series*, *162*, 301-306.

Baker, A., R. Rowan, and N. Knowlton (1997). Symbiosis ecology of two Caribbean acroporid corals. *Proceedings of the 8th International Coral Reef Symposium*, Vol. 2 (pp. 1295-1300).

Baker, A.C. (2001), Ecosystems: reef corals bleach to survive change, *Nature*, *411*, 765-766.

Baker, A.C. (2003), Flexibility and specificity in coral-algal symbiosis: diversity, ecology, and biogeography of *Symbiodinium*, *Annual Review of Ecology, Evolution, and Systematics*, 661-689.

Baker, A.C., C.J. Starger, T. McClanahan, and P.W. Glynn (2004), Coral Reefs: Corals' adaptive response to climate change, *Nature*, *430*, 741.

Baker, D.M., J.P. Andras, A.G. Jordán-Garza, and M.L. Fogel (2013), Nitrate competition in a coral symbiosis varies with temperature among Symbiodinium clades, *The ISME journal*.

Barnes, D.D., and C.C. Crossland (1980), Diurnal and seasonal variations in the growth of a Staghorn coral measured by time-lapse photography, *Limnology and Oceanography,* 1113-1117.

Barnes, D.J., and M.J. Devereux (1984), Productivity and calcification on a coral reef: A survey using pH and oxygen electrode techniques, *Journal of Experimental Marine Biology and Ecology*, *79*, 213-231.

Baskett, M.L., S.D. Gaines, and R.M. Nisbet (2009), Symbiont diversity may help coral reefs survive moderate climate change, *Ecological Applications*, *19*, 3-17.

Bates, N.R. (2002), Seasonal variability of the effect of coral reefs on seawater CO_2 and air-sea CO_2 exchange, *Limnology and Oceanography*, 43-52.

Bates, N.R. (2007), Interannual variability of the oceanic CO_2 sink in the subtropical gyre of the North Atlantic Ocean over the last 2 decades, *Journal of Geophysical Research*, *112*, C09013.

Bates, N.R. (2011), Multi-decadal uptake of carbon dioxide into subtropical mode water of the North Atlantic Ocean, *Biogeosciences Discussions*, *8*, 12451-12476.

Bates, N.R., A. Amat, and A.J. Andersson (2010), Feedbacks and responses of coral calcification on the Bermuda reef system to seasonal changes in biological processes and ocean acidification, *Biogeosciences*, *7*, 2509-2530.

Blackwood, J.C., A. Hastings, and P.J. Mumby (1999), A model-based approach to determine the long-term effects of multiple interacting stressors on coral reefs, *Ecological Applications*, *21*, 2722-2733.

Brading, P., M.E. Warner, P. Davey, D.J. Smith, E.P. Achterberg, and D.J. Suggett (2011), Differential effects of ocean acidification on growth and photosynthesis among phylotypes of *Symbiodinium* (Dinophyceae), *Limnology and Oceanography*, *56*, 927.

Brock, J.C., C.W. Wright, I.B. Kuffner, R. Hernandez, and P. Thompson (2006), Airborne lidar sensing of massive stony coral colonies on patch reefs in the northern Florida reef tract, *Remote Sensing of Environment*, *104*, 31-42.

Bruno, J.F., and M.D. Bertness (2001), Habitat modification and facilitation in benthic marine communities. , *Pages 201-218 in Bertness MD, Gaines SD, Hay ME, eds. Marine Community Ecology. Sunderland (MA): Sinauer*.

Bruno, J.F., and E.R. Selig (2007), Regional decline of coral cover in the Indo-Pacific: timing, extent, and subregional comparisons, *PloS One*, *2*, e711.

Bucher, D.J., V.J. Harriott, and L.G. Roberts (1998), Skeletal micro-density, porosity and bulk density of acroporid corals, *Journal of Experimental Marine Biology and Ecology*, *228*, 117-136.

Buddemeier, R.W., J.A. Kleypas, and R.B. Aronson (2004), Potential contributions of climate change to stresses on coral reef ecosystems, *Coral Reefs and Global Climate Change. Pew Center on Global Climate Change, Virginia, USA*,

Burdige, D.J., X. Hu, and R.C. Zimmerman (2010), The widespread occurrence of coupled carbonate dissolution/reprecipitation in surface sediments on the Bahamas Bank, *American Journal of Science*, *310*, 492-521.

Burdige, D.J., and R.C. Zimmerman (2002), Impact of sea grass density on carbonate dissolution in Bahamian sediments, *Limnology and Oceanography*, *47*, 1751-1763.

Burman, S.G., R.B. Aronson, and R. van Woesik (2012), Biotic homogenization of coral assemblages along the Florida reef tract, *Marine Ecology Progress Series*, *467*, 89.

Caldeira, K., and M.E. Wickett (2005), Ocean model predictions of chemistry changes from carbon dioxide emissions to the atmosphere and ocean, *Journal of Geophysical Res*, *110*, C09S04.

Cantin, N.E., A.L. Cohen, K.B. Karnauskas, A.M. Tarrant, and D.C. McCorkle (2010), Ocean warming slows coral growth in the central Red Sea, *Science*, *329*, 322-325.

Cao, L., K. Caldeira, and A.K. Jain (2007), Effects of carbon dioxide and climate change on ocean acidification and carbonate mineral saturation, *Geophysical Research Letters*, *34*, L05607.

Carpenter, R.C. (1985), Relationships between primary production and irradiance in coral reef algal communities, *Limnology and Oceanography*, 784-793.

Causey, B., J. Delaney, E. Diaz, D. Dodge, J. Garcia, J. Higgins, B. Keller, R. Kelty, W. Jaap, and C. Matos (2002). *Status of Coral Reefs in the US Caribbean and Gulf of Mexico: Florida, Texas, Puerto Rico, US Virgin Islands, Navassa*. Townsville, Australia: Australian Institute of Marine Science.

Chan, N.C.S., and S.R. Connolly (2012), Sensitivity of coral calcification to ocean acidification: A meta-analysis, *Global Change Biology*, *19*, 282-290.

Chiappone, M., L.M. Rutten, S.L. Miller, and D.W. Swanson (2007). Large-scale distributional patterns of the encrusting and excavating sponge *Cliona delitrix* Pang on Florida Keys coral substrates. *Porifera research: Biodiversity, Innovation and Sustainability. Proceedings of the 7th International Sponge Symposium* (pp. 255-263).

Cohen, A.L., and M. Holcomb (2009), Why corals care about ocean acidification: Uncovering the mechanism, *Oceanography*, *22*, 118-127.

Cohen, A.L., and T.A. McConnaughey (2003), Geochemical perspectives on coral mineralization, *Reviews in Mineralogy and Geochemistry*, *54*, 151-187.

Cohen, A.L., D.C. McCorkle, S. De Putron, G.A. Gaetani, and K.A. Rose (2009), Morphological and compositional changes in the skeletons of new coral recruits reared in acidified seawater: Insights into the biomineralization response to ocean acidification, *Geochemistry Geophysics Geosystems*, *10*, 1-12.

Cohen, S., and M. Fine (2012), Measuring gross and net calcification of a reef coral under ocean acidification conditions: methodological considerations, *Biogeosciences Discussions*, *9*, 8241-8272.

Collado-Vides, L., L.M. Rutten, and J.W. Fourqurean (2005), Spatiotemporal variation of the abundance of calcareous green macroalgae in the Florida keys: A study of synchrony within a macroalgal functional-form group, *Journal of Phycology*, *41*, 742-752.

Comeau, S., R.C. Carpenter, and P. Edmunds (2013a), Effects of feeding and light intensity on the response of the coral *Porites rus* to ocean acidification, *Marine Biology*, 1-8.

Comeau, S., P. Edmunds, N.B. Spindel, and R.C. Carpenter (2013b), The responses of eight coral reef calcifiers to increasing partial pressure of CO_2 do not exhibit a tipping point, *Limnology and Oceanography*, *58*, 288-398.

Conand, C., P. Chabanet, P. Cuet, and Y. Letourneur (1997). The carbonate budget of a fringing reef in La Reunion Island (Indian Ocean): sea urchin and fish bioerosion and net calcification. *Proceedings of the 8th International Coral Reef Symposium*, Vol. 1 (pp. 953-958).

Cooper, T.F., P.V. Ridd, K.E. Ulstrup, C. Humphrey, M. Slivkoff, and K.E. Fabricius (2008), Temporal dynamics in coral bioindicators for water quality on coastal coral reefs of the Great Barrier Reef, *Marine and Freshwater Research*, *59*, 703-716.

Costanza, R., R. d'Arge, R. De Groot, S. Farber, M. Grasso, B. Hannon, K. Limburg, S. Naeem, R.V. O'Neill, and J. Paruelo (1997), The value of the world's ecosystem services and natural capital, *Nature*, *387*, 253-260.

Crawley, A., D.I. Kline, S. Dunn, K. Anthony, and S. Dove (2010), The effect of ocean acidification on symbiont photorespiration and productivity in *Acropora formosa*, *Global Change Biology*, *16*, 851-863.

Crossland, C., D. Barnes, and M. Borowitzka (1980), Diurnal lipid and mucus production in the Staghorn coral *Acropora acuminata*, *Marine Biology*, *60*, 81-90.

Cunning, R., and A.C. Baker (2012), Excess algal symbionts increase the susceptibility of reef corals to bleaching, *Nature Climate Change*, *3*, 259-262.

Cyronak, T., I. Santos, D. Erler, and B. Eyre (2012), Groundwater and porewater as a major source of alkalinity to a fringing coral reef lagoon (Muri Lagoon, Cook Islands), *Biogeosciences Discussions*, *9*, 15501.

Davies, M.S., and J. Hawkins (1998), Mucus from marine molluscs, *Advances in Marine Biology*, *34*, 1-71.

Davies, S.P. (1989), Short-term growth measurements of corals using an accurate buoyant weighing technique, *Marine Biology*, *101*, 389-395.

de Putron, S.J., D.C. McCorkle, A.L. Cohen, and A. Dillon (2011), The impact of seawater saturation state and bicarbonate ion concentration on calcification by new recruits of two Atlantic corals, *Coral Reefs*, *30*, 321-328.

De'ath, G., J.M. Lough, and K.E. Fabricius (2009), Declining coral calcification on the Great Barrier Reef, *Science*, *323*, 116-119.

Dickson, A. (1990), Thermodynamics of the dissociation of boric acid in synthetic seawater from 273.15 to 318.15°K., *Deep Sea Research*, *37*.

Dickson, A., and F. Millero (1987), A comparison of the equilibrium constants for the dissociation of carbonic acid in seawater media, *Deep Sea Research Part A. Oceanographic Research Papers*, *34*, 1733-1743.

Dickson, A., C.L. Sabine, and J. Christian (eds) (2007), *Guide to best practices for ocean CO_2 measurements*. PICES Special Publication 3, North Pacific Marine Science Organization http://cdiac.oml.giv/oceans/Handbook_2007.html.

DiSalvo, L.H. (1971), Regenerative functions and microbial ecology of coral reefs: Labelled bacteria in a coral reef microcosm, *Journal of Experimental Marine Biology and Ecology*, *7*, 123-136.

Doney, S.C., V.J. Fabry, R.A. Feely, and J.A. Kleypas (2009), Ocean acidification: The other CO_2 problem, *Annual Review of Marine Science*, *1*, 169-192.

Dore, J.E., R. Lukas, D.W. Sadler, M.J. Church, and D.M. Kari (2009), Physical and biogeochemical modulation of ocean acidification in the central North Pacific, *Proceedings of the National Academy of Sciences*, *106*, 12235-12240.

Drenkard, E., A. Cohen, D. McCorkle, S. de Putron, V. Starczak, and A. Zicht (2013), Calcification by juvenile corals under heterotrophy and elevated CO_2, *Coral Reefs*, 1-9.

Drew, E.A. (1972), The biology and physiology of alga-invertebrates symbioses. II. The density of symbiotic algal cells in a number of hermatypic hard corals and alcyonarians from various depths, *Journal of Experimental Marine Biology and Ecology*, *9*, 71-75.

Duarte, C.M., N. Marbà, E. Gacia, J.W. Fourqurean, J. Beggins, C. Barrón, and E.T. Apostolaki (2010), Seagrass community metabolism: Assessing the carbon sink capacity of seagrass meadows, *Global Biogeochemical Cycles*, *24*.

Duarte, C.M., M. Merino, N.S. Agawin, J. Uri, M.D. Fortes, M.E. Gallegos, N. Marbá, and M.A. Hemminga (1998), Root production and belowground seagrass biomass, *Marine Ecology Progress Series*, *171*, 97-108.

Dubinsky, Z., N. Stambler, A. Tribollet, and S. Golubic (2011). Reef Bioerosion: Agents and Processes, in *Coral Reefs: An Ecosystem in Transition*, vol., edited, pp. 435-449, Springer Netherlands.

Edmunds, P., and P.S. Davies (1986), An energy budget for *Porites porites* (Scleractinia), *Marine biology*, *92*, 339-347.

Edmunds, P., and R. Gates (2002), Normalizing physiological data for scleractinian corals, *Coral Reefs*, *21*, 193-197.

Edmunds, P.J. (2011), Zooplanktivory ameliorates the effects of ocean acidification on the reef coral *Porites* spp, *Limnology and Oceanography*, *56*, 2402.

Edmunds, P.J., V.R. Cumbo, and T.-Y. Fan (2013), Metabolic costs of larval settlement and metamorphosis in the coral *Seriatopora caliendrum* under ambient and elevated pCO_2, *Journal of Experimental Marine Biology and Ecology*, *443*, 33-38.

Entsch, B., K.G. Boto, R.G. Sim, and J.T. Wellington (1983), Phosphorus and nitrogen in coral reef sediments, *Limnology and Oceanography*, *28*, 465-476.

Epifano, C., and J. Ewart (1977), Maximum ration of four algal diets for the oyster *Crassostrea virginica* Gmelin, *Aquaculture*, *11*, 9.

Epstein, N., and B. Rinkevich (2001), From isolated ramets to coral colonies: The significanceof colony pattern formation in reef restoration practices, *Basic and Applied Ecology*, *2*, 219-222.

Erez, J., and A. Braun (2007), Calcification in hermatypic corals is based on direct seawater supply to the biomineralization site, *Geochimica et Cosmochimica Acta*, *71*, A260-A260.

Erez, J., S. Reynaud, J. Silverman, K. Schneider, and D. Allemand (2011), Coral calcification under ocean acidification and global change, *Coral Reefs: An Ecosystem in Transition*, 151-176.

Espinosa, E.P., and B. Allam (2006), Comparative growth and survival of juvenile hard clams, *Mercenaria mercenaria*, fed commercially available diets, *Zoo Biology*, *25*, 513-525.

Fabricius, K.E., T.F. Cooper, C. Humphrey, S. Uthicke, G. De'ath, J. Davidson, H. LeGrand, A. Thompson, and B. Schaffelke (2012), A bioindicator system for water quality on inshore coral reefs of the Great Barrier Reef, *Marine Pollution Bulletin*, *65*, 320-332.

Fabricius, K.E., C. Langdon, S. Uthicke, C. Humphrey, S. Noonan, G. De'ath, R. Okazaki, N. Muehllehner, M.S. Glas, and J.M. Lough (2011), Losers and winners in coral reefs acclimatized to elevated carbon dioxide concentrations, *Nature Climate Change*, *1*, 165-169.

Fabricius, K., G. De'ath, L. McCook, E. Turank, and D.M. Williams (2005), Changes in algal, coral and fish assemblages along water quality gradients on the inshore Great Barrier Reef, *Marine Pollution Bulletin*, *51*, 384-398.

Fagoonee, I., H. Wilson, M. Hassell, and J. Turner (1999), The dynamics of zooxanthellae populations: a long-term study in the field, *Science*, *283*, 843-845.

Falkowski, P., R. Scholes, E. Boyle, J. Canadell, D. Canfield, J. Elser, N. Gruber, K. Hibbard, P. Högberg, and S. Linder (2000), The global carbon cycle: A test of our knowledge of earth as a system, *Science*, *290*, 291-296.

Falkowski, P.G., Z. Dubinsky, L. Muscatine, and J.W. Porter (1984), Light and the bioenergetics of a symbiotic coral, *BioScience*, *34*, 705-709.

Falter, J.L., R.J. Lowe, M.J. Atkinson, and P. Cuet (2012), Seasonal coupling and de-coupling of net calcification rates from coral reef metabolism and carbonate chemistry at Ningaloo Reef, Western Australia, *Journal of Geophysical Research*, *117*, C05003.

Falter, J.L., and F.J. Sansone (2000), Hydraulic control of pore water geochemistry within the oxic-suboxic zone of a permeable sediment, *Limnology and oceanography*, *45*, 550-557.

Feely, R.A., S.C. Doney, and S.R. Cooley (2009), Ocean acidification: present conditions and future changes in a high-CO_2 world, *Oceanography*, *22*, 36-47.

Ferrier-Pagés, C., D. Allemand, J. Gattuso, J. Jaubert, and F. Rassoulzadegan (1998), Microheterotrophy in the zooxanthellate coral *Stylophora pistillata*: effects of light and ciliate density, *Limnology and Oceanography*, *43*, 1639-1648.

Ferrier-Pagés, C., C. Rottier, E. Beraud, and O. Levy (2010), Experimental assessment of the feeding effort of three scleractinian coral species during a thermal stress: Effect on the rates of photosynthesis, *Journal of Experimental Marine Biology and Ecology*, *390*, 118-124.

Fine, M., and D. Tchernov (2007), Scleractinian coral species survive and recover from decalcification, *Science*, *315*, 1811.

Fitt, W.K., F.K. McFarland, M.E. Warner, and G.C. Chilcoat (2000), Seasonal patterns of tissue biomass and densities of symbiotic dinoflagellates in reef corals and relation to coral bleaching, *Limnology and Oceanography*, 677-685.

Fourqurean, J.W., M.J. Durako, M.O. Hall, and L.N. Hefty (2002), Seagrass distribution in south Florida: a multi-agency coordinated monitoring program, *The Everglades, Florida Bay, and Coral Reefs of the Florida Keys. An Ecosystem Sourcebook. CRC Press, Boca Raton, Florida*, 497-522.

Fourqurean, J.W., A. Willsie, C.D. Rose, and L.M. Rutten (2001), Spatial and temporal pattern in seagrass community composition and productivity in South Florida, *Marine Biology*, *138*, 341-354.

Frankignoulle, M., G. Abril, A. Borges, I. Bourge, C. Canon, B. Delille, E. Libert, and J.-M. Th'eate (1998), Carbon dioxide emission from European estuaries, *Science*, *282*, 434-436.

Frankignoulle, M., M. Elskens, R. Biondo, I. Bourge, C. Canon, S. Desgain, and P. Dauby (1996), Distribution of inorganic carbon and related parameters in surface seawater of the English Channel during spring 1994, *Journal of Marine Systems*, *7*, 427-434.

Furla, P., I. Galgani, I. Durand, and D. Allemand (2000), Sources and mechanisms of inorganic carbon transport for coral calcification and photosynthesis, *Journal of Experimental Biology*, *203*, 3445-3457.

Gagnon, A.C., J.F. Adkins, and J. Erez (2012), Seawater transport during coral biomineralization, *Earth and Planetary Science Letters*, *329*, 150-161.

Gagnon, A.C., J.F. Adkins, J. Erez, J.M. Eiler, and Y. Guan (2012), Sr/Ca sensitivity to aragonite saturation state in cultured subsamples from a single colony of coral: Mechanism of biomineralization during ocean acidification, *Geochimica et Cosmochimica Acta*.

Gardner, T.A., I.M. Côté, J.A. Gill, A. Grant, and A.R. Watkinson (2003), Long-term region-wide declines in Caribbean corals, *Science*, *301*, 958-960.

Gattuso, J., M. Pichon, B. Delesalle, C. Canon, and M. Frankignoulle (1996), Carbon fluxes in coral reefs. I. Lagrangian measurement of community metabolism and resulting air-sea CO_2 disequilibrium, *Marine Ecology Progress Series*, *145*, 109-121.

Gattuso, J.P., M. Pichon, B. Delesalle, and M. Frankignoulle (1993), Community metabolism and air-sea CO_2 fluxes in a coral reef ecosystem (Moorea, French Polynesia), *Marine Ecology Progress Series*, *96*, 259-267.

Gattuso, J.P., M. Pichon, J. Jaubert, M. Marchioretti, and M. Frankignoulle (1996), Primary production, calcification and air-sea CO_2 fluxes in coral reefs: organism, ecosystem and global scales, *Bulletin-Institut Oceanographique Monaco-Numero Special*, 39-46.

Gattuso, J.-P., D. Allemand, and M. Frankignoulle (1999a), Photosynthesis and calcification at cellular, organismal and community levels in coral reefs: A review on interactions and control by carbonate chemistry, *American Zoologist*, *39*, 160-183.

Gattuso, J.-P., M. Frankignoulle, and S.V. Smith (1999b), Measurement of community metabolism and significance in the coral reef CO_2 source-sink debate, *Proceedings of the National Academy of Sciences*, *96*, 13017-13022.

Gattuso, J.-P., C.E. Payri, M. Pichon, B. Delesalle, and M. Frankignoulle (1997), Primary production, calcification, and air-sea CO_2 fluxes of a macroalgal-dominated coral reef community (Moorea, French Polynesia), *Journal of Phycology*, *33*, 729-738.

Gledhill, D.K., R. Wanninkhof, F.J. Millero, and M. Eakin (2008), Ocean acidification of the greater Caribbean region 1996–2006, *Journal of Geophysical Research*, *113*, C10031.

Glynn, P.W. (1993), Coral reef bleaching: ecological perspectives, *Coral Reefs*, *12*, 1-17.

Glynn, P.W. (1997). Bioerosion and coral-reef growth: A dynamic balance, in *Life and death of coral reefs*, vol., edited by C. Birkeland, pp. 68-95, Chapman and Hall. New York.

Glynn, P.W., J.L. Mate, A.C. Baker, and M.O. Calderon (2001), Coral bleaching and mortality in Panama and Ecuador during the 1997-1998 El Nino Southern Oscillation Event: spatial/temporal patterns and comparisons with the 1982-1983 event, *Bulletin of Marine Science*, *69*, 79-109.

Goiran, C., S. Al-Moghrabi, D. Allemand, and J. Jaubert (1996), Inorganic carbon uptake for photosynthesis by the symbiotic coral/dinoflagellate association. 1. Photosynthetic performance of symbionts and dependence on seawater bicarbonate, *Journal of Experimental Marine Biology and Ecology*, *199*, 207-225.

Gray, S.E.C., M.D. DeGrandpre, C. Langdon, and J.E. Corredor (2012), Short-term and seasonal pH, pCO_2 and saturation state variability in a coral-reef ecosystem, *Global Biogeochemical Cycles*, *26*, GB3012.

Grottoli, A.G. (2002), Effect of light and brine shrimp on skeletal δ^{13} C in the Hawaiian coral *Porites compressa*: A tank experiment, *Geochimica et Cosmochimica Acta*, *66*, 1955-1967.

Grottoli, A.G., L.J. Rodrigues, and J.E. Palardy (2006), Heterotrophic plasticity and resilience in bleached corals, *Nature*, *440*, 1186-1189.

Grover, R., J.-F. Maguer, D. Allemand, and C. Ferrier-Pagès (2008), Uptake of dissolved free amino acids by the scleractinian coral *Stylophora pistillata*, *Journal of Experimental Biology*, *211*, 860-865.

Hallock, P. (1981), Production of carbonate sediments by selected large benthic foraminifera on two Pacific coral reefs, *Journal of Sedimentary Research*, *51*, 467-474.

Hall-Spencer, J.M., R. Rodolfo-Metalpa, S. Martin, E. Ransome, M. Fine, S.M. Turner, S.J. Rowley, D. Tedesco, and M.-C. Buia (2008), Volcanic carbon dioxide vents show ecosystem effects of ocean acidification, *Nature*, *454*, 96-99.

Hixon, M.A., and J.P. Beets (1993), Predation, prey refuges, and the structure of coral reef assemblages, *Ecological Monographs*, *63*, 77-101.

Hoegh-Guldberg, O. (2005), Low coral cover in a high-CO_2 world, *Journal of Geophysical Research*, *110*, 1-11.

Hoegh-Guldberg, O., P.J. Mumby, A.J. Hooten, R.S. Steneck, P. Greenfield, E. Gomez, C.D. Harvell, P.J. Sale, A.J. Edwards, K. Caldeira, N. Knowlton, C.M. Eakin, R. Iglesias-Prieto, N. Muthiga, R.H. Bradbury, A. Dubi, and M.E. Hatziolos (2007), Coral reefs under rapid climate change and ocean acidification, *Science*, *318*, 1737-1742.

Hofmann, G.E., J.E. Smith, K.S. Johnson, U. Send, L.A. Levin, F. Micheli, A. Paytan, N.N. Price, B. Peterson, Y. Takeshita, P.G. Matson, E.D. Crook, K.J. Kroeker, M.C. Gambi, E.B. Rivest, C.A. Frieder, P.C. Yu, and T.R. Martz (2011), High-frequency dynamics of ocean pH: A multi-ecosystem comparison, *PLoS ONE*, *6*, e28983.

Holbrook, S.J., A.J. Brooks, and R.J. Schmidt (2002), Variation in structural attributes of patch-forming corals and patterns of abundances of associated fishes, *Marine and Freshwater Research*, *53*, 1045-1053.

Holcomb, M., A. Cohen, and D. McCorkle (2011), A gender bias in the calcification response to ocean acidification, *Biogeosciences Discussion*, *8*, 8485-8513.

Hoogenboom, M., R. Rodolfo-Metalpa, and C. Ferrier-Pagés (2010), Co-variation between autotrophy and heterotrophy in the Mediterranean coral *Cladocora caespitosa*, *Journal of Experimental Biology*, *213*, 2399-2409.

Houlbréque, F., B. Delesalle, J. Blanchot, Y. Montel, and C. Ferrier-Pagés (2006), Picoplankton removal by the coral reef community of La Prévoyante, Mayotte Island, *Aquatic Microbial Ecology*, *44*, 59-70.

Houlbréque, F., and C. Ferrier-Pagés (2009), Heterotrophy in tropical scleractinian corals, *Biological Reviews*, *84*, 1-17.

Houlbrèque, F., E. Tambutté, D. Allemand, and C. Ferrier-Pagès (2004a), Interactions between zooplankton feeding, photosynthesis and skeletal growth in the scleractinian coral *Stylophora pistillata*, *Journal of Experimental Biology*, *207*, 1461-1469.

Houlbrèque, F., E. Tambutté, and C. Ferrier-Pagès (2003), Effect of zooplankton availability on the rates of photosynthesis, and tissue and skeletal growth in the scleractinian coral *Stylophora pistillata*, *Journal of Experimental Marine Biology and Ecology*, *296*, 145-166.

Houlbréque, F., E. Tambutté, C. Richard, and C. Ferrier-Pagés (2004b), Importance of a micro-diet for scleractinian corals, *Marine Ecology Progress Series*, *282*, 151-160.

Huettel, M., and A. Rusch (2000), Transport and degradation of phytoplankton in permeable sediment, *Limnology and Oceanography*, *45*, 534-549.

Huettel, M., W. Ziebis, and S. Forster (1996), Flow-induced uptake of particulate matter in permeable sediments, *Limnology and Oceanography*, *41*, 309-322.

Hughes, T.P., M.J. Rodrigues, D.R. Bellwood, D. Ceccarelli, O. Hoegh-Guldberg, L. McCook, N. Moltschaniwskyj, M.S. Pratchett, R.S. Steneck, and B. Willis (2007), Phase shifts, herbivory, and the resilience of coral reefs to climate change, *Current Biology*, *17*, 360-365.

Idjadi, J.A., and P.J. Edmunds (2006), Scleractinian corals as facilitators for other invertebrates on a Caribbean reef, *Marine Ecology Progress Series*, *319*, 209-211.

Iglesias-Prieto, R., V.H. Beltran, T.C. LaJeunesse, H. Reyes-Bonilla, and P.E. Thome (2004), Different algal symbionts explain the vertical distribution of dominant reef corals in the Eastern Pacific, *Proceedings of the Royal Society of London, Series B: Biological Sciences*, *271*, 1757-1763.

IPCC (2007). *Climate Change 2007: The Physical Science Basis: Contribution of Working Group I to theThird Assessment Report of the Intergovernmental Panel on Climate Change* New York: Cambridge University Press.

Jackson, J.B., M.X. Kirby, W.H. Berger, K.A. Bjorndal, L.W. Botsford, B.J. Bourque, R.H. Bradbury, R. Cooke, J. Erlandson, and J.A. Estes (2001), Historical overfishing and the recent collapse of coastal ecosystems, *Science*, *293*, 629-637.

Jones, C.G., J.H. Lawton, and M. Shachak (1997), Positive and negative effects of organisms as physical ecosystem engineers, *Ecology*, *78*, 1946-1957.

Kadko, D. (2000), Modeling the evolution of the Arctic mixed layer during the fall 1997 SHEBA project using measurements of ^{7}Be, *Journal of Geophysical Research*, *105*, 3369-3378.

Kadko, D., and D. Olson (1996), ^{7}Be as a tracer of surface water seduction and mixed layer history, *Deep Sea Research*, *43*, 89-116.

Kaniewska, P., P.R. Campbell, D.I. Kline, M. Rodriguez-Lanetty, D.J. Miller, S. Dove, and O. Hoegh-Guldberg (2012), Major cellular and physiological Impacts of ocean acidification on a reef building coral, *PloS One*, *7*, e34659.

Kawahata, H., A. Suzuki, T. Ayukai, and K. Goto (2000), Distribution of the fugacity of carbon dioxide in the surface seawater of the Great Barrier Reef, *Marine Chemistry*, *72*, 257-272.

Kawahata, H., A. Suzuki, and K. Goto (1997), Coral reef ecosystems as a source of atmospheric CO_2: Evidence of pCO_2 measurements of surface waters, *Coral Reefs*, *16*, 261-266.

Kinsey, D.D. (1985). Metabolism, calcification and carbon production. I. System level studies. *Proceedings of the 5th International Coral Reef Congress, Tahiti, 27 May-1 June 1985-pages: 4: 503-542*.

Kleypas, J.A., K. Anthony, and J.P. Gattuso (2011), Coral reefs modify their seawater carbon chemistry–case study from a barrier reef (Moorea, French Polynesia), *Global Change Biology*, *17*, 3667-3678.

Kleypas, J.A., R.W. Buddemeier, D. Archer, J.-P. Gattuso, C. Langdon, and B.N. Opdyke (1999), Geochemical consequences of increased atmospheric carbon dioxide on coral reefs, *Science*, *284*, 118-120.

Kleypas, J.A., R.W. Buddemeier, and J.-P. Gattuso (2001), The future of coral reefs in an age of global change, *International Journal of Earth Sciences*, *90*, 426-437.

Kleypas, J.A., R.A. Feely, V.J. Fabry, C. Langdon, C.L. Sabine, and L.L. Robbins (2006). *Impacts of ocean acidification on coral reefs and other marine calcifiers. A guide for future research. 88pp.* St. Petersburg, Florida.

Kleypas, J.A., and C. Langdon (2006), Coral reefs and changing seawater carbonate chemistry, *Coastal and Estuarine Studies*, *61*, 73-110.

Kleypas, J.A., J.W. McManus, and L. AB MEÑEZ (1999), Environmental limits to coral reef development: Where do we draw the line?, *American Zoologist*, *39*, 146-159.

Kleypas, J.A., and K.K. Yates (2009), Coral reefs and ocean acidification, *Oceanography*, *22*.

Kline, D.I., L. Teneva, K. Schneider, T. Miard, A. Chai, M. Marker, K. Headley, B. Opdyke, M. Nash, and M. Valetich (2012), A short-term in situ CO2 enrichment experiment on Heron Island (GBR), *Scientific Reports*, *2*.

Koch, M., G. Bowes, C. Ross, and X.H. Zhang (2012), Climate change and ocean acidification effects on seagrasses and marine macroalgae, *Global Change Biology*, *19*, 103-132.

Kraines, S., Y. Suzuki, K. Yamada, and H. Komiyama (1996), Separating biological and physical changes in dissolved oxygen concentration in a coral reef, *Limnology and Oceanography*, 1790-1799.

Krief, S., E.J. Hendy, M. Fine, R. Yam, A. Meibom, G.L. Foster, and A. Shemesh (2010), Physiological and isotopic responses of scleractinian corals to ocean acidification, *Geochimica et Cosmochimica Acta*, *74*, 4988-5001.

Kroeker, K.J., R.L. Kordas, R.N. Crim, and G.G. Singh (2010), Meta-analysis reveals negative yet variable effects of ocean acidification on marine organisms, *Ecology Letters*, *13*, 1419-1434.

LaJeunesse, T.C. (2001), Investigating the biodiversity, ecology, and phylogeny of endosymbiotic dinoflagellates in the genus *Symbiodinium* using the ITS region: in search of a "species" level marker, *Journal of Phycology*, *37*, 866-880.

Langdon, C. (2000a), Review of experimental evidence for effects of CO_2 on calcification of reef builders. *In*: Proceedings of the 9th International Coral Reef Symposium, Bali, Indonesia 2:1092-1098, *In: Proceedings of the 9th International Coral Reef Symposium, Bali, Indonesia*, 1092-1098.

Langdon, C., and M. Atkinson (2005), Effect of elevated pCO_2 on photosynthesis and calcification of corals and interactions with seasonal change in temperature/irradiance and nutrient enrichment, *Journal of Geophysical Research*, *110*, C09S07.

Langdon, C., T. Takahashi, C. Sweeney, D. Chipman, J. Goddard, F. Marubini, H. Aceves, H. Barnett, and M.J. Atkinson (2000b), Effect of calcium carbonate saturation state on the calcification rate of an experimental coral reef, *Global Biogeochemical Cycles*, *14*, 639-654.

Lannig, G., S. Eilers, H. Portner, I. Sokolova, and C. Bock (2010), Impact of ocean acidification on energy metabolism of oyster, *Crassostrea gigas* - Changes in metabolic pathways and thermal response, *Marine Drugs*, *8*, 2318-2339.

Lasker, H.R. (1981), A comparison of the particulate feeding abilities of three species of gorgonian soft coral, *Marine Ecoogy Progress Series*, *5*.

LeClercq, N., J.P. Gattuso, and J. Jaubert (2002), Primary production, respiration, and calcification of a coral reef mesocosm under increased CO_2 partial pressure, *Limnology and Oceanography*, 558-564.

LeClercq, N., J.-P. Gattuso, and J. Jaubert (2000), CO_2 partial pressure controls the calcification rate of a coral community, *Global Change Biology*, *6*, 329-334.

Lee, T., E. Barg, and D. Lal (1991), Studies of vertical mixing in the Southern California Bight with cosmogenic radionuclides ^{32}P and ^{7}Be, *Limnology and Oceanography*, *365*, 1044-1053.

Lee, T.N., and E. Williams (1999), Mean distribution and seasonal variability of coastal currents and temperature in the Florida Keys with implications for larval recruitment, *Bulletin of Marine Science*, *64*, 35-56.

Lee, T.N., E. Williams, E. Johns, D. Wilson, and N.P. Smith (2002), Transport processes linking South Florida coastal ecosystems, *The Everglades, Florida Bay, and Coral Reefs of the Florida Keys: An Ecosystem Sourcebook*, 309-342.

Leggat, W., M.R. Badger, and D. Yellowlees (1999), Evidence for an inorganic carbon-concentrating mechanism in the symbiotic dinoflagellate *Symbiodinium* sp, *Plant Physiology*, *121*, 1247-1255.

Lesser, M. (2012), Using energetic budgets to assess the effects of environmental stress on corals: are we measuring the right things?, *Coral Reefs*, *32*, 25-33.

Lewis, J., and W. Price (1975), Feeding mechanisms and feeding strategies of Atlantic reef corals, *Journal of Zoology*, *176*, 527-544.

Lidz, B., C. Reich, and E. Shinn (2007), Systematic mapping of bedrock and habitats along the Florida Reef Tract-central Key Largo to Halfmoon Shoal (Gulf of Mexico), *US Geological Survey Professional Paper Electronic Resource*, *1751*.

Lidz, B.H., and P. Hallock (2000), Sedimentary petrology of a declining reef ecosystem, Florida Reef Tract (U.S.A.), *Journal of Coastal Research*, *16*, 675-697.

Lidz, B.H., C.D. Reich, R.L. Peterson, and E.A. Shinn (2006), New maps, new information: coral reefs of the Florida Keys, *Journal of Coastal Research*, *22*, 260-282.

Lirman, D., and P. Biber (2000), Seasonal dynamics of macroalgal communities of the Northern Florida Reef Tract, *Botanica Marina*, *43*, 305.

Little, A.F., M.J.H. van Oppen, and B.L. Willis (2004), Flexibility in algal endosymbioses shapes growth in reef corals, *Science*, *304*, 1492-1494.

Manzello, D.P. (2010), Ocean acidification hot spots: Spatiotemporal dynamics of the seawater $C0_2$ system of Eastern Pacific coral reefs, *Limnology and Oceanography*, *55*, 239.

Manzello, D.P., I.C. Enochs, N. Melo, D.K. Gledhill, and E.M. Johns (2012), Ocean acidification refugia of the Florida Reef Tract, *PloS One*, *7*, e41715.

Marubini, F., and M. Atkinson (1999), Effects of lowered pH and elevated nitrate on coral calcification, *Marine Ecology Progress Series*, *188*, 117-121.

Marubini, F., H. Barnett, C. Langdon, and M. Atkinson (2001), Dependence of calcification on light and carbonate ion concentration for the hermatypic coral *Porites compressa*, *Marine Ecology Progress Series*, *220*, 153-162.

Marubini, F., C. Ferrier–Pages, and J.P. Cuif (2003), Suppression of skeletal growth in scleractinian corals by decreasing ambient carbonate-ion concentration: A cross-family comparison, *Proceedings of the Royal Society of London. Series B: Biological Sciences*, *270*, 179-184.

Marubini, F., C. Ferrier-Pages, P. Furla, and D. Allemand (2008), Coral calcification responds to seawater acidification: A working hypothesis towards a physiological mechanism, *Coral Reefs*, *27*, 491-199.

Maxwell, D.P., S. Falk, and N.P.A. Huner (1995), Photosystem II excitation pressure and development of resistance to photoinhibition (I. light-harvesting complex II abundance and zeaxanthin content in *Chlorella vulgaris*), *Plant Physiology*, *107*, 687-694.

McConnaughey, T. (1998), Acid secretion, calcification, and photosynthetic carbon concentrating mechanisms, *Canadian Journal of Botany*, *76*, 1119-1126.

McConnaughey, T., and J. Whelan (1997), Calcification generates protons for nutrient and bicarbonate uptake, *Earth-Science Reviews*, *42*, 95-117.

McCulloch, M.T., J.L. Falter, J. Trotter, and P. Montagna (2012), Coral resilience to ocean acidification and global warming through pH up-regulation, *Nature Climate Change*, *2*, 623-627.

McGillis, W.R., C. Langdon, B. Loose, K.K. Yates, and J. Corredor (2011), Productivity of a coral reef using boundary layer and enclosure methods, *Geophysical Research Letters*, *38*.

Mehrbach, C., C. Culberson, J. Hawley, and R. Pytkowicz (1973), Measurement of the apparent dissociation constants of carbonic acid in seawater at atmospheric pressure, *Limnology and Oceanography*, 897-907.

Middlebrook, R., O. Hoegh-Guldberg, and W. Leggat (2008), The effect of thermal history on the susceptibility of reef-building corals to thermal stress, *Journal of Experimental Biology*, *211*, 1050-1056.

Mieog, J.C., M.J. van Oppen, R. Berkelmans, W.T. Stam, and J.L. Olsen (2009), Quantification of algal endosymbionts (*Symbiodinium*) in coral tissue using real-time PCR, *Molecular Ecology Resources*, *9*, 74-82.

Miller, J., E. Muller, C. Rogers, R. Waara, A. Atkinson, K.R.T. Whelan, M. Patterson, and B. Witcher (2009), Coral disease following massive bleaching in 2005 causes 60% decline in coral cover on reefs in the US Virgin Islands, *Coral Reefs*, *28*, 925-937.

Moberg, F., and C. Folke (1999), Ecological goods and services of coral reef ecosystems, *Ecological Economics*, *29*, 215-233.

Moran, S.B., S.E. Weinstein, H.N. Edmonds, J.N. Smith, R.P. Kelly, M.E.Q. Pilson, and W.G. Harrison (2003), Does $^{234}Th/^{238}U$ disequilibrium provide an accurate record of the export flux of particulate organic carbon from the upper ocean?, *Limnology and Oceanography*, *48*, 1018-1029.

Moses, C.S., S. Andrefouet, C.J. Kranenburg, and F.E. Muller-Karger (2009), Regional estimates of reef carbonate dynamics and productivity using Landsat 7 ETM+, and potential impacts from ocean acidification, *Marine Ecology Progress Series*, *380*, 103-115.

Moya, A., S. Tambutté, A. Bertucci, E. Tambutté, S. Lotto, D. Vullo, C.T. Supuran, D. Allemand, and D. Zoccola (2008), Carbonic anhydrase in the scleractinian coral *Stylophora pistillata* characterization, localization, and role in biomineralization, *Journal of Biological Chemistry*, *283*, 25475-25484.

Muir, G.K.P., J.M. Pates, A.P. Karageorgis, and H. Kaberi (2005), $^{234}Th:^{238}U$ disequilibrium as an indicator of sediment resuspension in Thermaikos Gulf, northwestern Aegean Sea, *Continental Shelf Research*, *25*, 2476-2490.

Muscatine, L. (1973), Nutrition of corals, *book: In O. A. Jones and R. Endean [eds.], Biology and Geology of Coral Reefs, v. 2, Academic*, 77-115.

Muscatine, L. (1990), The role of symbiotic algae in carbon and energy flux in reef corals. *In*: Coral Reefs, Z. Dubinsky (eds.). Elsevier Science Publishers, Amsterdam, *Coral Reefs*.

Muscatine, L., L. McCloskey, and R. Marian (1981), Estimating the daily contribution of carbon from zooxanthellae to coral animal respiration, *Limnology and Oceanography*, 601-611.

Muscatine, L., and J.W. Porter (1977), Reef corals: mutualistic symbioses adapted to nutrient-poor environments, *BioScience*, *27*, 454-460.

Nakamura, M., S. Ohki, A. Suzuki, and K. Sakai (2011), Coral larvae under ocean acidification: survival, metabolism, and metamorphosis, *PloS One*, *6*, e14521.

Nanami, A., and M. Nishihira (2004), Microhabitat association and temporal stability in reef fish assemblages on massive *Porites* microatolls, *Ichthyologist Research*, *51*, 165-171.

Odum, H.T., and E.P. Odum (1955), Trophic structure and productivity of a windward coral reef community on Eniwetok Atoll, *Ecological Monographs*, *25*, 291-320.

Ohde, S., and R. van Woesik (1999), Carbon dioxide flux and metabolic processes of a coral reef, Okinawa, *Bulletin of Marine Science*, *65*, 559-576.

Paddack, M.J., R.K. Cowen, and S. Sponaugle (2006), Grazing pressure of herbivorous coral reef fishes on low coral cover reefs, *Coral Reefs*, *25*, 461-472.

Palandro, D.A., S. Andréfouët, C. Hu, P. Hallock, F.E. Müller-Karger, P. Dustan, M.K. Callahan, C. Kranenburg, and C.R. Beaver (2008), Quantification of two decades of shallow-water coral reef habitat decline in the Florida Keys National Marine Sanctuary using Landsat data (1984-2002), *Remote Sensing of Environment*, *112*, 3388-3399.

Palardy, J.E., A.G. Grottoli, and K.A. Matthews (2005), Effects of upwelling, depth, morphology and polyp size on feeding in three species of Panamanian corals, *Marine Ecology Progress Series*, *300*, 79-89.

Palardy, J.E., A.G. Grottoli, and K.A. Matthews (2006), Effect of naturally changing zooplankton concentrations on feeding rates of two coral species in the Eastern Pacific, *Journal of Experimental Marine Biology and Ecology*, *331*, 99-107.

Pandolfi, J.M., S.R. Connolly, D.J. Marshall, and A.L. Cohen (2011), Projecting coral reef futures under global warming and ocean acidification, *Science*, *333*, 418-422.

Patten, N.L., A.S. Wyatt, R.J. Lowe, and A.M. Waite (2011), Uptake of picophytoplankton, bacterioplankton and virioplankton by a fringing coral reef community (Ningaloo Reef, Australia), *Coral Reefs*, *30*, 555-567.

Peng, T.-H., J.-J. Hung, R. Wannikof, and F. Millero (1999), Carbon budget in the East China Sea in spring, *Tellus*, *51B*, 531-540.

Perry, C., G. Murphy, P. Kench, S. Smithers, E. Edinger, R. Steneck, and P. Mumby (2013), Caribbean-wide decline in carbonate production threatens coral reef growth, *Nature Communications*, *4*, 1402.

Perry, C.T., E.N. Edinger, P.S. Kench, G.N. Murphy, S.G. Smithers, R.S. Steneck, and P.J. Mumby (2012), Estimating rates of biologically driven coral reef framework production and erosion: A new census-based carbonate budget methodology and applications to the reefs of Bonaire, *Coral Reefs*, *31*, 853-868.

Piniak, G. (2002), Effects of symbiotic status, flow speed, and prey type on prey capture by the facultatively symbiotic temperate coral *Oculina arbuscula*, *Marine Biology*, *141*, 449-455.

Piniak, G.A., and F. Lipschultz (2004), Effects of nutritional history on nitrogen assimilation in congeneric temperate and tropical scleractinian corals, *Marine Biology*, *145*, 1085-1096.

Pitts, P.A. (2002), Near-shore circulation in the lower Florida Keys, *Journal of Coastal Research*, *18*, 662-673.

Pochon, X., J. Pawlowski, L. Zaninetti, and R. Rowan (2001), High genetic diversity and relative specificity among Symbiodinium-like endosymbiotic dinoflagellates in soritid foraminiferans, *Marine Biology*, *139*, 1069-1078.

Porter, J., K. Porter, J. Porter, and K. Porter (2002), Introduction: The Everglades, Florida Bay, and coral reefs of the Florida Keys: an ecosystem sourcebook, *The Everglades, Florida Bay, and Coral Reefs of the Florida Keys: An Ecosystem Sourcebook*.

Porter, J.W., S.K. Lewis, and K.G. Porter (1999), The effect of multiple stressors on the Florida Keys coral reef ecosystem: A landscape hypothesis and a physiological test, *Limnology and Oceanography*, *44*, 941-949.

Raupach, M.R., G. Marland, P. Ciais, C. Le Quéré, J.G. Canadell, G. Klepper, and C.B. Field (2007), Global and regional drivers of accelerating CO_2 emissions, *Proceedings of the National Academy of Sciences*, *104*, 10288-10293.

Reaka-Kudla, M.L. (1996), The global biodiversity of coral reefs: A comparison with rain forests. *In*: M. Reaka-Kudla, D. E. Wilson and E. O Wilson (eds), Biodiversity II, pp 83-108. Joseph Henry Press, Washington D.C., *Biodiversity II: Understanding and Protecting Our Biological Resources*.

Reipschläger, A., H. Pörtner, and (1996), Metabolic depression during environmental stress: The role of extra- versus intracellular pH in *Sipunculus nudus*, *J Exp Biol 199*, 1801–1807.

Renegar, D.A., and B.M. Riegl (2005), Effect of nutrient enrichment and elevated CO_2 partial pressure on growth rate of Atlantic scleractinian coral *Acropora cervicornis*, *Marine Ecology Progress Series*, *293*, 69-76.

Reynaud, S., N. LeClercq, S. Romaine-Lioud, C. Ferrier-Pages, J. Jaubert, and J.-P. Gattuso (2003), Interacting effects of CO_2 partial pressure and temperature on photosynthesis and calcification in a scleractinian coral, *Global Change Biology*, *9*, 1660-1668.

Riahi, K., A. Grübler, and N. Nakicenovic (2007), Scenarios of long-term socio-economic and environmental development under climate stabilization, *Technological Forecasting and Social Change*, *74*, 887-935.

Riebesell, U., K.G. Schulz, R. Bellerby, M. Botros, P. Fritsche, M. Meyerhöfer, C. Neill, G. Nondal, A. Oschlies, and J. Wohlers (2007), Enhanced biological carbon consumption in a high CO_2 ocean, *Nature*, *450*, 545-548.

Ries, J.B. (2011), A physicochemical framework for interpreting the biological calcification response to CO_2-induced ocean acidification, *Geochimica et Cosmochimica Acta*, *75*, 4053-4064.

Ries, J.B., A.L. Cohen, and D.C. McCorkle (2010), A nonlinear calcification response to CO_2-induced ocean acidification by the coral Oculina arbuscula, *Coral Reefs*, *29*, 661-674.

Rodolfo-Metalpa, R., A. Peirano, F. Houlbrèque, M. Abbate, and C. Ferrier-Pagès (2008), Effects of temperature, light and heterotrophy on the growth rate and budding of the temperate coral *Cladocora caespitosa*, *Coral Reefs*, *27*, 17-25.

Rost, B., and U. Riebesell (2004). Coccolithophores and the biological pump: Responses to environmental changes, in *Coccolithophores*, vol., edited, pp. 99-125, Springer.

Rowan, R., and N. Knowlton (1995), Intraspecific diversity and ecological zonation in coral-algal symbiosis, *Proceedings of the National Academy of Sciences*, *92*, 2850-2853.

Russill, C., and Z. Nyssa (2009), The tipping point trend in climate change communication, *Global Environmental Change*, *19*, 336-344.

Sabine, C.L., R.A. Feely, N. Gruber, R.M. Key, K. Lee, J.L. Bullister, R. Wanninkhof, C.S. Wong, D.W.R. Wallace, B. Tilbrook, F.J. Millero, T.-H. Peng, A. Kozyr, T. Ono, and A.F. Rios (2004), The Oceanic Sink for Anthropogenic CO_2, *Science*, *305*, 367-371.

Sansone, F.J., G.W. Tribble, C.C. Andrews, and J.P. Chanton (1990), Anaerobic diagenesis within recent, Pleistocene, and Eocene marine carbonate frameworks, *Sedimentology*, *37*, 997-1009.

Santos, I.R., R.N. Glud, D. Maher, D. Erler, and B.D. Eyre (2011), Diel coral reef acidification driven by porewater advection in permeable carbonate sands, Heron Island, Great Barrier Reef, *Geophysical Research Letters*, *38*.

Schneider, K., and J. Erez (2006), The effect of carbonate chemistry on calcification and photosynthesis in the hermatypic coral *Acropora eurystoma*, *Limnology and Oceanography*, 1284-1293.

Semesi, I.S., S. Beer, and M. Bjork (2009), Seagrass photosynthesis controls rates of calcification and photosynthesis of calcareous macroalgae in a tropical seagrass meadow, *Marine Ecology Progress Series*, *382*, 41-47.

Semina, H.J. (1978). *Phytoplankton manual*. Paris: United Nations Educational, Scientific.

Shamberger, K.E.F., R.A. Feely, C.L. Sabine, M.J. Atkinson, E.H. DeCarlo, F.T. Mackenzie, P.S. Drupp, and D.A. Butterfield (2011), Calcification and organic production on a Hawaiian coral reef, *Marine Chemistry*, *127*, 64-75.

Shaw, E.C., B.I. McNeil, and B. Tilbrook (2012), Impacts of ocean acidification in naturally variable coral reef flat ecosystems, *Journal of Geophysical Research: Oceans (1978–2012)*, *117*.

Shaw, E.C., B.I. McNeil, B. Tilbrook, R. Matear, and M.L. Bates (2013), Anthropogenic changes to seawater buffer capacity combined with natural reef metabolism induce extreme future coral reef CO_2 conditions, *Global Change Biology*.

Silverman, J., D.I. Kline, L. Johnson, T. Rivlin, K. Schneider, J. Erez, B. Lazar, and K. Caldeira (2012), Carbon turnover rates in the One Tree Island reef: A 40-year perspective, *Journal of Geophysical Research-Part G-BioGeochemistry*.

Silverman, J., B. Lazar, L. Cao, K. Caldeira, and J. Erez (2009), Coral reefs may start dissolving when atmospheric CO_2 doubles, *Geophysical Research Letters*, *36*, L05606.

Silverman, J., B. Lazar, and J. Erez (2007a), Community metabolism of a coral reef exposed to naturally varying dissolved inorganic nutrient loads, *Biogeochemistry*, *84*, 67-82.

Silverman, J., B. Lazar, and J. Erez (2007b), Effect of aragonite saturation, temperature and nutrients on the community calcification rate of a coral reef, *Journal of Geophysical Research*, *112*, 1-14.

Smith, N.P. (2002), Tidal, low-frequency and long-term mean transport through two channels in the Florida Keys, *Continental Shelf Research*, *22*, 1643-1650.

Smith, S.V., and R. Buddemeier (1992), Global change and coral reef ecosystems, *Annual Review of Ecology and Systematics*, 89-118.

Smith, S.V., and G.S. Key (1975), Carbon dioxide and metabolism in marine environments, *Limnology and Oceanography*, *20*, 493-495.

Smith, S.V., and D.W. Kinsey (1976), Calcium carbonate production, coral reef growth, and sea level change, *Science*, *194*, 937-939.

Solomon, S., D. Qin, M. Manning, Z. Chen, M. Marquis, K. Averyt, M. Tignor, and H. Miller (2007), The physical science basis, *Contribution of working group I to the fourth assessment report of the intergovernmental panel on climate change*, 235-337.

Somero, G. (2012), The physiology of global change: Linking patterns to mechanisms, *Annual Review of Marine Science*, *4*, 39-61.

Sorokin, Y. (1991), Biomass, metabolic rates and feeding of some common reef zoantharians and octocorals, *Marine and Freshwater Research*, *42*, 729-741.

Sorokin, Y.I. (1973), Data on biological productivity of the western tropical Pacific Ocean, *Marine Biology*, *20*, 177-196.

Soto, I.M., F.E. Muller-Karger, P. Hallock, and C. Hu (2011), Sea surface temperature variability in the Florida Keys and its relationship to coral cover, *Journal of Marine Biology*, *2011*.

Sponaugle, S., T. Lee, V. Kourafalou, and D. Pinkard (2005), Florida current frontal eddies and the settlement of coral reef fishes, *Limnology and Oceanography*, *50*, 1033-1048.

Stabenau, E., R. , R. Zepp, G. , and R. Zika, G. (2004), Role of the seagrass *Thalassia testudinum* as a source of chromophoric dissolved organic matter in coastal south Florida, *Marine Ecology Progress Series*, *282*, 59-72.

Stambler, N., and Z. Dubinsky (2005), Corals as light collectors: an integrating sphere approach, *Coral Reefs*, *24*, 1-9.

Stanley, S.M. (1966), Paleoecology and diagenesis of Key Largo limestone, Florida, *AAPG Bulletin*, *50*, 1927-1947.

Stimson, J. (1997), The annual cycle of density of zooxanthellae in the tissues of field and laboratory-held *Pocillopora damicornis* (Linnaeus), *Journal of Experimental Marine Biology and Ecology*, *214*, 35-48.

Stimson, J., and R.A. Kinzie III (1991), The temporal pattern and rate of release of zooxanthellae from the reef coral *Pocillopora damicornis* (Linnaeus) under nitrogen-enrichment and control conditions, *Journal of Experimental Marine Biology and Ecology*, *153*, 63-74.

Suggett, D.J., L.F. Dong, T. Lawson, E. Lawrenz, L. Torres, and D.J. Smith (2013), Light availability determines susceptibility of reef building corals to ocean acidification, *Coral Reefs*, 1-11.

Suggett, D.J., R.K. Kikuchi, M.D. Oliveira, S. Spanó, R. Carvalho, and D.J. Smith (2012), Photobiology of corals from Brazil's near-shore marginal reefs of Abrolhos, *Marine Biology*, *159*, 1461-1473.

Suzuki, A., and H. Kawahata (2003), Carbon budget of coral reef systems: and overview of observations in fringing reefs, barrier reefs and atolls in the Indo-Pacific regions, *Tellus*, *55B*, 428-444.

Suzuki, A., and H. Kawahata (2004), Reef water CO_2 system and carbon production of coral reefs: Topographic control of system-level performance, *Global Environmental change in the Ocean and on Land*.

Suzuki, A., T. Nakamori, and H. Kayanne (1995), The mechanism of production enhancement in coral reef carbonate systems: model and empirical results, *Sedimentary Geology*, *99*, 259-280.

Takahashi, T., J. Olafsson, J.G. Goddard, D.W. Chipman, and S.C. Sutherland (1993), Seasonal variation of CO_2 and nutrients in the high-latitude surface oceans: a comparative study, *Global Biogeochemical Cycles*, *7*, 843-878.

Tambutté, É., D. Allemand, E. Mueller, and J. Jaubert (1996), A compartmental approach to the mechanism of calcification in hermatypic corals, *Journal of Experimental Biology*, *199*, 1029-1041.

Taylor, J.A., and J. Lloyd (1992), Sources and sinks of atmospheric CO_2, *Australian Journal of Botany*, *40*, 407-418.

Tentori, E., and D. Allemand (2006), Light-enhanced calcification and dark decalcification in isolates of the soft coral *Cladiella* sp. during tissue recovery, *The Biological Bulletin*, *211*, 193-202.

Thayer, G.W., K.A. Bjorndal, J.C. Ogden, S.L. Williams, and J.C. Zieman (1984), Role of larger herbivores in seagrass communities, *Estuaries and Coasts*, *7*, 351-376.

Thayer, G.W., D.W. Engel, and K. A. Bjorndal (1982), Evidence for short-circuiting of the detritus cycle of seagrass beds by the green turtle, *Chelonia mydas* L., *Journal of Experimental Marine Biology and Ecology*, *62*, 173-183.

Titlyanov, E., V. Leletkin, and Z. Dubinsky (2000b), Autotrophy and predation in the hermatypic coral *Stylophora pistillata* in different light habitats, *Symbiosis*, *29*, 263-281.

Titlyanov, E., T. Titlyanova, K. Yamazato, and R. Van Woesik (2001), Photo-acclimation of the hermatypic coral *Stylophora pistillata* while subjected to either starvation or food provisioning, *Journal of Experimental Marine Biology and Ecology*, *257*, 163-181.

Titlyanov, E., J. Tsukahara, T. Titlyanova, V. Leletkin, R. Van Woesik, and K. Yamazato (2000a), Zooxanthellae population density and physiological state of the coral *Stylophora pistillata* during starvation and osmotic shock, *Symbiosis*, *28*, 303-322.

Tremblay, P., M. Fine, J.F. Maguer, R. Grover, and C. Ferrier-Pagés (2013), Ocean acidification increases photosynthate translocation in a coral-dinoflagellates symbiosis, *Biogeosciences Discuss*, *10*, 83-109.

Trench, R. (1974), Nutritional potentials in *Zoanthus sociathus* (Coelenterata, Anthozoa), *Helgoland Marine Research*, *26*, 174-216.

Tribble, G.W. (1993), Organic matter oxidation and aragonite diagenesis in a coral reef, *Journal of Sedimentary Research*, *63*.

Tribble, G.W., F.J. Sansone, and S.V. Smith (1990), Stoichiometric modeling of carbon diagenesis within a coral reef framework, *Geochimica et Cosmochimica Acta*, *54*, 2439-2449.

Tribollet, A., M.J. Atkinson, and L. Christopher (2006), Effects of elevated pCO_2 on epilithic and endolithic metabolism of reef carbonates, *Global Change Biology*, *12*, 2200-2208.

Tribollet, A., C. Godinot, M. Atkinson, and C. Langdon (2009), Effects of elevated pCO_2 on dissolution of coral carbonates by microbial euendoliths, *Global Biogeochemical Cycles*, *23*, GB3008.

Tribollet, A., and S. Golubic (2011). Reef bioerosion: agents and processes, in *Coral Reefs: An Ecosystem in Transition*, vol., edited, pp. 435-449, Springer.

Tribollet, A., C. Langdon, S. Golubic, and M. Atkinson (2006), Endolithic microflora are major primary producers in dead carbonate substrates of Hawaiian coral reefs, *Journal of Phycology*, *42*, 292-303.

Unsworth, R.K.F., C.J. Collier, G.M. Henderson, and L.J. McKenzie (2012), Tropical seagrass meadows modify seawater carbon chemistry: implications for coral reefs impacted by ocean acidification, *Environmental Research Letters*, *7*, 024026.

Veal, C., G. Homes, M. Nunez, O. Hoegh-Guldberg, and J. Osborn (2010), A comparative study of methods for surface area and three-dimensional shape measurement of coral skeletons, *Limnology and Oceanography: Methods*, *8*, 241-253.

Venn, A., E. Tambutté, M. Holcomb, D. Allemand, and S. Tambutté (2011), Live tissue imaging shows reef corals elevate pH under their calcifying tissue relative to seawater, *PloS One*, *6*, e20013.

Venn, A., E. Tambutté, S. Lotto, D. Zoccola, D. Allemand, and S. Tambutté (2009), Imaging intracellular pH in a reef coral and symbiotic anemone, *Proceedings of the National Academy of Sciences*, *106*, 16574-16579.

Venn, A.A., E. Tambutté, M. Holcomb, J. Laurent, D. Allemand, and S. Tambutté (2013), Impact of seawater acidification on pH at the tissue–skeleton interface and calcification in reef corals, *Proceedings of the National Academy of Sciences*, *110*, 1634-1639.

Venti, A., D. Kadko, A.J. Andersson, C. Langdon, and N.R. Bates (2012), A multi-tracer model approach to estimate reef water residence times, *Limnology and Oceanography, Methods*, *10*, 1078-1005.

Veron, J., O. Hoegh-Guldberg, T. Lenton, J. Lough, D. Obura, P. Pearce-Kelly, C. Sheppard, M. Spalding, M. Stafford-Smith, and A. Rogers (2009), The coral reef crisis: The critical importance of< 350ppm CO_2, *Marine Pollution Bulletin*, *58*, 1428-1436.

Vidal-Dupiol, J., D. Zoccola, E. Tambutté, C. Grunau, C. Cosseau, K.M. Smith, M. Freitag, N.M. Dheilly, D. Allemand, and S. Tambutté (2013), Genes related to ion-transport and energy production are upregulated in response to CO_2-driven pH decrease in corals: New insights from transcriptome analysis, *PloS One*, *8*, e58652.

Walter, L.M., and E.A. Burton (1990), Dissolution of recent platform carbonate sediments in marine pore fluids, *American Journal of Science*, *290*, 601-643.

Ware, J.R. (1991), Coral Reefs: sources or sinks of atmospheric CO_2, *Coral Reefs*, *11*, 127.

Warner, M., G. Chilcoat, F. McFarland, and W. Fitt (2002), Seasonal fluctuations in the photosynthetic capacity of photosystem II in symbiotic dinoflagellates in the Caribbean reef-building coral *Montastraea*, *Marine Biology*, *141*, 31-38.

Watanabe, A., H. Kayanne, H. Hata, S. Kudo, Y. Ikeda, and H. Yamano (2006), Analysis of the seawater CO_2 system in the barrier reef-lagoon system of Palau using total alkalinity-dissolved inorganic carbon diagrams, *Limnology and Oceanography*, *51*, 1614-1628.

Wei, G., M.T. McCulloch, G. Mortimer, W. Deng, and L. Xie (2009), Evidence for ocean acidification in the Great Barrier Reef of Australia, *Geochimica et Cosmochimica Acta*, *73*, 2332-2346.

Wilkinson, C. (2008). *Status of coral reefs of the world*. Townsville, Australia.

Wisshak, M., L. Tapanila, and A. Tribollet (2008). The boring microflora in modern coral reef ecosystems: a review of its roles, in *Current Developments in Bioerosion*, vol., edited, pp. 67-94, Springer Berlin Heidelberg.

Wood, H.L., J.I. Spicer, and S. Widdicombe (2008), Ocean acidification may increase calcification rates, but at a cost, *Proceedings of the Royal Society B: Biological Sciences*, *275*, 1767-1773.

Xu, J., A. Takasaki, H. Kobayashi, T. Oda, J. Yamada, R.E. Mangindaan, K. Ukai, H. Nagai, and M. Namikoshi (2006), Four new macrocyclic trichothecenes from two strains of marine-derived fungi of the genus *Myrothecium*, *The Journal of Antibiotics*, *59*, 451-455.

Xu, Y., T.M. Wahlund, L. Feng, Y. Shaked, and F.M.M. Morel (2006), A novel alkaline phosphatase in the coccolithophore *Emiliania huxelyi* (Prymnessiophycea) and its regulation by phosphorus *Journal of Phycology*, *42*, 835-844.

Yahel, G., F.P. Anton, K. Fabricius, D. Marie, D. Vaulot, and A. Genin (1998), Phytoplankton distribution and grazing near coral reefs, *Limnology and Oceanography*, *43*, 551-563.

Yahel, R., G. Yahel, and A. Genin (2005), Near- bottom depletion of zooplankton over coral reefs: I: Diurnal dynamics and size distribution, *Coral Reefs*, *24*, 75-85.

Yates, K., and R. Halley (2006), Diurnal variation in rates of calcification and carbonate sediment dissolution in Florida Bay, *Estuaries and Coasts*, *29*, 24-39.

Yates, K.K., and R.B. Halley (2003), Measuring coral reef community metabolism using new benthic chamber technology, *Coral Reefs*, *22*, 247-255.

Zieman, J.C., J.W. Fourqurean, and T.A. Frankovich (1999), Seagrass die-off in Florida Bay: Long-term trends in abundance and growth of turtle grass, *Thalassia testudinum*, *Estuaries*, *22*, 460-470.

Zoccola, D., A. Moya, G.E. Béranger, E. Tambutté, D. Allemand, G.F. Carle, and S. Tambutté (2009), Specific expression of BMP2/4 ortholog in biomineralizing tissues of corals and action on mouse BMP receptor, *Marine Biotechnology*, *11*, 260-269.

Zoccola, D., E. Tambutté, E. Kulhanek, S. Puverel, J.-C. Scimeca, D. Allemand, and S. Tambutté (2004), Molecular cloning and localization of a PMCA P-type calcium ATPase from the coral *Stylophora pistillata*, *Biochimica et Biophysica Acta (BBA)-Biomembranes*, *1663*, 117-126.